METABOLIC AND ENERGETIC STUDIES OF RECOMBINANT *ESCHERICHIA COLI* STRAINS: APPLICATIONS OF NMR TECHNIQUES

Thesis by

Ruizhen Chen

In Partial Fulfillment of the Requirements
for the Degree of
Doctor of Philosophy

California Institute of Technology
Pasadena, California
1994

(Submitted May 18, 1994)

To my daughter

Jennifer Yitian Dou

ACKNOWLEDGEMENTS

I would like to thank my advisor, Dr. James E. Bailey, for his support and able guidance over the course of the work.

I am deeply appreciative of the help and stimulus that I have received over the years from many group members. Particularly, I wish to thank Dr. Thomas Hottiger for showing me around when I first came to the lab, for helping me with many lab basics and for being a good friend and officemate. Thanks are given to Drs. Pauli Kallio, Thomas Hottiger and Wilfred Chen for their key roles in shaping a friendly environment which I enjoyed very much. I am grateful to Neilay Dedhia for sharing much the same experience and the lonely times after the majority of the group moved to Switzerland.

Support from my family and family-in-law is tremendous. Without their help, I could not have made it this far. Especially, I thank my mother-in-law and my parents, who travelled across the Pacific Ocean, for taking care of my baby. Thanks are due to my brother and sisters for their love and confidence in me.

Technical assistances of Drs. Bog Kusta, Gerard Riedy and Robert Lee are very much appreciated. Thanks to Tom Dunn for his help with instrumental repair.

Finally, I thank my husband, Ming, for his support, understanding and constant encouragement and for sharing many joys and sorrows during my stay at Caltech.

ABSTRACT

This work concerns applications of NMR techniques in metabolic engineering studies. As demonstrated here, NMR is a valuable tool in analyzing intracellular metabolic and energetic states. When combined with growth and fermentation studies, it greatly enhances the understanding of cellular responses to particular genetic modifications.

A novel on-line NMR system has been developed in this work which extends the capacities of *in vivo* NMR to growing cell cultures. This new approach eliminates possible artifacts and time limitations associated with conventional NMR methods. Furthermore, experiments can be conducted under well-defined conditions. New types of physiological states and experimental regimes are accessible with this on-line system.

Steady-state levels of ATP and ΔpH have been measured using the on-line NMR system for strains with and without *Vitreoscilla* hemoglobin (VHb) (GRO21 and MG1655, respectively) during their growth under oxygen-limited conditions. GRO21 has similar levels of ATP and ΔpH while exhibiting a higher specific growth rate, indicating that the net ATP accumulation rate is enhanced. Studies on ATP synthase (ATPase) kinetics show that the presence of VHb accelerates ATP synthesis rate catalyzed by ATPase by 30%.

Switching from the phosphotransferase system (PTS) to the galactose-proton symport system for glucose uptake brings about many changes in cell energetics and

metabolism. The extra energy cost in the non-PTS glucose uptake has a greater effect on the specific growth rates in anaerobic conditions than in aerobic conditions, Fermentation patterns are significantly different in the non-PTS strain, compared to the PTS strain. The non-PTS strain has a much lower NTP and ΔpH and higher NDP; NAD(H) is also considerably reduced. Different levels of glycolytic intermediates have also been observed in these two strains.

The non-PTS strain carrying a phenylalanine overproduction plasmid exhibits much lower energy level (NTP and ΔpH), lower sugar phosphate (S-P) total concentration, NAD(H) and PEP concentrations than its PTS counterpart. The compositions of S-P are significantly different between the two strains. Phenylalanine production is not increased in the non-PTS strain and a larger portion of carbon is oxidized to CO_2.

TABLE OF CONTENTS

Chapter 1

Introduction

1.1 METABOLIC ENGINEERING

Metabolic engineering is defined as application of recombinant DNA technology to restructure metabolic networks for improvement of production of bioproducts (Bailey, 1991). It provides many possibilities to optimize cellular functions for a particular purpose, for example, for production of a valuable metabolite. These include deregulating a biosynthesis pathway by mutating a regulatory element; augmenting a set of enzymes catalyzing the rate-limiting steps of the pathway; introducing mutations in a particular enzyme to increase precursor pools, eliminating existing or installing new pathways. All of these approaches have been used in different processes with varying successes. Examples of each category can be found in references (Bailey, 1991; Cameron and Tong, 1993).

For a few microorganisms such as *E. coli*, with the current state of recombinant DNA technology, genetic modification can be made precisely. In contrast to the precision that recombinant DNA techniques offer to change cell genome at the molecular level, prediction of how the cell will respond to a genetic modification is much more difficult. This is due to the complexity of cellular machinery which encompasses a large number of reactions with branched and interacting pathways, and sophisticated regulatory strategies evolved over millions of years. Although many biochemical pathways have been elucidated for years, interactions among different pathways are largely unknown.

With the unpredictability of cell behavior, a legitimate choice of a target gene to manipulate is difficult. The current trial and error approach in metabolic engineering often leads to unexpected and undesired results. For example, abolishing both acetyl

phosphotransferase (PTA) and acetate kinase (ACK) activities in an *E. coli* strain resulted in an accumulation of pyruvate as an unusual product (Diaz-Ricci et al. 1991). Mutation in the *ppc* gene coding for phosphoenolpyruvate carboxylase led to unwanted products, acetate and pyruvate (Miller, 1987).

Studies also show that redirection of carbon flux distributions in the primary metabolism may not readily occur because metabolic flux alterations are directly opposed by the control mechanisms whose main object is to maintain a distribution for optimal growth, not for overproduction of a particular metabolite (Stephanopoulos and Vallino, 1991).

While the effectiveness of genetic manipulation can be easily determined by simply measuring the target product, full assessment of the consequence of even a single mutation is not trivial. The mutation of a single gene or of its expression control can elicit changes and responses not only directly associated with the gene product, but also in processes distant from the pathway in which the mutation acts directly. In order to analyze what has been changed and to gain insight into how much room is left for further improvement and guidance on the next round genetic modification, often one has to include the whole pathway and sometimes, other interacting pathways for analysis. This requires some analytical tools that allow one to look into the cell, measure quantities such as intracellular metabolite concentrations, and also knowledge of the pathway, kinetics of the enzymes involved and their regulation, and ideally also a mathematical model to aid the analysis.

1.2 NMR TECHNIQUES

Many analytical methods and classic biochemical techniques find important applications in metabolic engineering. Among others, NMR stands out as a method of choice because the measurement is essentially non-invasive so that intracellular environmental and metabolic changes, energetics and other cellular events can be observed as they exist within an unperturbed living system. This leads to the possibility of investigating details of cellular biochemistry previously obscured by separation and purification procedures. The other feature that makes NMR particularly attractive in biological studies is its informativeness. NMR spectroscopy can be used to identify metabolites and determine their concentrations, and simultaneously, it provides information regarding the locations of these metabolites and environments such metabolites are experiencing such as pH and binding to ions or proteins.

Since the first account of using NMR for studies in cells in which Moon and Richards (1973) showed that phosphorylated metabolites could be detected non-invasively in ^{31}P NMR spectra of intact red blood cells, NMR has been widely used as a routine method for studying metabolism and bioenergetics. The broad spectrum of NMR applications can be summarized as follows.

(i) *Intracellular pH measurements*

^{31}P NMR analysis is the most frequently used method, which is based on the strong dependence of ^{31}P chemical shifts of phosphorylated compounds such as inorganic phosphate, glucose-6-phosphate, ATP and 2, 3- diphosphoglycerate. For some organisms such as *E. coli*, inorganic phosphate is a good pH probe because it is one of the most abundant compounds in this organism and is present within cells at

sufficiently high concentrations (usually above 10 mM) to allow rapid detection by NMR. Moreover, its pKa value is close to physiological pH and thus inorganic phosphate affords high pH sensitivity of chemical shift in the range of most interest. The accuracy of this probe is estimated to be 0.1-0.2 pH unit (Lundberg et al. 1990; Roberts and Jardetzky, 1981).

Spectra of other nuclei such as ^{13}C, ^{1}H, ^{15}N have also been reported to be used in intracellular pH measurements.

(ii) *Metabolite concentrations and fluxes*

The inherent low sensitivity of NMR limits in vivo detection of metabolites to those that have relatively high concentration (0.1 mM or higher) and only low molecular weight (less than 1000 daltons). Only freely mobile molecular species can be measured. Nevertheless, NMR is a useful tool in quantifying metabolites from energy and carbon metabolism including glycolysis, the TCA cycle, pathways from amino acids and fatty acids metabolism, and lipid-related metabolites.

Adenosine diphosphate and triphosphate nucleotide (ADP and ATP) and inorganic phosphate can be measured by ^{31}P NMR. The measurement gives the total nicotinamide adenine dinucleotide NAD(H) (total of oxidized and reduced species). Sugar phosphate can also be determined by ^{31}P spectra, but these peaks are normally too broad (linewidth 50 Hz or higher) and too poorly separated to distinguish between individual sugars. Much narrower linewidths can be obtained in cell extracts, allowing quantification of many individual phosphorylated sugars. Certain amino acids such as glutamate, alanine and valine and low molecular weight metabolites such as lactate, acetate, succinate and ethanol can be measured by ^{13}C and ^{1}H NMR spectra.

In some cases, metabolic flux partition between overlapping pathways, for example, glycolysis and the TCA cycle and glycolysis and gluconeogenesis, can be evaluated in ^{13}C NMR spectra, by observing labeling patterns after feeding ^{13}C-labeled carbon substrates. The applicability of this method depends on the existence of a label pattern which can differentiate fluxes to different pathways, which is not always available and obvious. Sometimes computer models are necessary to extract information obtained (Tran-Dinh et al. 1992).

(iii) *Ion concentrations other than proton*

Intracellular concentration and transmembrane gradients of monovalent and other cations and anions are suggested to be modulators in a variety of cellular and tissue functions such as signal transduction in nerves, contractile activity of the heart, cellular proliferation, differentiation, volume regulation and hormone control (Gupta et al, 1984) and thus measurement of these ions are critical in assessing their regulatory roles. ^{23}Na, ^{39}K, ^{7}Li, ^{35}Cl, ^{87}RB, ^{133}Cs, ^{19}F and ^{43}Ca NMR have been used in studies of these ions (Gupta et al, 1984; Lundberg et al. 1990).

(iv) *Enzyme kinetics*

An exciting aspect of NMR spectroscopy is its ability to measure enzyme kinetics *in vivo* and non-invasively. These features are particularly important in the case of membrane proteins whose isolation, purification and reconstitution are not an easy task.

E. coli was one of the first *in vivo* systems to be studied using NMR techniques (In particular, saturation transfer was used to study ATPase kinetics). Other enzymes that have been studied include: creastine kinase, lactate dehydrogenase (LDH), glyceraldehyde 3-phosphate dehydrogenase (GAPDH), β-hydroxybutyrate dehydrogenase and adenylate kinase (Brindle and Campbell, 1987). Although the list is still short, NMR holds the potential for more wide applications.

1.3 SCOPE OF THESIS

^{1}H, ^{2}H, ^{13}C, ^{15}N, ^{19}F, ^{31}P, ^{23}Na and ^{39}K are among the nuclei which have been frequently observed in cells and tissues by NMR. ^{31}P NMR has been chosen as an analytical tool in this study since the focus of this thesis is energetics and metabolism. Half of the intermediates involved in *E. coli* central carbon metabolism pathways are phosphorylated, and several important high-energy compounds such as ATP, ADP, NAD(H) etc., which are supposed to be important in regulation of carbon fluxes, are also phosphorylated. Additionally, inorganic phosphate is a good pH probe and can be readily measured in ^{31}P NMR spectroscopy as explained above and therefore can provide not only intracellular pH but also the pH gradient across the cytoplasmic membrane, which is another important energetic parameter. Further, since ^{31}P is a natural isotope, experiments do not require feeding labeled substrates, and the simplest one-pulse FT-NMR can be implemented to obtain a ^{31}P NMR spectrum. Furthermore, ^{31}P NMR spectra are usually simpler than ^{13}C and ^{1}H spectra, allowing easier interpretation.

Despite many advantages, the insensitivity of the technique has many consequences that need to be addressed before it can be used to study particular physiological problems. Conventional non-growing suspension NMR procedures have three major drawbacks: (i) possible artifacts associated with sample preparation; (ii) time limitation of the experiments. For example, for *E. coli* glycolysis experiments, the total time available is on the scale of 30 minutes at 25°C, with longer time possible at lower temperature; and (iii) ill-defined experimental conditions, especially oxygen supply in "aerobic" experiments.

A novel on-line NMR system based on circulation of cell culture between the NMR sample chamber and fermentor has been developed in this work. In addition to eliminating the aforementioned problems, it extends the powerful NMR tool to active, growing cell samples. Many intracellular properties of growing cells can be probed, and new types of experiments can be done. For example, growth-related physiological problems can be studied using this system. Described in Chapter 2 are detailed configurations, strategies used in constructing the on-line system, and operation procedures as well as the development of the high-cell-density fed-batch fermentation process which is an essential part of the on-line system. Examples illustrating the use of this system are also included. Observations of growing cell energetics, mechanistic studies of acetate inhibitory effects on cell growth and oxygen effect on cell energetics of a glycolysing stationary phase culture are the first few applications of this on-line system.

The on-line system was further used to investigate responses of host *E. coli* cells to expression of *Vitreocilla* hemoglobin (VHb). The on-line approach,

combining with the special saturation transfer NMR technique to measure the kinetics of ATP synthase, provided valuable information on the energetics of the metabolic-engineered *E. coli* cells. This work is presented in Chapter 3.

A comparative study of *E. coli* strains using different glucose uptake systems is given in Chapter 4. A strain carrying a deletion of mutation of genes in the phosphotransferase (PTS) system, ptsHI-*crr* was further modified so that it expresses galactose permease consititutively, and glucose can then be transported by galactose permease and subsequent phosphorylation is catalyzed by the native *E. coli* glucokinase. A strain with a wild-type PTS system and no galactose permease activity was used as control. Fermentation studies were conducted to investigate the altered growth and metabolism patterns under both aerobic and anaerobic conditions. ^{31}P NMR was used to study the alterations in cell energetics and other changes in carbon metabolism.

The conventional non-growing method was used for these last experiments for the reason that the on-line system is not readily applicable to this case due to lack of a universal approach to obtain high-cell density culture required for NMR measurements. Care was exercised to keep any artifacts due to the method to minimum. Sample preparation procedures were standardized and vortex was omitted (as described in Chapter 4, Materials and Methods) to avoid any complications in interpreting experimental data. The problem of oxygen supply in aerobic experiments was also addressed by using relatively low cell density (adequacy of aeration under these conditions was determined by separate experiments outside the magnet in which dissolved oxygen concentration was measured by a micro-oxygen electrode) and by

using a double-bubbled apparatus to ensure sufficient oxygenation. Perchloric acid (PCA) extract NMR experiments were conducted to give data complementary to the whole cell experiments.

The same methodology described in Chapter 4 was applied to the study of phenylalanine overproduction using PTS and non-PTS host strains. Fermentation and shake-flask results are both included in Chapter 5 as well as NMR characterizations. The combined information is useful to understand the difference in phenylalanine production between these two strains.

1.4 REFERENCES

Bailey, J. E. Toward a science of metabolic engineering. Science. 1991, 252, 1668-1675.

Brindle, K. M. and Campbell, I. D. NMR studies of kinetics in cells and tissues. Quart. Rev. Biophy. 1987, 19(3/4), 159-182.

Cameron, C. D. and Tong, I. Cellular and metabolic engineering. Applied biochemistry and biotechnology. 1993, 38, 105-140.

Diaz-Ricci, J. C.; Regan, L. and Bailey, J. E. Effect of alteration of the acetic acid synthesis pathway on the fermentation pattern of *Escherichia coli*. Biotechnol. Bioeng. 1991, 38, 1318-1324.

Lundberg, P.; Harmsen, E.; Ho, C. and Vogel, H. J. Nuclear magnetic resonance studies of cellular metabolism. Anal. Biochem. 1990, 191, 193-222.

Miller, J. E.; Backman, K. C.; O'Connor, M. J. and Hatch, R. T. Production of phenylalanine and organic acids by phosphoenolpyruvate carboxylase-deficient mutants of *Escherichia coli*. J. industrial Microbiol. 1987, 2, 143-149.

Moon, R. N.; and Richards, J. H. Determination of intracellualr pH by ^{31}P magnetic resonance. J. Biol. Chem. 1973, 248, 7276-7278.

Roberts, J. K. M.; and Jardetzky, O. Monitoring of cellular metabolism by NMR. Biochim. Biophys. Acta. 1981, 639, 53-76.

Stephanopoulos, G. and Vallino, J. J. Network rigidity and metabolic engineering in metabolite overproduction. Science. 1991, 252, 1675-1681.

Tran-Dinh, S; Wietzerbin, J. and Herve, M. Mathematical model for the determination of metabolite fluxes in *Saccharomyces cerevisae*. J. Chim. Phys. 89, 65-76.

Chapter 2

Observations of Aerobic, Growing *Escherichia coli* Metabolism Using An On-Line Nuclear Magnetic Resonance Spectroscopy System

Source: Chen, R. and Bailey, J. E. 1993. Biotechnol. Bioeng. 42: 215-221

2.1 ABSTRACT

An experimental system has been constructed which enables on-line measurements of phosphorous-31 (^{31}P) nuclear magnetic resonance (NMR) spectra for growing bacterial suspensions under anaerobic or aerobic conditions. A sample stream from a laboratory bioreactor is circulated to the NMR sample chamber in a gas exchange system which permits maintenance of aerobic conditions for high cell density cultures. ^{31}P NMR spectra with resolution comparable to that obtained traditionally using dense, concentrated, non-growing cell suspensions can be obtained at cell densities above 25 g/L with acquisition times ranging from 14 to 3 minutes which decline as cell density increases. This system has been employed to characterize the changes in intracellular state of a stationary phase culture which is subjected to a transition from aerobic to anaerobic conditions. Both intracellular NTP level and cytoplasmic pH are substantially lower under anaerobic conditions. Also, the system has been employed to observe the response of a growing culture to external addition of acetate. Cells are able to maintain pH difference across the cytoplasmic membrane at extracellular acetate concentrations of 5 and 10 g/L. However, acetate concentrations of 20 g/L cause collapse of the transmembrane ΔpH and sharp reduction of the growth rate of the culture. The experimental configuration described should also permit NMR observations of many other types of microbial cultures and of other nuclei.

2.2 INTRODUCTION

The last two decades have witnessed tremendous progress in application of nuclear magnetic resonance (NMR) spectroscopic techniques for non-invasive characterization of the internal composition and activities of many different types of living systems. In particular, NMR data has provided detailed insights into composition and function of microorganisms (6,12,29) and cultured cells (13,16,26) which are inaccessible by other methods. Previous researchers have typically studied highly concentrated cell suspensions (often at cell densities of more than 100 gDW (grams dry weight)/L) in their NMR studies of microbial metabolism.

Several investigators have commented on artifacts which can easily be generated in study of higher cells using traditional harvest-concentration-observation protocols. Sample preparations can occupy periods from 2 to 4 hours which include repeated centrifugations, washings, and resuspensions by vortexing. Gindsberg *et al.* point out that metabolites such as polyphosphate and inorganic phosphate are liberated from cells in such procedures and that supernatant fluid in some conditions showed strong spectral intensities due to cell lysis (17). Laws *et al.* reported that washing and centrifuging *Ehrlich ascites* tumor cells reduces the level of ATP, the utilization of glucose, and the respiration rate by about 30% (20). Although comparable studies have not been conducted with microorganisms, the severe changes of conditions to which cells are exposed in traditional sample preparation are certainly potential sources for physiological perturbations. Thus, the metabolic features observed for non-growing, glucose-consuming cell samples subjected to such sample preparation protocols may not be representative of the metabolic state of well-adapted cells in a growing state.

Previous investigators have analyzed NMR spectra of dense, non-growing, glycolyzing *E. coli* suspensions and suspensions of other types of cells under both anaerobic and aerated conditions (1,6,8-10,23,32,33). Almost all studies of aerated suspensions relied on the existence of differences in spectra with air or oxygen introduced relative to spectra without such addition of oxygen to conclude that aerobic metabolism was observed. However, due to the high oxygen uptake rates of microorganisms, it is not certain that these samples possessed fully aerobic metabolism; only partially aerobic conditions may have been achieved. Indeed, previous investigators of aerated algae have suggested that earlier studies with more dense cell suspensions likely do not involve completely aerobic conditions (17). Only one mass transfer study of oxygen exchange devices for NMR studies of cell suspensions has been reported (19), and, although data are provided on oxygen transfer rates, the relationship of these rates to maximum cell densities which can be fully aerated is complicated by absence of information on oxygen uptake rates of glycolyzing aerated cultures.

Although significant progress has been made recently in maintaining viable, growing cells within an NMR magnet to enable observations of growing cells by immobilizing cells using hollow fibers (4,5), agarose beads (3,18,25) and κ-carrageenan supported threads (30), entrapped cells may be exposed to a nonuniform environment because of mass transfer resistance within hollow fibers, beads and threads (4,5,7). Further, other studies have shown that immobilization may cause many profound changes in cell metabolism. For alginate-entrapped *Saccharomyces cerevisiae*, for example, the glucose uptake increases by a factor of two compared to suspended cells (15); thus NMR data on immobilized cells are not necessarily representative of conditions in suspended cells. Thus, circulation of a suspension of

cell culture to the NMR magnet appears to be a good alternative. De Graaf *et al.* (7) described an NMR bioreactor positioned above the magnet with circulation of cell cultures through the magnet achieved by a pump. As a result of fast continuous flow, relaxation times were reduced and sensitivity was thus increased. The similar strategy was adopted by Meehan *et al* .(21) in building their NMR cultivator in which an air turbine was used to circulate the cell culture.

The present approach is based on circulation of a sample of culture from a well-instrumented, carefully controlled bioreactor to the NMR sample chamber and back to the bioreactor. An aeration system was designed to transfer oxygen to the bacterial culture during circulation in the sample loop. This was achieved by employing an oxygen-permeable thin tube for carrying the cells and also by providing aeration within the NMR sample chamber itself. The ability to maintain aerobic conditions throughout the circulation loop for dense, actively respiring bacterial cultures differentiates this design and the initial experiments reported here from strategies and systems previously reported.

The application of this system to observe the intracellular state of *E. coli* under aerobic and anaerobic conditions is described here, as are studies on the effect of externally added acetate on the pH difference across the cytoplasmic membrane. Acetate has been suggested to act as an uncoupler of energy metabolism (2). Such effects are observed here in a growing fed-batch culture.

2.3 MATERIALS AND METHODS

On-line NMR system

The on-line NMR measurement system developed in this work is illustrated schematically in Figure 2.1. This system was designed to maintain cells under investigation in well-defined conditions, with special attention to dissolved oxygen measurement and control. Since no ferromagnetic material is allowed within 1.5 m of the magnet of the spectrometer, cells removed from the fermentor must travel about 10 m to traverse the sample loop. In order to avoid oxygen depletion as the sample traverses the external sampling loop, the circulation time in the sample loop should be minimized. However, there is an upper limit to the sample circulation rate which is imposed by a combination of physical factors and also by the requirement that the sample should reside in the magnet for some time (depending on T_1, which is approximately 0.4 seconds for intracellular inorganic phosphorus [22]) prior to measurement so that phosphorous nuclei can be equilibrated with the applied constant magnetic field. Given these contradictory demands, maintaining cells in defined D.O. conditions in the sample loop requires construction of a system to aerate the circulating cells (see Figure 2.1 for detailed arrangements). Highly oxygen-permeable silastic tubing of 0.00198 m inner diameter was used to carry the circulating cell culture. This silastic tubing was supported by spacer inserts within polyester tubes (0.032 m inner diameter). Oxygen or/and nitrogen gas, with each flow rate controlled by an FC-260 gas flow multichannel controller (Tylan corporation, Torrance, CA), flowed

continuously through the space between the inner and outer tubing. The D.O. in the loop could be controlled to some extent by varying the flow rates of nitrogen and oxygen passing through this shell-side space. The D.O. of the circulating culture exiting the NMR sample tube was monitored by a micro-oxygen electrode inserted into the circulating sample. The flow rate of the culture and NMR pulse sequence were chosen to minimize the saturation of the signal, with consideration of D.O. conditions in the whole circulating loop. In all cases, the culture residence time in the sample loop was less than 1.5 minutes.

The standard 20 mm NMR sample tube was used, with the inbuilt sample flow design as detailed in Figure 2.2. A safeguard line was introduced to control the liquid level in the sample tube and avoid accidental overflow of sample fluid from the sample tube. To avoid cell mass sedimentation and further to supply oxygen in aerobic conditions or nitrogen to maintain anaerobic conditions, oxygen or nitrogen was introduced directly to the NMR sample tube, with flow rate controlled by a Tylan FC -260 mass flow controller .

Cell Growth

Escherichia coli MG1655, a wild-type K12 strain, was used in these experiments. A 100 ml seed culture was prepared using complex medium CM4 (27). The growth medium, denoted hereafter RZ, is a modification of MM2 (27) and the medium described by Riesenberg et al .(28); the composition of RZ medium is given in Table 2.1. The feeding solution from (28) was used which contained glucose 500g/l +19.7 g/l $MgSO_4.7H_2O$. The trace element solution consisted of (mg/l): $AlCl_3 .6H_2O$,

20; $CoCl_2$. $6H_2O$, 8; $CuCl_2$.$2H_2O$, 2; H_3BO_4, 1; KI, 20; $MnSO_4$.H2O, 20; $NiCl_2.6H_2O$, 1.23; $Na_2MoO_4.2H_2O$, 4; $ZnSO_4.7H_2O$, 4.

The square of the NMR acquisition time for a given level of spectral resolution is inversely proportional to the cell density in the bioreactor and therefore in the sample tube; in order to enable relatively short acquisition times, a fed-batch procedure was applied in these studies. An L-H 3.5 l fermentor with 2000 series pH, temperature, foam, and agitator speed control package was used for all experiments. The initial medium volume was 1.4 l. Feeding followed a predetermined schedule which provided an extended interval of exponential growth. The feeding was initiated when O.D.(660 nm) was about 6: subsequent feedings were implemented at 2 hour intervals by turning on a pre-calibrated polystaltic pump (Buchler Instruments) for 1 minute using an EC72D two channel time control (Cole Parmer). After each feeding the glucose concentration in the medium was approximately 5 g/l. This feeding scheme was repeated three times. Afterwards, the interval between successive feedings was shortened to 1 hour in order to maintain exponential growth of the culture. After 3 repetitions, the interval between feed additions was further reduced to 0.5 hours until the end of the experiment. Care was exercised so that glucose was not exhausted before each feeding to avoid an undesired sudden change of the dissolved oxygen. In order to obtain high cell density, in addition to controlled glucose feeding, a suboptimal growth temperature (30^{o}C) was used to reduce the growth rate and thus the accumulation of inhibitory metabolic by-products.

When the cell density reached the desired level (typically about 30 g dry weight/l in these experiments), circulation of cell culture in the sample loop was

initiated, with sample loop aeration and D.O. control as described above. In most cases, D.O. in the sample line exiting the NMR sample tube was controlled at the same level as in the fermentor.

NMR operation

Phosphorus-31 NMR spectra were obtained in the Fourier-transform mode at 121 MHz on a Bruker AM300 NMR spectrometer. The spectra were accumulated in consecutive 3.5 minute blocks (300 transients), except where otherwise indicated, with a spectral width of 8000 Hz, and the free induction decays (FID) were sequentially stored on disk (8K). Pulse angle 40^{o} and relaxation delay 0.2 seconds were chosen to optimize the intensity of NTP peaks, resulting in a saturation factor of approximately 1.2 (greater than 1 because of flow effects). Routine tuning, lock, and shimming were applied. The spectrometer temperature was controlled at the same temperature (30^{o}C) as the fermentor. A 20 mm broadband probe was used. An external standard containing 0.1M methylene diphosphonic acid (MDP) sealed in a capillary was placed inside the sample tube as a chemical shift and concentration reference. MDP resonates at 18.6 ppm (downfield) relative to 85% orthophosphoric acid, which is assigned to zero ppm. A line broadening of 20 Hz was used in all the spectra shown in this study. Peak integration was performed on a VT240 computer using the LAB ONE (TM) NMR1 Spectroscopic Data Analysis Software System[32].

2.4 RESULTS

I. On-line NMR measurements for an exponentially growing E. coli culture

Using the medium and the fed-batch protocol developed in this work, *E. coli* MG1655 maintains exponential growth for more than 25 hours before attaining a maximum cell density of approximately 40 gDW/L (Figure 2.3). In this case, the specific growth rate was 0.180 h^{-1}, corresponding to a doubling time of 3.8 hours. In this cultivation, a stream of culture was diverted from the fermentor and circulated through the sample loop depicted schematically in Figure 2.1. Phosphorous-31 NMR spectra were acquired between 22.5 and 27 gDW/L (late exponential phase); spectra for different acquisition times during this interval are displayed in Figure 2.4. At these cell densities, some features of the spectrum are obscured by noise when the acquisition time is 2.9 minutes (Figure 2.4c). However, for acquisition times of 8 minutes and 14 minutes, the spectra contain all of the characteristic resonances observed previously in dense suspension measurements of non-growing cells (Figures 2.4a & 2.4b). Assignments of resonances were done according to these previous investigations (10,11,23,34). Peaks at -4.9 ppm, -10.0 ppm, and -18.6 ppm were assigned to NTPγ, NTPα + NDPα and NTPβ, respectively. Other metabolites observed in these ^{31}P NMR spectra include the composite sugar phosphate (SP), NAD(H), and UDPG resonating at 4.2 ppm, -10.6 ppm, and -12.1 ppm, respectively. Positions of the inorganic phosphate resonances enable estimates of cytoplasmic and extracellular pH; calibration for these estimates was taken from the pH-inorganic phosphate chemical shift standard given in Reference 31. According to these estimates, growing MG1655

cells maintain cytoplasmic pH at approximately 7.3 during exponential growth at the specific growth rate of 0.180 h^{-1} which is approximately 0.7 pH units higher than the extracellular pH.

Cells in the bioreactor are exposed to an environment of controlled pH, dissolved oxygen, and temperature. Cells flowing through the sample loop are subject to indirect control of dissolved oxygen and temperature and no control of pH. It is possible, however, to make realistic engineering estimates of the fluctuations in these important environmental parameters which are expected in the circulation loop. Assuming plug flow in the sample line, neglecting the heat transfer resistance of the liquid side and the silastic tubing, and estimating heat transfer coefficient of the sample line to be 2.0 $w/m^2/^oC$, which corresponds to a temperature fluctuation in the loop about 0.15 ^oC. The fluctuation of the pH in the sample line was also estimated for the following typical operating condition of the system: cell dry weight 30 g/l, specific growth rate 0.18 hr^{-1}, glucose yield factor 0.5; residence time 1.2 min, and pH in the fermentor controlled at 6.8. Assuming that half of the glucose consumed is converted to acetate, the pH change thus calculated is 0.07 units. In order to evaluate the likely fluctuation of the dissolved oxygen in the sample line, we calculated the D.O. at the point just before NMR sample tube, assuming that the silastic tubing, which has oxygen permeability about 50 x 10^{-9} $cm^2/s/cm\text{-}Hg$, is the dominant mass transfer resistance. The D.O. at this point is about 10% lower than the controlled level in the fermentor. In this calculation, we used a specific oxygen uptake rate of 5 mmol/g/h, and oxygen saturation concentration of 1.16 mmol/l. In the NMR sample tube, oxygen was further supplied by bubbling through the tube. Although it is impossible to measure dissolved oxygen level in the sample tube, direct measurement of dissolved oxygen in the sample line after exit from the NMR sample tube provides a good check

on the extent to which the dissolved oxygen concentration which cells experience when circulating through the sample loop differs from the dissolved oxygen level in the bioreactor. Accordingly, it is a reasonable approximation to assume that conditions within the NMR sample tube are essentially identical to the controlled conditions within the bioreactor. This approximation and the calculations which support its reasonability are not highly sensitive to the particular conditions employed in this experiment; therefore such an approximation is expected to be appropriate under a broad range of operating conditions.

These considerations show that the experimental system depicted in Figure 2.1 and described in detail in the Materials and Methods Section affords an opportunity for essentially on-line NMR observations of the intracellular state of growing cultures under a broad range of well-controlled and well-defined conditions. We note that, in the case of chemostat operation, we expect similar possibilities to acquire intracellular composition information using this system, employing either long acquisition times (which are feasible due to the steady-state conditions maintained in the culture for an extended period) or by employing partial cell recycle to the chemostat in order to boost cell density to high enough to allow NMR measurement on the time scale within which no substantial intracellular changes would occur and time averaged results are acceptable.

II. Observations Of The Intracellular Metabolic State of Aerobic and Anaerobic Stationary Phase Cells

As an illustration of the capability of observing directly via ^{31}P NMR changes in cellular state resulting from changes in culture conditions, an experiment was performed in which the cells were grown aerobically using the fed-batch procedure described in the Materials and Methods Section. After the cells reached stationary phase, during which the cells remain active and continue to glycolyze, spectra were taken under these aerobic conditions. Figure 2.5a displays one of these aerobic glycolyzing culture spectra. Subsequently, oxygen supply to the fermentor, the NMR sample tube, and the sample loop aeration system was replaced by nitrogen, switching all parts of the experimental system to anaerobic conditions. Figure 2.5b displays one of a reproducible series of spectra obtained under anaerobic operation.

Pronounced changes in the ^{31}P spectra are evident following the switch from aerobic to anaerobic conditions. In anaerobic conditions, the pH difference between the cytoplasm and the extracellular medium have diminished so that two distinct resonances of inorganic phosphate are no longer evident (Figure 2.5b). This decrease in intracellular pH was also manifested by the shift of the sugar phosphate chemical shift from around 4.3 ppm under aerobic conditions to around 4.0 ppm under anaerobic conditions (Figure 6). Since the extracellular pH was controlled at 6.8±0.1 in both cases, the decrease of the cytoplasmic pH under anaerobic conditions reflects a decline in pH difference across the cytoplasmic membrane under anaerobic conditions. Consistent with this decline in the proton gradient across the cytoplasmic membrane is concomitant reduction in intracellular NTP levels accompanying the shift from aerobic to anaerobic conditions. For example, the NTPβ resonance is clearly resolved under

aerobic conditions but is not evident under anaerobic operation. A quantitative comparison of NTP level was obtained by integrating peak areas for the better resolved γ-NTP peak. Although β-NDP resonates at a nearby position, a previous study indicates that it contributes less than 10% to the overall signal (8). For simplicity, we refer to the peak at -5 ppm as γ-NTP. The area ratios of γ-NTP to the reference MDP were 0.55±0.07 and 0.19±0.05 under aerobic and anaerobic conditions, respectively. Both numbers were averages of results of 12 individual spectra (such as shown in Figure 2.5) from two separate experiments. Therefore, anaerobic glycolysing cells contained a much smaller NTP pool (by 20% to 50%) than cells in aerobic conditions.

Immediately after the anaerobic spectra were taken, aerobic conditions were restored and a few aerobic spectra were taken. Those spectra were found to be similar to those in Figure 2.5a. Thus the cellular state change observed here is attributable to the availability of oxygen and not to a change in cell state due to aging of the culture.

III. Observations of Cytoplasmic pH Responses to Exogenous Acetate

Another series of experiments employed the on-line NMR system to investigate the influence of exogenous acetate on *E. coli* metabolism. When high cell densities were obtained late in the exponential phase of the fed-batch protocol, acetate was added to the culture at 3 successive time points in order to provide acetate concentrations in the medium of 5, 10, and 20 g/L following the first, second, and third additions, respectively. Figure 2.7 illustrates the three time points of acetate addition relative to the growth curve of the fed-batch culture. Although there is not a large quantity of data to resolve the precise point of transition, it was found that the specific

growth rate declines from that existing prior to acetate addition (0.18 hr^{-1}) to 0.12 hr^{-1} at some point following the third acetate addition. Reduction in metabolic activity following the third acetate addition was also manifested by a substantial increase in culture dissolved oxygen using conditions of constant air sparging and agitation in the bioreactor.

Acetate has been reported to serve as an uncoupler of membrane energetics, a process which has been directly observed here by acquiring ^{31}P NMR spectra previous to and following acetate addition (Figure 2.8). Based upon the chemical shifts of the cytoplamic and extracellular inorganic phosphate resonances, the corresponding pH values have been estimated at 3.5 minutes intervals (Figure 2.9). First, it is evident that a qualitative change has occurred in the culture after the final and highest level of acetate addition. In spectrum d in Figure 2.8, it is not possible to distinguish intracellular and extracellular inorganic phosphate resonances; only a single resonance corresponding to the overall inorganic phosphorus P_i is apparent. Therefore, the ability of the cells to maintain an energized membrane in terms of an observable proton concentration difference has failed at these high levels of external acetate. Following the first acetate addition, there is a transient decline in the transmembrane ΔpH (Figure 2.10) which is followed by a recovery of the transmembrane ΔpH over approximately 12 minutes to its value before acetate addition. After the acetate concentration in the medium has been increased to 10 g/l (after the second arrow in the Figures 2.7, 2.9 and 2.10), there is a larger transient decline in the transmembrane ΔpH and a subsequent recovery to large ΔpH values. However, the cytoplasmic pH is observed to decline somewhat throughout this interval (Figure 2.9).

2.5 DISCUSSION

The on-line NMR measurement system for studying growing cells under aerobic or anaerobic conditions which has been constructed and which is described in this work can be implemented with relatively simple and inexpensive additions to an NMR spectrometer and controlled bioreactor. The on-line system avoids the complications and possible artifacts involved in removing and concentrating cells from the bioreactor prior to measurement, while it provides data with information content comparable to that obtained in traditional, glycolyzing dense cell suspension measurements. Maintenance of the culture in a well-controlled bioreactor with dissolved oxygen monitoring and control in the sample loop ensures that the cells are maintained under well-defined conditions, permitting more rigorous studies of relationships between cell environment and cell internal state. Furthermore, new types of physiological states and experimental regimes are accessible with this on-line system. For example, as has been shown in the illustrative studies here, this NMR system can be used to observe intracellular state in exponentially growing cells. Further, at high density, time-dependent changes in cell metabolism can be followed with a resolution of approximately 3 minutes, permitting studies of intracellular transients. Furthermore, the NMR measurements can be combined with other on-line or off-line measurements to provide a more enriched data set for analyzing and interpreting cellular function.

Use of this system requires a cell culture of sufficiently high cell density to enable NMR data acquisition within a reasonable time interval. In separate experiments, we observed that cell densities of around 14 gDW/L are sufficient for ^{31}P spectra accumulation in 14 minutes with resolution and sensitivity similar to that shown in Figure 2.4b (acquisition time 8 min.). Consequently, with appropriate choice of

medium (26), some measurements can be accomplished in ordinary batch cultures. However, for consistent and convenient use of this on-line NMR system, higher cell densities are more suitable. This generally necessitates fed-batch cultivation or, in the case of continuous culture, implementation of partial cell recycle. Our experiments reported here show that fairly simple feeding strategies which do not require any feedback control can be implemented to achieve sustained exponential growth and cell densities greater than 40 gDW/l. If off-gas measurement capability exists, adjusting the feeding to maintain a respiratory quotient of one or less is a generally useful strategy for effective high cell density fed-batch culture for *E. coli* or for other types of cultivated cells (34).

Although this paper reports only experiments involving *E. coli* and only phosphorous-31 NMR measurements, the experimental system described here is general and can be applied to other organisms and to other nuclei.

2.6 ACKNOWLEDGMENTS

This work was supported by the Advanced Industrial Concepts Division of the U.S. Department of Energy and the National Science Foundation (Grant. No. BCS 891284). The LH fermentor and instrumentation were generously provided by LH Fermentation (Hayward, CA). Gerard Riedy provided important assistance in conducting early NMR experiments.

2.7 REFERENCES

1. Alam, K. Y., and Clark, D. P.1989. Anaerobic fermentation balance of *Escherichia coli* as observed by *in vivo* nuclear magnetic resonance spectroscopy. J. Bacteriol. **171**: 6213-6217.

2. Baronofsky, J. J., Schreurs, W. J. A. and Kashket, E. R. 1984. Uncoupling by acetic acid limits growth of and acetogenesis by *Clostridium thermoaceticum.* Appl. Environ. Microbiol. **48**(6): 1134-1139.

3. Bental, M., Pick, U., Avoron, M. and Degani, H. 1990. Metabolic studies with NMR spectroscopy of the alga *Dunaliella salina* trapped within agarose beads, Eur. J. Biochem. **188**, 111-116.

4. Briasco, C. A., Ross, D. A.and Robertson, C. R. 1990. A hollow-fiber reactor design for NMR studies of microbial cells, Biotechnol. Bioeng. 36: 879-886.

5. Briasco, C. A., Karel,S. F. and Robertson, C. R. 1990. Diffusional limitations of immobilized *Escherichia coli* in hollow-fiber reactors: Influence on ^{31}P NMR spectroscopy. Biotechnol. Bioeng. **36**: 887-901.

6. Campbell-Burk, S. L., Shulman, R. G. 1987. High-resolution NMR studies of *Saccharomyces cerevisiae.* Ann. Rew. Microbiol. **41**:595-616.

7. De Graaf, A. A., Wittg, R. M., Probst, U., Strohhaecker, J., Schoberth, S. M. and Sahm, H. 1992. Continuous-flow NMR bioreactor for *in vivo* studies of microbial cell suspensions with low biomass concentrations, J. Magnetic Resonance **98:**654-659

8. den Hollander, J. A., Ugurbil, K., Brown, T. R. and Shulman, R. G. 1981. Phosphorus-31 nuclear magnetic resonance studies of the effect of oxygen upon glycolysis in Yeast. Biochemistry. **20**: 5871-5880.

9. den Hollander, J. A., Ugurbil, K. and Shulman, R. G. 1986. ^{31}P and ^{13}C studies of intermediates of aerobic and anaerobic glycolysis in *Saccharomyces cerevisiae*. Biochemistry. **25**: 212-219.

10. Diaz-Ricci, J. C., Hitzmann, B., Rinas, U. and Bailey, J. E. 1990. Comparative Studies of glucose catabolism by *Escherichia coli* grown in a complex medium under aerobic and anaerobic conditions. Biotechnol. Prog., **6**(5): 326-332.

11. Diaz-Ricci, J. C. Hitzmann, B., Bailey, J. E. 1991. In vivo NMR analysis of the influence of pyruvate decarboxylase and alcohol dehydrogenase of *Zymomonas mobilis* on the anaerobic metabolism of *Escherichia coli*. Biotechnol. Prog., **7**: 305-310.

12. Fernandez, E. J. and Clark D. S. 1986. NMR spectroscopy: a non-invasive tool for studying intracellular processes. Enzyme Microb. Technol. **9**:259-271.

13. Fernandez, E. J., Marcuso, A. and Clark D. S. 1988. NMR spectroscopy studies of hybridoma metabolism in a simple membrane reactor. Biotechnol. Prog. **4**(3): 173-183.

14. Fernandez, E. J., Marcuso, A., Murphy, M. K., Blanch, H. W. and Clark D. S. 1990. Nuclear magnetic resonance methods for observing the intracellular environment of mammalian cells. Ann. N. Y. Acad. Sci., **589:**458-475.

15. Galazzo, J. L. and Bailey, J. E. 1989. *In vivo* Nuclear magnetic resonance analysis of immobilization effects on glucose metabolism of yeast *Saccharomyces cerevisiae,* Biotechnol. and Bioeng. **33,** 1283-1289.

16. Gillies, R. J., MacKenzie, N. E. and Dale, B. E. 1989. Analyses of bioreactor performance by nuclear magnetic resonance spectroscopy. Biotechnology. **7**:50-54.

17. Ginzburg, M., Ratcliffe, R. G. and Southon, T. E. 1988. Phosphorus metabolism and intracellular pH in the halotolerant alga *Dunaliella parva* studied by ^{31}P NMR, Biochim. Biophys.Acta **969**: 225-235.

18. Katz, A., Bental, M., Degani, H. and Avron, M. 1991. In vivo pH regulation by a Na^+/H^+ antiporter in the halotorant alga *Dunaliella salina,* Plant Physiol. **96**, 110-115.

19. Kramer, H. W. and Bailey, J. E. 1991. Mass transfer characterization of an airlift probe for oxygenating and mixing cell suspensions in an NMR spectrometer. Biotechnol. Bioeng.**37**: 205-209.

20. Laws, J.O., Stickland, L.H. 1963. The effect of washing procedures on the phosphate metabolism of *Ehrlich ascites* tumor cells. Biochem J. **87**: 520-525.

21.Meehan, A.J., Eskey, C.J., Koretsky, A.P.and Domach, M.M.1992. Cultivator for NMR studies of suspended cell cultures. Biotechnol. Bioeng.**40:**1427-1434.

22. Mitsumori, F., Rees, D., Brindle, K. M., Rsdda, G. K. and Campbell, I. D. 1988. ^{31}P-NMR saturation transfer studies of aerobic *Escherichia coli* cells, Biochim. Biophys. Acta, **969:** 185-193.

23. Navon, G., Shulman, R. G., Yamane, T., Eccleshall, T. R., Lam, K., Baronofsky, J. J. and Marmuur, J. 1979. Phosphorus-31 nuclear magnetic resonance studies of wild-type and glycolytic pathway mutants of *Saccharomyces cerevisiae*. Biochemistry. **18**(21):4487-4499.

24. Navon, G, Ogawa, S., Shulman, R. G. and Yamane, T. 1977. High-resolution ^{31}P nuclear magnetic resonance studies of metabolism in aerobic *Escherichia coli* cells, Proc. Natl. Acad. Sci. USA .**74**(3): 888-891.

25. Oren-Shamir, M., Avron, M. and Degani. H. 1988. In vivo NMR studies of the alga *Dunaliella salina* embedded in beads, FEBS Lett. **233**(1), 124-128.

26. Pendse, G. J., Riedy, G. and Bailey, J. E. 1991. NMR Spectroscopy of recombinant Chinese hamster ovary (CHO) cells in a packed bed reactor.Biotechnology Techniques. **5**(3): 193-198.

27. Reiling, H. E., Laurila, H. and Fiechter, A. 1985. Mass culture of *Escherichia coli:* Medium development for low and high density cultivation of *Escherichia coli* B/r in minimal and complex media. Journal of Biotechnology. **2**: 191-206.

28. Riesenberg, D., Schultz, V., Knorre,W. A., Pohl, H._d., Korz, D., E. A. Sanders, E. A., Rob, A. and Deckwer, W._D. 1991. High cell density cultivation of *Escherichia coli* at controlled specific growth rate, Journal of Biotechnology, **20:** 17-28.

29. Roberts, J. K. M. and Jardetzky, O. 1981. Monitoring of cellular metabolism by NMR. Biochim. Biophys. Acta. **639**:53-76.

30. Santos, H., Pereira, H., Crespo, J., Moura, M., Carrondo, M. and Xavier, A. 1989.In vivo NMR studies of propionic-acid fermentation by *Propionibacterium acidi-Propionici.* p.685-688. In: J.A.M., de Bont, J. Visser and J. Tramper (ed.), Physiology of Immobilized Cells, Proceedings of an International Symposium held at Wageningen, The Netherlands, 10-13 December 1989. Elsevier Science Publishers, Amsterdam.

31. Shanks, J. V. and Bailey, J. E. 1988. Estimation of intracellular sugar phosphate concentrations in *Saccharomyces cerevisiae* using 31P nuclear magnetic resonance spectroscopy. Biotechnol. Bioeng. **32**: 1138-1152.

32. Shanks, J. V., Bailey, J. E. 1990. Comparison of wild-type and reg1 mutant *Saccharomyces cerevisiae* metabolic levels during glucose and galactose metabolism using 31P NMR. Biotechnol. Bioeng. **35**: 395-407

33. Ugurbil, K., Rottenberg, H., Glynn, P. and Shulman, R. G. 1982. Phosphorus-31 nuclear magnetic resonance studies of bioenergetics in wild-type and adenosinetriphosphatase (1-) *Escherichia coli* cells. Biochemistry. **21**:1068-1075.

34. Wang, H. Y., Cooney, C. L. and Wang, D. I. C. 1979.Computer Control of bakers' yeast production. Biotechnol. Bioeng. **21**: 975-995.

2.8 TABLES

Table 2.1. Composition of RZ medium

(components of the trace element solution are detailed in the Materials and Methods)

Components	concentration g/l
KH_2PO_4	2.98
$(NH)_2HPO_4$	1.90
$MgSO_4.7H_2O$	1.46
$FeSO_4.7H_2O$	64.2(mg)
D_2O	5%
Trace elements	10 ml/l
Glucose	15

2.9 FIGURES

Figure caption

Figure 2.1 A simplified schematic diagram of the on-line NMR system.

Figure 2.2 NMR sample tube build-up (units in centimeters).

Figure 2.3 Growth profile of a typical *E. coli* fed-batch cultivation in RZ medium.

Figure 2.4 ^{31}P NMR spectra acquired during aerobic exponential growth of *E.coli* MG1655. The spectra were taken when cell density was between 22.5 and 27 gDW/l. a. NS (number of scans; the corresponding acquisition time follows each scan number in parentheses): 1200 (14 min.), b. NS: 700 (8.2 min.), c. NS: 250 (2.9 min.). Spectra were obtained using 40^{o} pulse and a relaxation delay of 0.2 s, other parameters as in the Materials and Methods. Abbreviations: MDP: methylene diphosphonic acid; SP: sugar phosphate; P_i^{cyt}: intracellular inorganic phosphate; P_i^{ex}: extracellular inorganic phosphate; NTP: nucleoside triphosphate; NDP: nucleoside diphosphate; NAD(H): nicotinamide adenine dinucleotide; UDPG: uridinediphosphoglucose.

Figure 2.5 ^{31}P spectra during aerobic and anaerobic glucose glycolysis of *E.coli* in early stationary phase. a: aerobic spectrum ; b: anaerobic spectrum, both acquired at a cell density of about 45 gDW /l. NMR acquisition parameters were the same as in the caption of Figure 2 except here NS is 300.

Figure 2.6 Chemical shifts of the sugar-phosphate resonances under aerobic and anaerobic conditions. All experimental conditions are as described in the caption of Figure 2.4. (•) anaerobic, time zero corresponds 10 minutes after switch from aerobic condition; (○) aerobic, time zero corresponds the sart of NMR acqusition, with each data point corresponds the end of each individual spectrum which is accumulated in the period of approximately 3 minutes.

Figure 2.7 Growth profile of the fed-batch *E. coli* culture with external addition of acetate at the times indicated as arrows. After the first, second, and third additions, the medium acetate concentrations were approximately 5, 10, and 20 g/l, respectively.

Figure 2.8 P_i region of ^{31}P NMR spectra before and after external acetate addition. a. Prior to acetate addition, b. Following the first acetate addition to a final acetate concentration of about 5 g/l, c. After the second acetate addition to a final acetate concentration of about 10 g/l, d. Subsequent to

the third acetate addition to a final acetate concentration of about 20 g/l. NMR acquisition parameters are the same as indicated in the caption of Figure 2.4 except here NS is 300.

Figure 2.9 pH(cyt) and pH(ex) before and after acetate additions. (•) pH(cyt), (○) pH(ex).

Figure 2.10 pH difference across the cytoplasmic membrane before and after acetate additions.

Figure 2.1

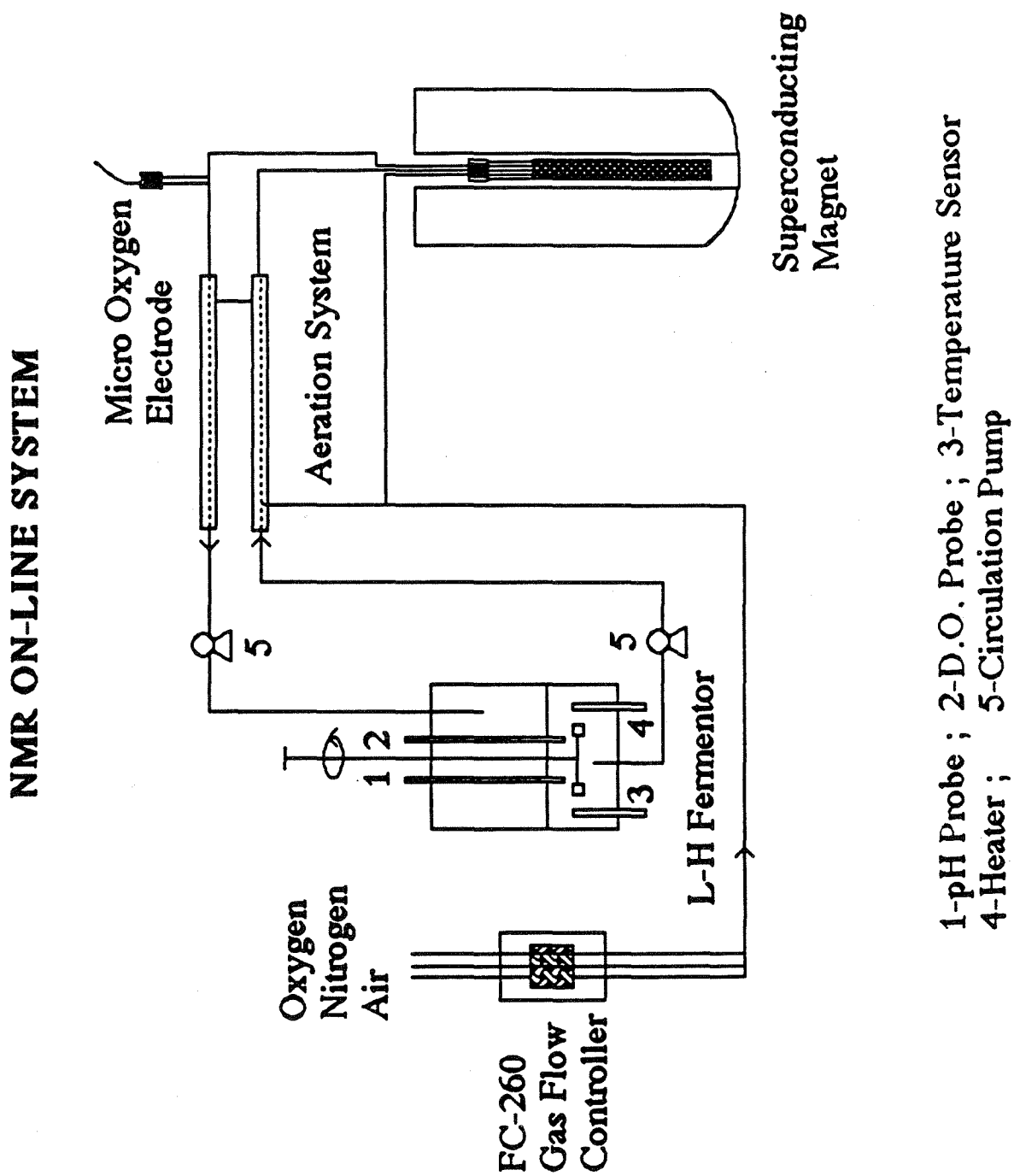
NMR ON-LINE SYSTEM
Micro Oxygen Electrode
Aeration System
Superconducting Magnet
5
5
1 2
3
4
Oxygen
Nitrogen
Air
FC-260 Gas Flow Controller
L-H Fermentor
1-pH Probe ; 2-D.O. Probe ; 3-Temperature Sensor
4-Heater ; 5-Circulation Pump

Figure 2.2

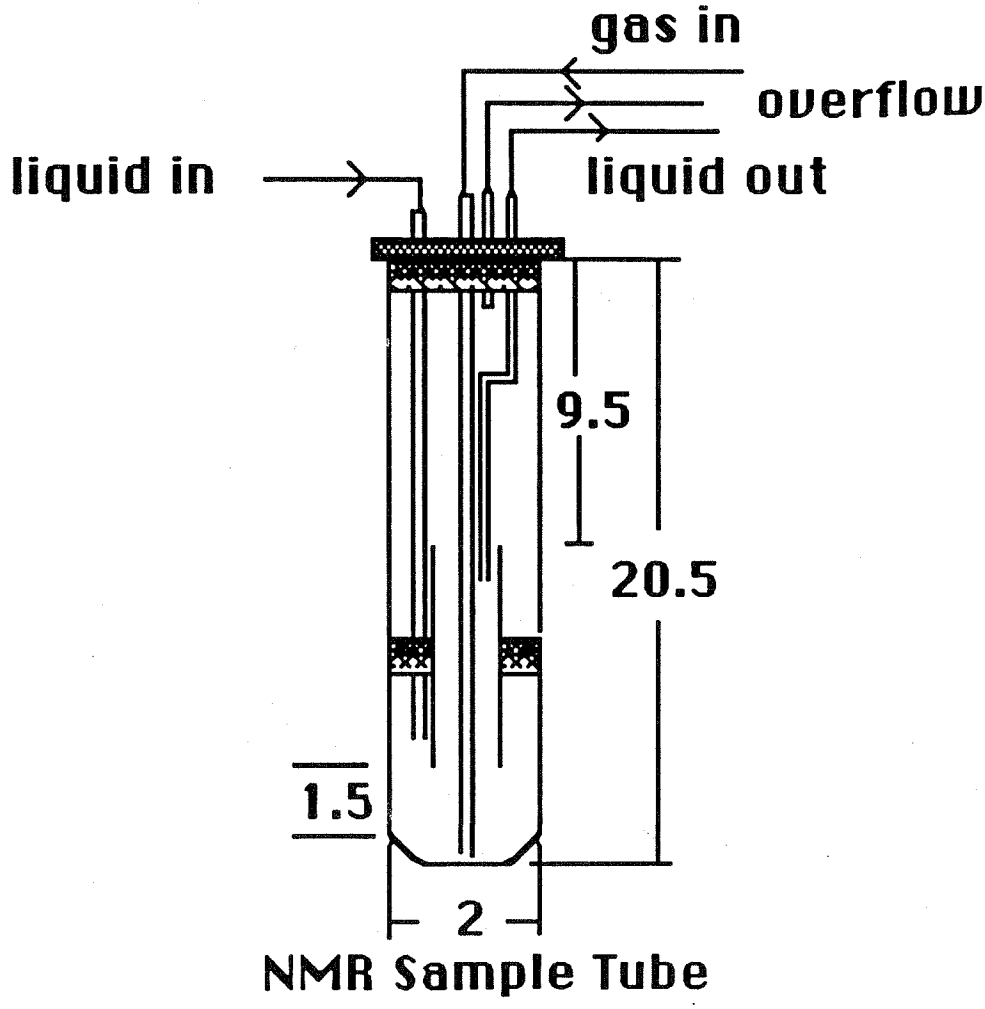
gas in
overflow
liquid in
liquid out
9.5
20.5
1.5
2
NMR Sample Tube

Figure 2.3

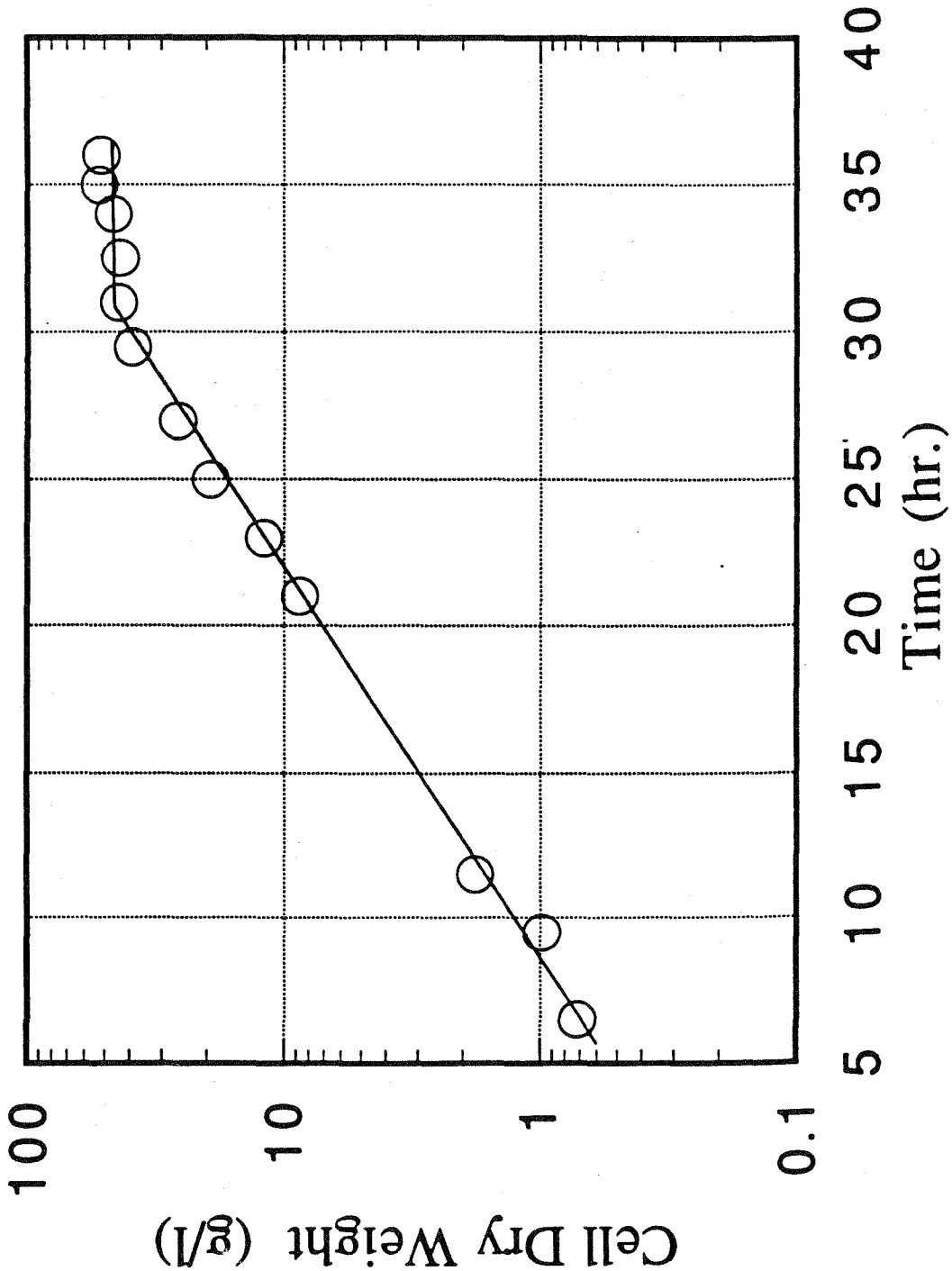

Figure 2.4

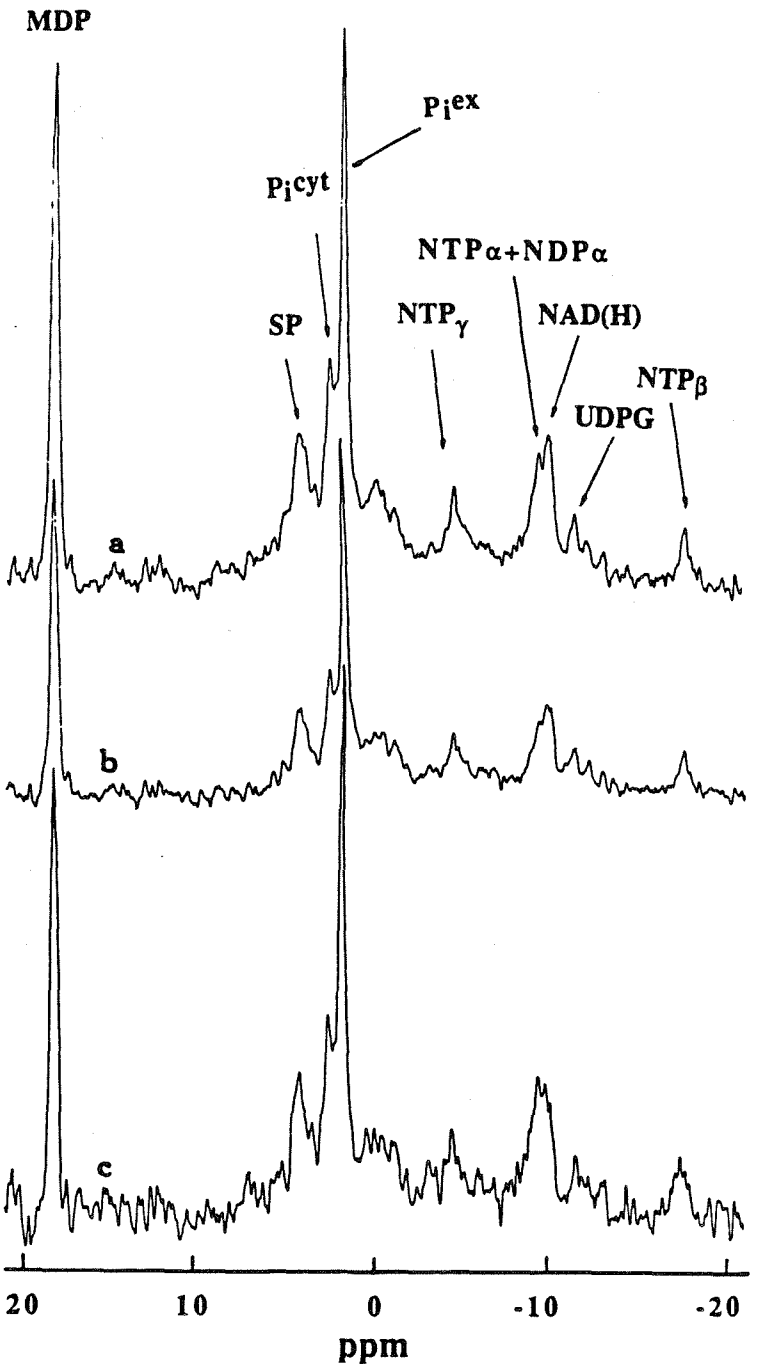
MDP
Pi ex
Pi cyt
NTPα+NDPα
SP
NTPγ
NAD(H)
NTPβ
UDPG
a
b
c
20
10
0
-10
-20
ppm

Figure 2.5

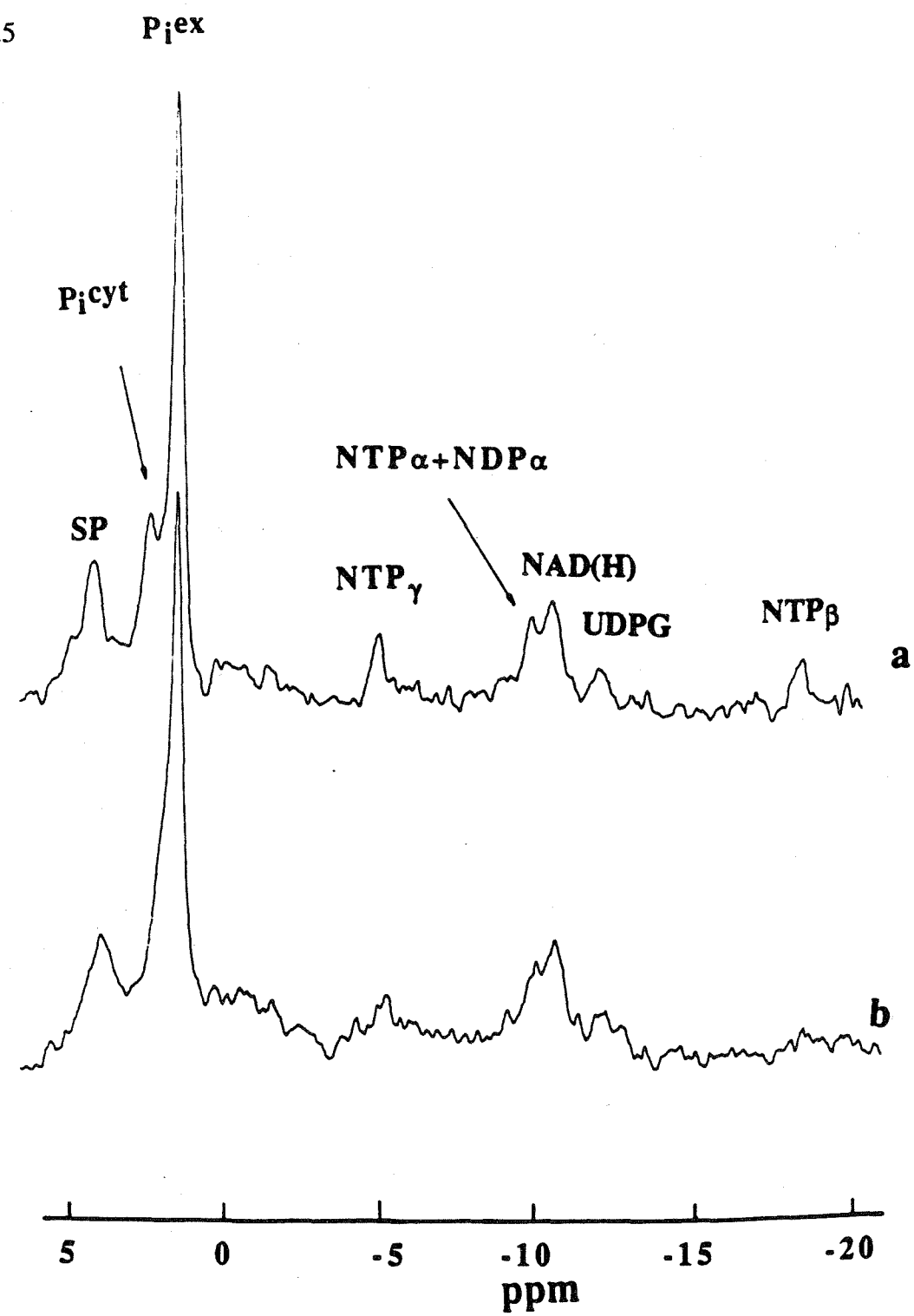

Figure 2.6

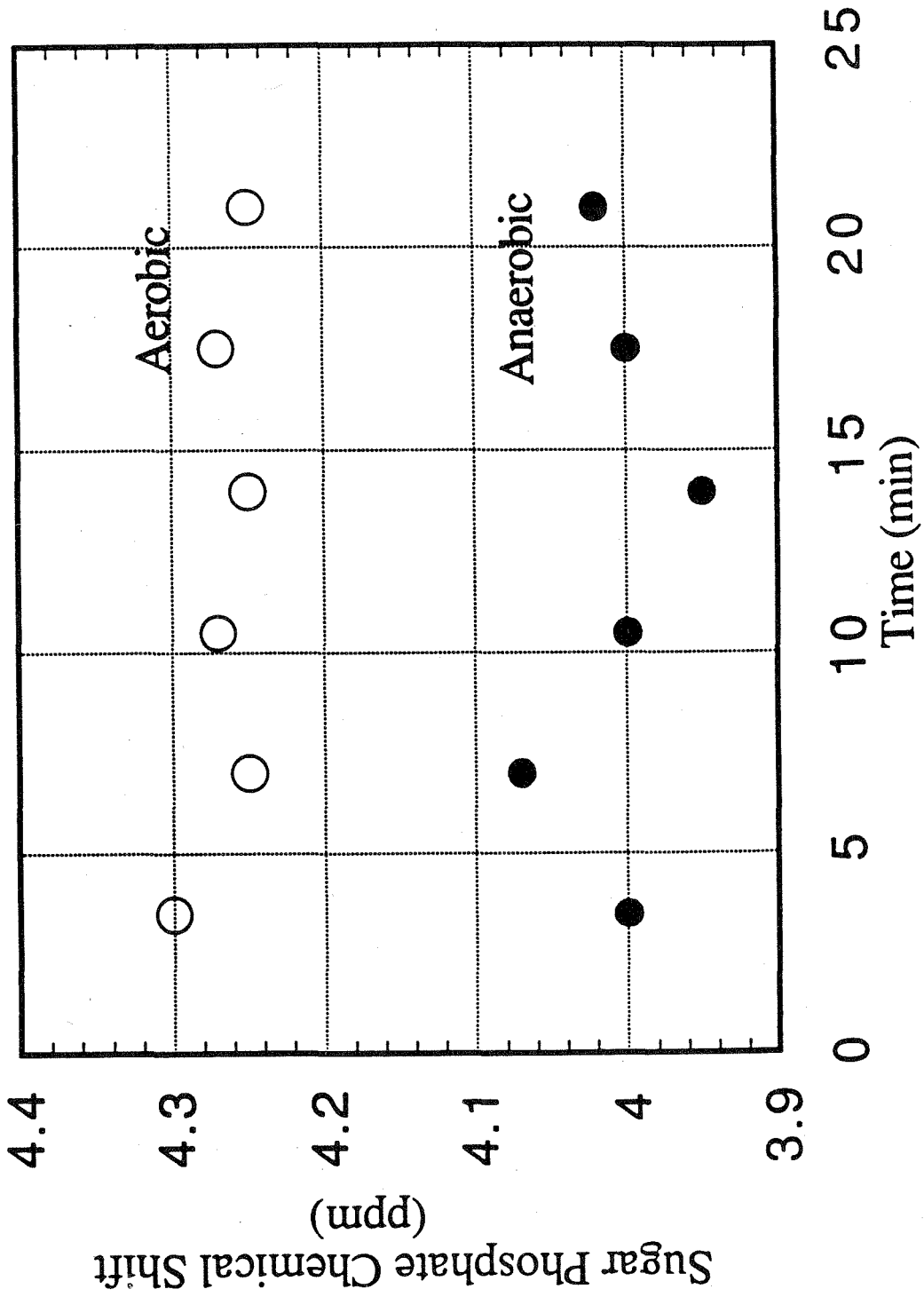
Sugar Phosphate Chemical Shift
(ppm)
4.4
4.3
4.2
4.1
4
3.9
0
5
10
15
20
25
Time (min)
Aerobic
Anaerobic

Figure 2.7

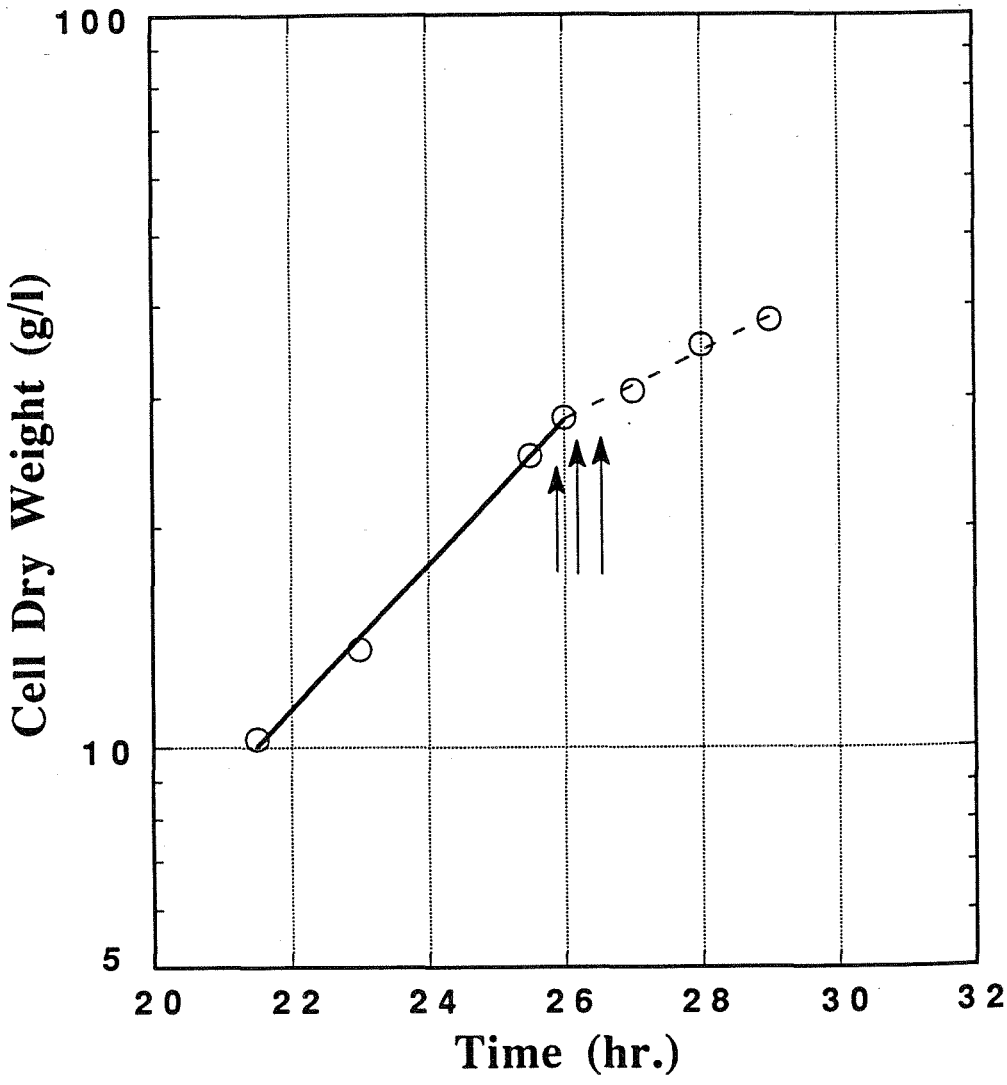

Figure 2.8

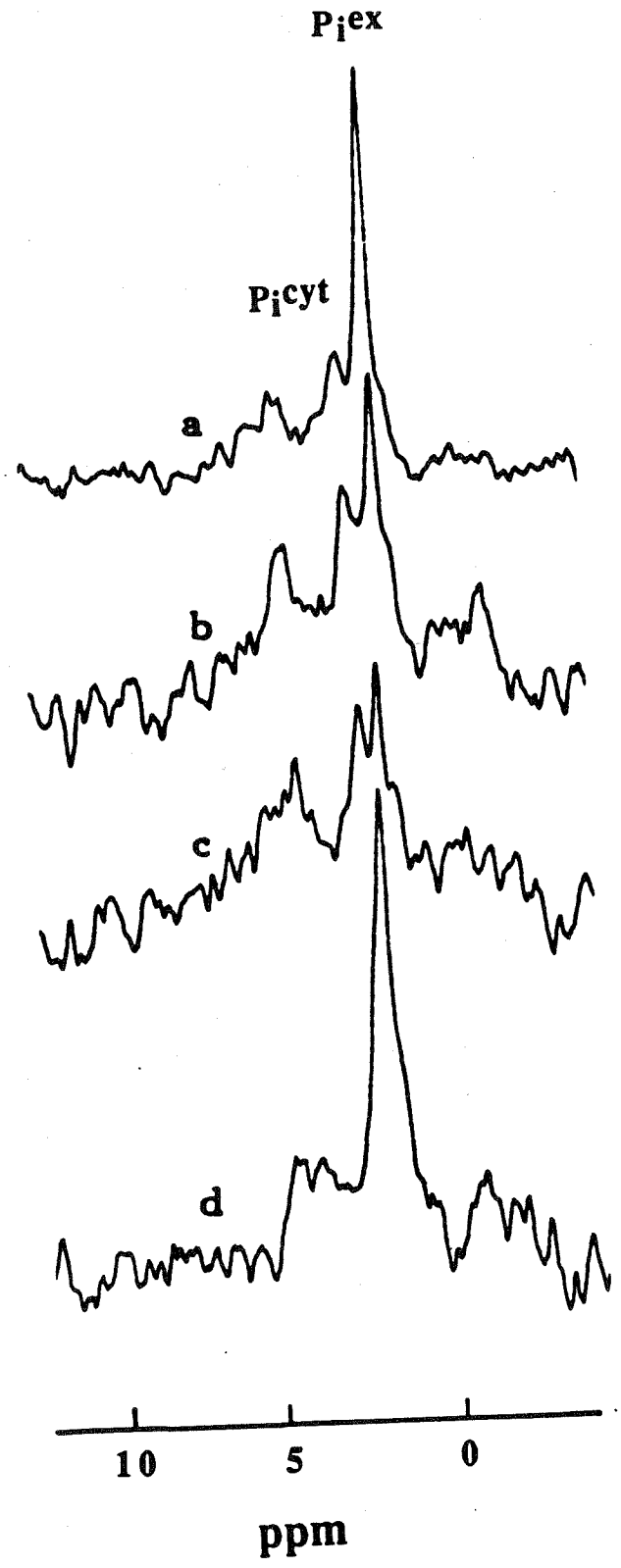

Figure 2.9

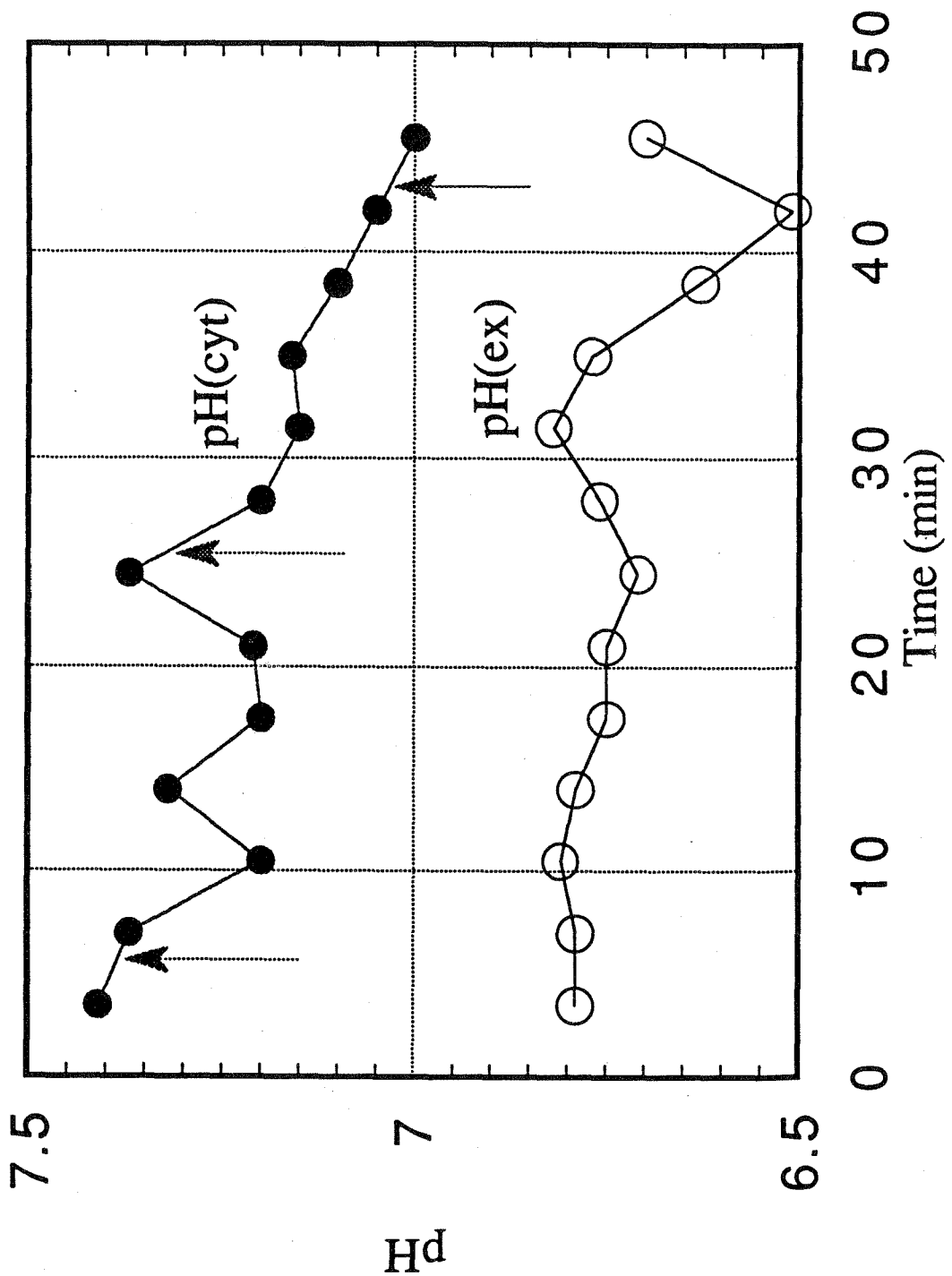

Figure 2.10

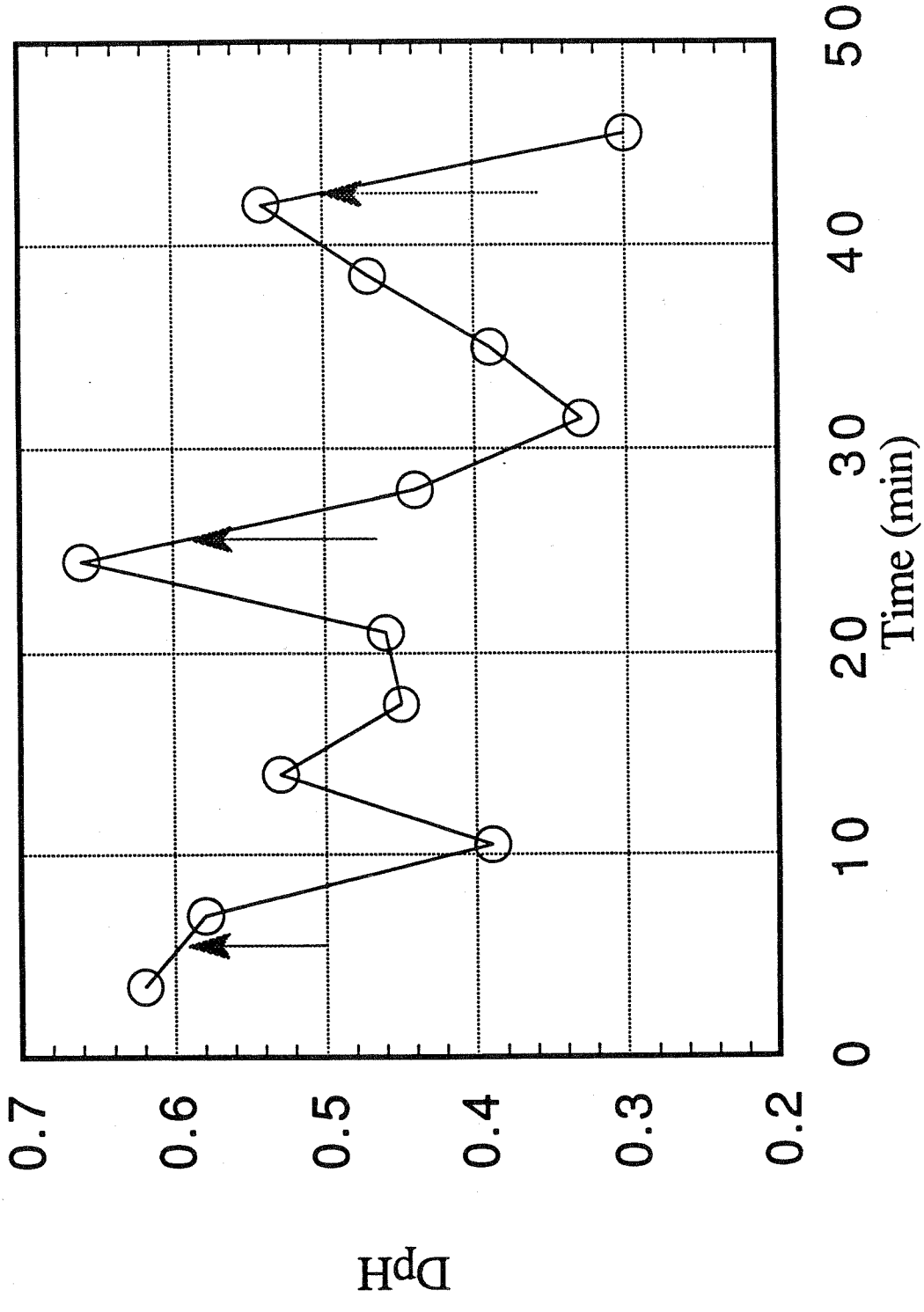

Chapter 3

The Energetic Effect of Expressing *Vitreoscilla* Hemoglobin (VHb) In *Escherichia coli:* An On-line ^{31}P NMR And A Saturation Transfer Study

Source: Chen, R. and Bailey, J. E. Biotechnol. Prog. In Press

3.1 ABSTRACT

A newly developed on-line ^{31}P NMR system has been used to investigate the effect of *Vitreoscilla* hemoglobin (VHb) expression on the steady-state level of ATP in *E. coli* under oxygen-limited conditions. The VHb-expressing strain GRO21 exhibited higher growth rate on a minimal fed-batch medium after the onset of oxygen-limitation and maintained the same level of ATP pool and transmembrane ΔpH as the slower growing wild-type strain MG1655, indicating that the net ATP accumulation rate (the rate at which ATP increases per unit volume of culture per unit time) was enhanced in VHb-expressing strain. Further direct evidence of enhanced flux of Pi-ATP (catalyzed by ATPase) in GRO21 was obtained in a saturation transfer study on respiring cells. VHb-expressing cells respiring on succinate exhibited a Pi-ATP flux $30\pm5\%$ higher than that of an otherwise isogenic strain which did not express VHb.

3.2 INTRODUCTION

Vitreoscilla is a gram negative obligate aerobe, living in low-oxygen environments such as stagnant ponds and decaying vegetable matter. One possible element of a genetic strategy by which species of this genus survive under oxygen-limiting conditions is synthesis of an intracellular hemoglobin (VHb) molecule, homodimeric with a polypeptide subunit molecular weight of 15,775 (Webster, 1988). The observation in *Vitreoscilla* that hemoglobin is only present when the dissolved oxygen in the growth medium falls below a threshold level implies that the relatively large amount of hemoglobin synthesized in response to hypoxic conditions is used to sustain cell growth, though at much lower growth rate. However, the mechanism by which the hemoglobin interacts with respiratory metabolism is yet to be discovered.

This naturally evolved genetic strategy has been extended to other organisms using recombinant DNA techniques. The VHb gene (*vhb*) was first cloned and expressed in *E. coli*, and the consequences for oxygen-limited growth were assessed (Khosla and Bailey, 1988a, 1988b). Strains engineered to express VHb exhibited enhanced specific growth rate as well as increased final cell density (Khosla and Bailey, 1988a). Intracellular expression of VHb increased overall protein synthesis about 20% and final activity of cloned chloramphenicol acetyltransferase about 30% (Khosla et al. 1990); expressing VHb improves the synthesis of plasmid-encoded α-amylase by *E. coli* up to 3.3 fold (Khosravi et al. 1990). Studies on location of VHb in *E. coli* showed that about half of the VHb synthesized is partitioned to the periplasm (Khosla and Bailey, 1989a).

The present work investigates the growth-promoting effect of VHb by probing the energetic consequences of expressing VHb. ^{31}P NMR is informative in revealing the energetic state of the cell, since information is obtained on ATP levels, cytoplasmic pH and transmembrane ΔpH. The recently developed on-line NMR system (Chen and Bailey, 1993, or Chap. 2), which extends NMR measurements to growing cell cultures, is particularly useful in studying the growth-enhancing effect of bacterial hemoglobin. Besides its non-invasive character, NMR also offers the possibility of measuring kinetics of some key enzyme-catalyzed reactions *in vivo*. In particular, the NMR saturation transfer technique has been used to measure kinetics of ATPase in microbial cells such as *E. coli* (Brown et al. 1977; Mitsumori et al. 1988), yeast (Alger et al. 1982; Brindle, 1988) and intact mammalian kidney (Shine et al. 1990). Different conclusions concerning whether or not the saturation transfer-visible flux should be attributed to ATPase were reported from two studies conducted on *E. coli* cells (Brown et al. 1977; Mitsumori et al. 1988). In the present study, saturation transfer experiments were conducted when cells respired on exogeneous succinate. Under this condition, it is expected that ATPase is the dominant ATP synthesis pathway. Further, the specific inhibitors dicyclohexylcarbodiimide (DCCD) and iodoacetic acid (IAA) were used to show that the flux measured here by the saturation transfer technique is attributable to the ATPase.

3.3 MATERIALS AND METHODS

Strains

E. coli strain MG1655, an unmutagenized wild-type K-12 strain, and GRO21, a derivative of MG1655 with one copy of the *vhb* gene integrated into its chromosome (Khosla and Bailey, 1989b), were used in this study. Transcription of the *vhb* gene in GRO21 is under control of an oxygen-regulated promoter. VHb is maximally synthesized when the dissolved oxygen level is below 5% of air saturation.

On-line NMR Study

The recently developed on-line NMR system, which connects a NMR spectrometer with a well-controlled fermentor through a circulation loop and thus permits direct circulation of growing cell culture to the NMR sample chamber for on-line NMR measurement (for details, see Chen and Bailey, 1993 or Chap. 2), was used here to measure steady state concentrations of ATP for both strains. Growth medium and fed-batch growth condition are the same as described elsewhere (Chen and Bailey, 1993 or Chap. 2), except the agitation speed and air supply to the fermentor were fixed at 500 rpm and 0.5 l/l/min respectively, in order to generate oxygen-limited growth conditions under which VHb is expressed.

Saturation Transfer Study

For a saturation transfer experiment a pair of spectra is needed to obtain a difference spectrum (γ-ATP non-saturated spectrum minus γ-ATP saturated one) from which kinetic information can be deduced. Since only a very small difference exists in

the γ-ATP saturated spectrum and γ-ATP non-saturated spectrum (Pi in the difference spectrum is only about 10% of that in the non-saturated spectrum), a large number of scans is required to obtain a difference spectrum with acceptable signal to noise ratio. Additionally, more time is required to implement two trains of pulses in the Dante sequence for selective saturation and to toggle between two saturation frequencies. Thus, even for a high cell density sample (over 100 gDW/l), the time required for a difference spectrum is on the scale of an hour whereas a normal spectrum can be obtained on the scale of minutes.

In order to reduce acquisition times for saturation transfer studies to intervals within which cellular state remains approximately constant, the saturation transfer experiment were done on highly concentrated (ca 100gDW/l) non-growing cell samples. Therefore a traditional growth-harvest-resuspension protocol was used here.

Growth: *E. coli* cells were grown in a 2-liter shaker flask in 1 liter of growth medium consisting of: 5 g/l yeast extract, 3.0 mM $(NH_4)_2SO_4$, 41.1 mM KH_2PO_4, 6.1 mM K_2HPO_4, 1mM $MgSO_4$, 0.05mM $CaCl_2$, 0.02mM $FeCl_3$, 1 ml/l trace solution (8.3mM Na_2MoO_4, 7.6mM $CuSO_4$, 8 mM H_3BO_4), pH adjusted to 7.0 with 4N NaOH. The cultivation of *E. coli* was carried out at 37°C and 275 rpm in an INNOVA 4000 rotary shaker (New Brunswick Scientific). Succinate at an initial concentration of 50mM was used as sole carbon source. A cultivation time of 14 hours was chosen so that cell density toward the end of the cultivation was sufficiently high to cause oxygen limitation and hemoglobin was expressed in GRO21. VHb expression as a consequence of this growth protocol was verified by CO difference spectrum analysis for hemoglobin activity (Webster and Liu, 1974).

^{31}P NMR sample preparation: Cell broth was harvested by centrifugation at 7000 rpm using a JA-14 rotor for 5 minutes. This was followed by two washings using ice cold buffer containing: 100 mM Pipes (1,4-piperazinediethanesulfonic acid), 50 mM MES (2-[N-Morpholino]ethanesulfonic acid), 10mM Na_2HPO_4, 10mM KH_2PO_4, 40mM NaCl, pH adjusted to 7.0. Afterward, cells were suspended in a buffer which is essentially the same as the washing buffer, except with lowered inorganic phosphate concentration (containing 2mM Na_2HPO_4, 2mM KH_2PO_4, 60 mM NaCl) at pH 6.5. The density of the sample cell suspension was approximately 100gDW/l [(grams dry weight)/l]. More accurate dry weight values, required to normalize measured fluxes, were measured by transferring the cell suspension after each experiment to a pre-weighed aluminum plate which was dried in a 105°C oven to constant weight. A 3 ml aliquot of the sample suspension was placed in a 10 mm (diameter) NMR sample tube, 0.5 ml D_2O was added as lock signal, and a sealed capillary with 0.1M methylene diphosphonic acid (MDP) was placed in the sample tube to provide a chemical shift and concentration reference. MDP resonates at 18.6 ppm downfield of 85% phosphoric acid which is assigned as 0 ppm.

^{31}P NMR Operation : Saturation transfer studies were performed on a Bruker AM300 NMR spectrometer in the Fourier transform mode at a frequency of 121.5 MHz. A 10 mm NMR broadband probe was used. This instrument was modified and the necessary hardware was incorporated so that the instrument could generate two types of pulses. A selective pulse sequence, namely, the Dante sequence, was used to saturate the γ-ATP peak. Blocks of 64 FIDs (free induction decays) were alternately collected with the saturation frequency at the γ-ATP signal and at a point of equal frequency distance to

the low field side of the P_i resonance. In this way the spectra were obtained essentially simultaneously and no artifacts were observed when this saturation effect was thus operated. Other acquisition parameters are indicated in the figure captions.

Aeration: The cell concentration in the saturation transfer experiments was sufficiently high to generate oxygen-limited conditions. A double oxygenation system within the NMR sample chamber was used, which consisted of one oxygen supply of 22.5 ml/min bubbling through the bottom of the sample and a second oxygen supply of 50 ml/min, 5mm below the surface of the sample. The flow rates were controlled by an FC-260 multichannel gas flow controller (Tylan Corporation, Torrance, CA). In a separate experiment outside the NMR magnetic field, an oxygen microelectrode was inserted into a 10 mm NMR sample tube, which contained the same amount of concentrated cell suspension prepared as detailed above. 10 minutes after the addition of 200µl of 1M succinate, the dissolved oxygen (D.O.) was found to be below the detection limit of the microelectrode for about 2 hours, indicating ongoing succinate utilization. The saturation transfer experiments were conducted during this interval.

Pi-ATP flux comparison: Saturation of the γ-ATP peak by selective pulses causes a decrease of the magnetization of the intracellular inorganic phosphate P_i, the extent of the decrease is given by a function of k:

$$\Delta M/Mo = k(1/T_1+k)^{-1} \qquad 3.1$$

where k is the rate constant of the first-order exchange between P_i and γ-ATP; T_1 is the intrinsic spin-lattice relaxation time of the P_i (in the absence of the exchange), and M_o is the non-disturbed steady state magnetization of the P_i (Brown et al, 1977; Mitsumori et al, 1988).

The Pi-ATP flux can be written as :

$$M_O\, k = M_O \Delta M (M_O - \Delta M)^{-1} T_1^{-1}. \qquad 3.2$$

Since ΔM never exceeds more than 10% of M_O, equation 2 can be simplified to :

$$M_O\, k = \Delta M T_1^{-1}. \qquad 3.3$$

Since M_O and T_1 are not changed by the presence of the VHb (T_1 for both strains are estimated to be approximately 0.4 s from our separate T_1 experiments, in which DCCD-treated cell samples were used in order to eliminate chemical exchange and obtain the intrinsic T_1), the ATP fluxes with and without VHb can be compared directly using ΔM values for the two cases. To correct for fluctuations in the noise level of different experiments, the ratio of ΔM to the reference MDP is used in this study.

It is important to note that, although the resonance at 5 ppm, labeled NTPγ, arises from the total nucleotide triphosphate pool, approximately 50% of this is ATP (Lowry et al. 1971; Navon et al. 1977). As an approximation, this peak is referred to as γ-ATP.

3.4 RESULTS

MG1655 and GRO21 cells were grown in a minimal medium in a fed-batch mode with fixed air supply and agitation speed as detailed in the Materials and Methods. Both strains showed the same growth features for the first few hours, but, as the culture grew to higher cell density, oxygen became limiting and the D.O. was below the probe detection limit. Accordingly, a significant amount of hemoglobin was synthesized in the VHb-expressing strain, GRO21, as judged by the slight pink tint of the cell paste and CO binding spectra using the method described by Webster and Liu

(1974). Specific growth rates of both GRO21 and MG1655 were reduced at this point of the cultivation because of oxygen limitation. Subsequently, the two growth profiles differed, with GRO21 exhibiting the higher specific growth rate as shown in Figure 3.1. The specific growth rates during oxygen-limited growth were estimated as $0.064 \pm 0.004\ h^{-1}$ for GRO21 and $0.038 \pm 0.004\ h^{-1}$ for MG1655. One possible explanation of this growth-promoting effect of VHb is a different energetic state of VHb expressing cells. This speculation was investigated by implementing ^{31}P NMR measurements on these two isogenic strains.

When the cell density was approximately 15 g/l, the cell culture began to circulate in a newly developed on-line NMR system, which allows NMR measurement on a growing cell culture (The detailed configuration of the system and operation are described in Chen and Bailey, 1993 or Chap. 2). A typical ^{31}P NMR spectrum is shown in Figure 3.2. The spectrum allows estimation of cytoplasmic pH, transmembrane ΔpH, and the sizes of the NTP, intracellular inorganic phosphate, sugar phosphate (S-P), NAD(H) and UDPG pools in GRO21 relative to those in MG1655. No significant differences were found between the two strains in terms of NTP pool (judged by both NTPβ and NTPγ peaks), Pi, cytoplasmic pH and transmembrane ΔpH. No significant differences were found in other ^{31}P NMR accessible parameters such as S-P, NAD(H) and UDPG pool sizes, when both strains were observed by NMR during oxygen-limited growth.

These data can be interpreted with the aid of a quasi-steady state ATP balance for growing cells, which can be stated by the following equation :

Net rate of ATP accumulation = rate of ATP dilution by growth 3.4

or:

$$r_{fATP} = \mu[ATP] \qquad 3.5$$

where r_{fATP} denotes the net ATP accumulation rate (the rate at which ATP increases per unit volume of culture per unit time in units of moles ATP per liter of cells per hour), μ is the specific growth rate (h^{-1}) and [ATP] is the steady-state intracellular ATP concentration (moles ATP per liter cells).

Therefore, the ratio of the rates of ATP accumulation in the strains with and without VHb can be calculated as:

$$r_{fATP}(GRO21)/r_{fATP}(MG1655)$$
$$=\mu(GRO21)[ATP\ (GRO21)]/\mu(MG1655)\ [ATP\ (MG1655)]$$
$$=1.68. \qquad 3.6$$

Therefore, the presence of VHb results in an increase in the net rate of ATP accumulation of more than 65% relative to the wild-type strain MG1655 in oxygen-limited growing cultures.

Direct observation of the flux of Pi-ATP can be obtained for oxygen-limited, nongrowing cultures using the saturation transfer NMR technique. Figure 3.3 shows a few spectra of GRO21 in saturation transfer experiments on a non-growing high density sample under oxygen-limited conditions. Figure 3.3a was obtained using a normal pulse sequence with 640 scans. Figures 3.3b and 3.3c were collected using the Dante sequence; arrows indicate the points of application of the saturation frequency. These two spectra are sums of 3840 scans, approximately 1.5 hour total acquisition time. Figure 3.3d is the difference spectrum of 3.3b-3.3c. Two peaks appear in Figure 3.3d, which correspond to intracellular Pi and γ-ATP, respectively. As explained in the Materials and Methods, the intracellular Pi peak in the difference spectrum is a measure of the Pi-ATP flux. The same methodology was applied to the wild-type MG1655

strain employing identical experimental conditions as used for GRO21(spectra not shown).

Interpretation of these data depends on existence of approximately the same intracellular Pi levels in MG1655 and GRO21. This approximation is supported by the following observations. The on-line measurement and spectra taken during the first 45 minutes for the dense non-growing sample using a normal pulse sequence (see Figure 3.2 and Figure 3.3a) do not show significant differences in intracellular Pi content in the two strains. Since the intracellular Pi appeared in these spectra as a shoulder of the extracellular Pi peak, the area of the intracellular Pi peak was estimated based on deconvolution using NMRONE software.

For internal calibration, the ratio of areas of the intracellular Pi peak in the difference spectrum to the MDP in the spectrum (γ-ATP non-saturated) was calculated for GRO21 and MG1655 for a number of experiments. This ratio was further normalized to the dry weight of the cell sample to correct for any differences in the sample cell density. The ratios were $(7.7\pm0.3)\times10^{-4}$ for GRO21 and $(6.0\pm0.3)\times10^{-4}$ for MG1655. The number of experiments for each strains was six. From this result, we can see that in GRO21 the flux of Pi-ATP is $30\pm5\%$ higher than that in MG1655 under oxygen-limited conditions.

To clarify that the Pi-ATP flux measured by saturation transfer is a result of ATPase activity, and not from activities of the glycolytic enzymes glyceraldehyde-3-phosphate dehydrogenase (GAPDH) and phosphoglycerate kinase (PGK) as claimed by Mitsumori et al. (1988), the specific inhibitors DCCD for ATPase and iodoacetic acid for GAPDH were used in additional experiments. It is important to note that, in contrast to the experiments of Mitsumori et al. (1988), DCCD was added to cells

utilizing succinate with a normal ATP level; no addition of glucose, which could easily alter ATP metabolism significantly, was necessary here to maintain ATP levels. The DCCD-treated cells were apparently able to maintain a normal ATP level, as observed in this study and also in an earlier study (Brown et al. 1977). Figure 3.3e shows a difference spectrum for GRO21 obtained using 1 mM DCCD to inhibit ATPase activity using otherwise identical experimental conditions, as described above. No ATP flux was observed. Only the γ-ATP peak appeared in the difference spectrum as the result of selective saturation. The same results were obtained on MG1655 samples. However, difference spectra for iodoacetic acid-treated cells were essentially identical to those for non-treated samples for both GRO21 and MG1655. Thus the ATP flux observed in the saturation transfer experiments is contributed by ATPase under the conditions used in this study.

3.5 DISCUSSION

We have shown that VHb-expressing strain GRO21 outgrows the wild type, VHb non-expressing strain, in minimal medium fed-batch cultivation under low-oxygen conditions. Both strains maintain similar ATP levels, indicating that the ATP accumulation rate in the VHb expressing strain is enhanced by approximately 65%. Our NMR saturation transfer studies also show that the ATPase catalyzed flux of Pi-ATP is accelerated by the presence of VHb.

Our results from saturation transfer experiments differ from those of Mitsumori et al (1988) concerning whether the flux of Pi to ATP is from ATPase. This difference

likely results from substantial difference in experimental protocols and different strains used. A conclusion qualitatively similar to ours was reached by Brown et al .(1977).

These results concerning VHb effects on energetics are also consistent with a hypothesis proposed to explain the mechanism of the VHb effect in *E. coli* (Kallio et al, 1994). According to this hypothesis, intracellular VHb increases the effective oxygen concentration inside the cell, thus shifting the distribution of terminal oxidase activities from cytochrome d toward cytochrome o which results in an increase in the number of protons extruded by the respiratory chain per oxygen reduced. Subsequent entry of these extra protons into the cell via the ATPase increases ATP production rate. This study proves that one prediction of this hypothesis is correct, but of course these data do not demonstrate anything about relative terminal oxidase activities or other critical aspects of the proposed mechanism.

3.6 ACKNOWLEDGMENTS

This work was supported by the Advanced Industrial Concepts Division of the U.S. Department of Energy and the National Science Foundation (Grant No. BCS 891284). The LH fermentor and instrumentation were generously provided by LH Fermentation (Hayward, CA). R.C appreciates assistance of Dr. Boguslaw Kuszta with the saturation transfer experiments.

3.7REFERENCES

Alger, J. R.; den Hollander, J. A. and Shulman, R. G. In vivo phosphorus-31 nuclear magnetic resonance saturation transfer studies of adenosinetriphosphatase kinetics in *Saccharomyces cerevisiae*. Biochemistry **1982**, 21, 2957-2963.

Brindle, K. M. ^{31}P NMR magnetization-transfer measurements of flux between inorganic phosphate and adenosine 5'-triphosphate in yeast cells genetically modified to overproduce phosphoglycerate kinase. Biochemistry **1988**, 27, 6187-6196.

Brown, T. R.; Ugurbil, K. and Shulman, R. G. ^{31}P nuclear magnetic resonance measurements of ATPase kinetics in aerobic *Escherichia coli* cells. Proc. Natl. Acad. Sci. USA. **1977**, 74, 5551-5553.

Chen, R. and Bailey, J. E. Observations of aerobic, growing *Escherichia coli* metabolism using an on-line nuclear magnetic resonance spectroscopy system. Biotechnol. Bioeng. **1993**, 42, 215-221.

Kallio, P. T.; Kim, D. J.; Tsai, P. T. and Bailey, J. E. Intracellular expression of *Vitreoscilla* Hemoglobin alters *Escherichia coli* energy metabolism under oxygen-limited conditions. Eur. J. Biochem. **1994.** In Press.

Khosla, C. and Bailey, J. E. Heterologous expression of a bacterial haemoglobin improves the growth properties of recombinant *Escherichia coli*. Nature, **1988a**, 331, 633-635.

Khosla, C. and Bailey, J. E. The *Vitreoscilla* hemoglobin gene: molecular cloning, nucleotide sequence and genetic expression in *Escherichia coli*. Mol. Gen. Genet. **1988b**, 214, 158-161.

Khosla, C. and Bailey, J. E. Evidence for partial export of *Vitreoscilla* hemoglobin into the periplasmic space in *Escherichia coli*----Implications for protein function. J. Mol. Biol. **1989a**, 210, 79-89.

Khosla, C. and Bailey, J. E. Characterization of the oxygen-dependent promotor of the *Vitreoscilla* hemoglobin gene in *Escherichia coli*. J. Bacteriol. **1989b**, 171, 5995-6004.

Khosla, C.; Curtis, J. E.; DeModena, J.; Rinas, U. and Bailey, J. E. Expression of intracellular hemoglobin improves protein synthesis in oxygen-limited *Escherichia coli*. Biotechnology **1990**, 8, 849-853.

Khosravi, M.; Webster, D. A. and Stark, B. C. Presence of the bacterial hemoglobin gene improves a-Amylase production of a recombinant *Escherichia coli* strain. Plasmid **1990**, 24, 190-194.

Lowry, O. H.; Carter, J. and Glaser, L. The effect of carbon and nitrogen sources on the level of metabolic intermediates in *Escherichia coli*. J. Bio. Chem. **1971**, 246, 6511-6521.

Mitsumori, F.; Rees, D.; Brindle, K. M.; Radda, G. K. and Campbell, I. D. ^{31}P-NMR saturation transfer studies of aerobic *Escherichia coli* cells. Biochim. Biophys. Acta **1988**, 969, 185-193.

Navon, G., Ogawa, S., Shulman, R. G. and Yamane, T. High-resolution ^{31}P nuclear resonance studies of metabolism in aerobic *Escherichia coli* cells. Proc. Natl. Acad. Sci. USA **1977**, 74, 888-891.

Shine, N.; Xuan, A. and Weiner, M. W. ^{31}P NMR studies of ATP concentrations and Pi-ATP exchange in the rat kidney in vivo: effects of inhibiting and stimulating renal metabolism. Magnetic Resonance In Medicine **1990**, 14, 445-460.

Webster, D. A. Structure and function of bacterial hemoglobin and related proteins. Advances in Inorganic Biochemistry **1988**, 7, 245-265.

Webster, D. A. and Liu, C. Y. Reduced nicotinamide adenine dinucleotide cytochrome o reductase associated with cytochrome o purified from *Vitreoscilla*. J. Biol. Chem. **1974**, 249, 4257-4260.

3.8 FIGURES

Figure Captions

Figure 3.1. Growth trajectories of MG1655 and GRO21 after the onset of oxygen limitation. The ordinate is log scale.

Figure 3.2. A typical ^{31}P NMR spectrum of GRO21 using an on-line NMR system. The spectrum was obtained under oxygen-limited conditions, observed in an interval of reduced specific growth rate in Figure 1. NMR acquisition parameters: 40° pulse and a relaxation delay of 0.2 s, 1200 scans, other parameters as in the Materials and Methods. Abbreviations: SP: sugar phosphate; P_i^{cyt}: intracellular inorganic phosphate; P_i^{ex}: extracellular inorganic phosphate; NTP: nucleoside triphosphate; NDP: nucleoside diphosphate; NAD(H): nicotinamide adenine dinucleotide; UDPG: uridinediphosphoglucose.

Figure 3.3. ^{31}P NMR spectra of GRO21 using a non-growing high-cell-density suspension. a. Obtained using a normal pulse sequence. NMR acquisition parameters were the same as as given for Figure 3.2, except the number of scans was 640. b. Dante sequence applied as shown by the arrow. c. Dante sequence applied at γ–ATP. d. Difference spectrum, d=b-c. e. A difference spectrum measured with 1mM DCCD added to inhibit ATPase. PEP is the abbreviation for

phosphoenolpyruvate, other abbreviations are the same as given in Figure 3.2 captions. Saturation transfer spectra were taken using 90^{o} pulse, acquisition time 0.5 s and relaxation delay 0.05 s.

Figure 3.1

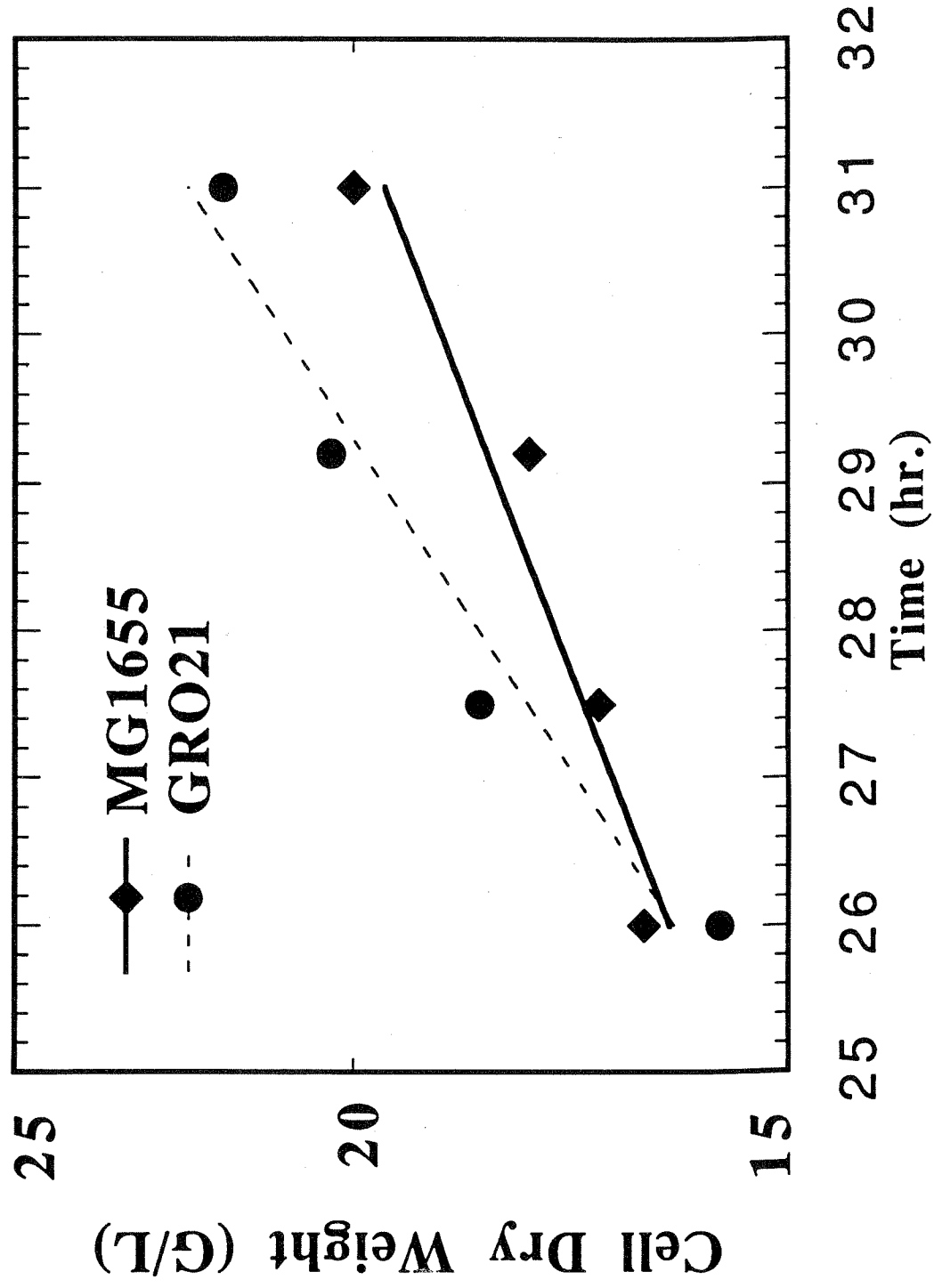
Cell Dry Weight (G/L)
25
20
15
25
26
27
28
29
30
31
32
Time (hr.)
MG1655
GRO21

Figure 3.2

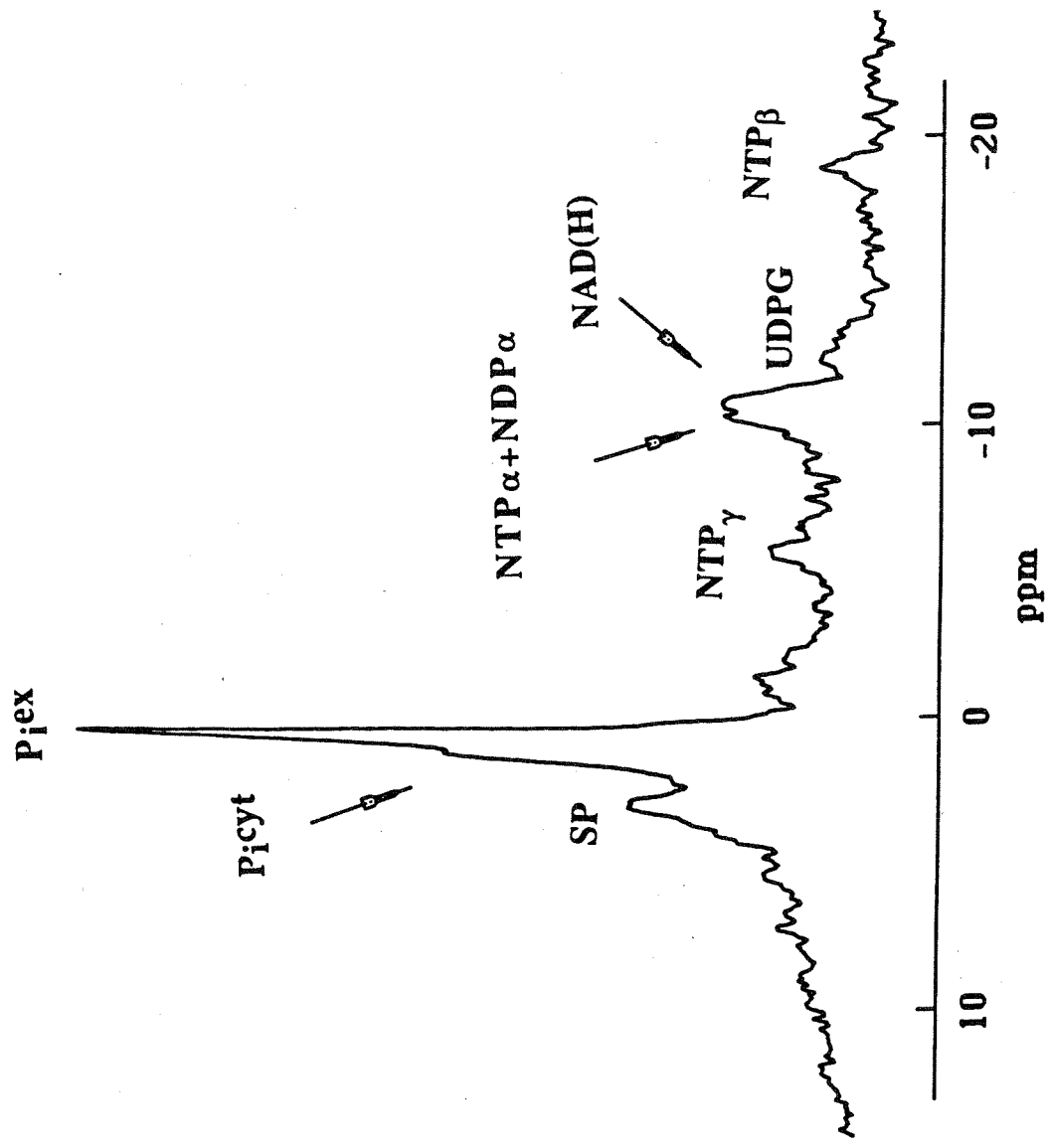

Figure 3.3

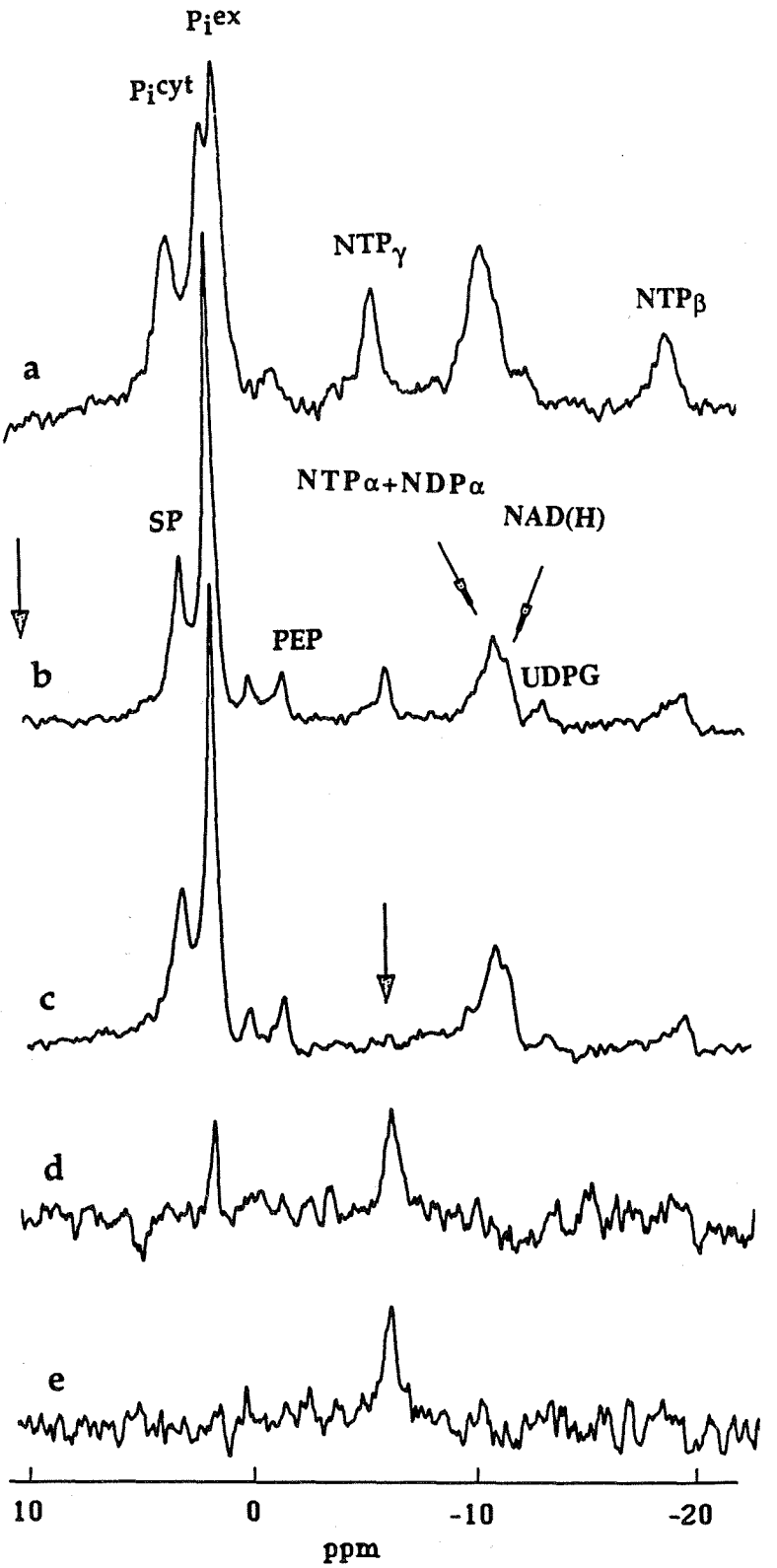
Pi ex
Pi cyt
NTPγ
NTPβ
a
NTPα+NDPα
SP
NAD(H)
PEP
b
UDPG
c
d
e
10
0
-10
-20
ppm

Chapter 4

Comparative Studies of *E. coli* Strains Using Different Glucose Uptake Systems: Metabolism and Energetics

4.1 ABSTRACT

The present study investigates energetic and metabolic changes brought about by the genetic modification of the glucose uptake and phosphorylation system of *E. coli*. The strain PPA316, using the galactose-proton symport system for glucose uptake, exhibited significantly altered metabolic patterns relative to the parent strain PPA305 due to the lower flux to pyruvate in both aerobic and anaerobic fermentation. The extra energy cost in substrate uptake had a greater effect on anaerobic specific growth rate, reducing the specific growth rate by a factor of five whereas the effect on aerobic specific growth was moderate, reaching a specific growth rate of 60% of that of the wild-type PTS strain. The maximal cell densities obtained were approximately 8% higher than the wild-type PTS strain under aerobic conditions and 14% lower under anaerobic conditions. NMR results showed that the mutant experienced a dramatically different intracellular environment, which was reflected by lower levels of total sugar phosphate (S-P), NAD(H), NTP, PEP and ΔpH across the cytoplasmic membrane and higher NDP. The S-P compositions, as measured by extract NMR, were considerably different between these two strains. Data suggest that glucokinase, glyceraldehyde-3-phosphate dehydrogenase, fructokinase (PFK) and pyruvate kinase (PK) may be responsible for the low rate of glucose metabolism in PPA316.

4.2 INTRODUCTION

Monosaccharides are one of the most widely utilized food materials of bacteria (Cooper, 1978). Before they can be subjected to the degradative reactions that yield energy and building blocks necessary for cell growth, they must pass from the growth medium into the cell. There are four mechanisms by which cells uptake exogenously supplied nutrients. They are: simple diffusion, facilitated diffusion, active transport and group translocation (Henderson and Maiden, 1987; Neidhardt et al. 1990).

Simple diffusion

The driving force of diffusion is the difference in concentrations of the solute across the membrane. Thus flow occurs only down a concentration gradient with its rate proportional to ΔC, P and A:

$$V=P\ A\ \Delta C \qquad 4.1$$

where P is the membrane's constant of permeability to the solute, ΔC is the difference in concentrations of the solute across the membrane, and A is the surface area over which diffusion can occur.

Facilitated diffusion

Facilitated diffusion is a non-energized transport process catalyzed by a protein (carrier). The protein that mediates facilitated diffusion does not concentrate a substrate within the cytoplasm. It merely provides a mechanism by which a particular solute can diffuse down a concentration gradient into the cell. It has saturable kinetics, typical of an enzyme-catalyzed process:

$$V = V\max[S] / \{Km + [S]\} \qquad 4.2$$

where V is the initial rate of transport, [S] denotes substrate concentration, Vmax is the maximum rate of transport and *K*m is the substrate concentration at which V is Vmax/2. The stereospecific carrier offers substrate specificity to the process. Glycerol transport is the only known example of facilitated diffusion in *E. coli*.

Active transport

Active transport resembles facilitated diffusion in that a stereospecific, membrane-located carrier (or permease) mediates the process, and saturation kinetics are seen (eqn. 4.2). By active transport, the intracellular concentration of a substrate can be maintained at a level many fold higher than its concentration in the medium (or vice-versa). For example, galactose is concentrated by its active transport system by a factor greater than 10^5. Obviously, the maintenance of a concentration gradient requires the expenditure of energy, and depending on the sources of the energy, active transport can be divided into two types: primary active transport, which involves the direct coupling of chemical or photosynthetic energy to the transport of substrate across the membrane barrier, and secondary active transport, where the transport of a solute

across the membrane is at the expense of a previously established ion gradient, usually of H^+ or Na^+ ions.

There are three types of secondary active transport: symport, antiport and uniport.

Symport is the transport of two substrates simultaneously in the same direction by a single carrier. As exemplified by the galactose-proton symport system, illustrated in figure 4.1, protons flow down its concentration gradient (previously created), galactose (or glucose in fig. 4.1) flows with it. Therefore, in this case the proton gradient drives the symport system. As a result of the transport, both proton concentration gradient and membrane potential, i.e., both components of the proton motive force, are diminished. Definitions and examples of uniport and antiport can be found in the references (Neidhardt et al. 1990).

Group translocation

Group translocations are mechanisms that chemically alter substrate to impermeable derivatives as they cross the cytoplasmic membrane. The best studied of the group translocations is the Phosphoenolpyruvate (PEP): carbohydrate phosphotransferase system (PTS). The mechanism was first characterized by Kundig (1974), and extensive subsequent studies were reviewed by Postma and Lengeler (1985) and Saier (1985). The major sugar transported by this route is glucose. Figure 4.2 illustrates the main features of the PEP: glucose phosphotransferase (PTS) system in *E. coli*. As can be seen from fig. 4. 2, one molecule of PEP is used per molecule of sugar transported by this system, reducing the yield of ATP from catabolism of the

sugar by one. However, glucose arrives in the cytoplasm as glucose-6-phosphate, ready for glycolysis without further modification or energy input. This is a distinct advantage over most other systems in which no modification of the substrate occurs during the transport and glucose has to be phosphorylated by ATP (as is the case illustrated in fig. 4.1) in addition to the energy expended on transport (Muir et al. 1985; Dawes, 1986; Cooper, 1986).

Glucokinase

As is clear from the above comments, except for the PTS system, glucose transported through other mechanisms is not modified and therefore phosphorylation is the first catabolic reaction in glycolysis. In *E. coli*, in addition to PTS-PEP dependent phosphorylation mechanism, glucokinase is an enzyme capable of phosphorylating glucose using adenosine-5'-triphosphate as phosphate donor, although it plays a minor role when the PTS functions (Curtis and Epstein, 1975). Studies have shown that, when deficient in PTS-dependent phosphorylation enzymes, *E. coli* cell can grow on glucose, albeit slowly, using glucokinase to phosphorylate glucose (Fukuda et al. 1983).

Glucokinase is an enzyme of two subunits each having a molecular weight of 24,500 (Fukuda et al. 1984). The optimal pH for activity is around 9.5, markedly decreasing its activity with decrease of pH, with only 20% of maximal activity at pH=7.5, the normal intracellular pH, and only approximately 5% of its maximal activity is left when pH is at 7.0. This enzyme has a *K*m value of 20 mM for glucose, which is 3 orders of magnitude higher than that of enzyme II^{glu} of PTS system and 2 orders of magnitude higher for glucokinases found in other organisms (for example,

Zymomonas mobilis). Glucokinase from *E. coli* B is highly specific to ATP with a *K*m of 0.67 mM. Phosphoenolpyruvate was found to be inert as phosphoryl donor. Glucose-6-phosphate (G-6-P) showed non-competitive inhibition against glucose, and ADP showed competitive inhibition against ATP. The *K*i of ADP for ATP was 0.3 mM. The inhibition was more severe when the concentration of G-6-P falls below 2 mM. The enzymatic activity varies depending on the ratios of Mg^{++}/ATP, with maximal activity obtained at ratios between 1.0 and 2.0.

NMR techniques

NMR techniques enjoy an increasing popularity in energetic and metabolic studies of a wide range of cell types such as bacteria, fungi, algae, plant cells and animal cells. There is an abundant literature that has recorded many elegant studies in bioenergetics and metabolic regulation (for reviews, see Lundberg et al. 1990; Campbell-Burk and Shulman, 1987; Roberts and Jardetzky, 1981). For example, using ATPase mutants, uncoupler FCCP and specific ATPase inhibitor DCCD, the relationship between ATP, ΔPH and electron transport was investigated extensively under both anaerobic and aerobic conditions (Ugurbil et al. 1979). Results from this study provided firm evidence to support the well-known chemiosmotic hypothesis, which was proposed by Peter Mitchell in 1961. A combination of whole-cell NMR experiments, to follow ATP, ADP, inorganic phosphate and intracellular pH and ΔpH, with NMR data also obtained from perchloric acid (PCA) extracts, to provide detailed information on concentrations of sugar phosphate components, has been proven to be very successful in analyzing metabolic changes brought about by specific genetic

modifications in metabolic pathways. Gil Navon et al. applied both whole cell and PCA extract NMR methods to a metabolic study of various mutants of *Saccharomyces cerevisiae*. Mutants, lacking phosphofructokinase activity, phosphoglucose isomerase activity and glucose catabolite repression of the fructose bisphosphatase activity, respectively, were found to accumulate characteristic sugar phosphates during glycolysis. Disruptions of glycolysis in these mutants were characterized by ^{31}P NMR spectra.

The present work explores the metabolic and physiological consequences of an alternative glucose uptake and phosphorylation system. In particular, a strain has been constructed (in the laboratory of Dr. P. Postma of the University of Amsterdam) which uses a galactose-proton symport system for glucose uptake. As illustrated in fig.4.1, glucose phosphorylation in this mutant is ATP-dependent and catalyzed by the native *E. coli* glucokinase. A comparison of PTS and symport system shows three major differences between these two substrate transport schemes (fig.4.1 and fig.4.2). First of all, PTS system is a PEP-dependent phosphorylation system while symport system uses ATP as phosphoryl donor. Secondly, PTS system is energetically more efficient in the sense that only one high-energy compound (PEP) or only one ATP equivalent is used during the process. The cost of glucose uptake and phosphorylation in a symport system is one ATP plus one proton per each glucose molecule transported; this is equivalent to one and half ATPs (Driessen et al. 1987). Finally, there is also a difference in pyruvate coproduced between these two systems, i.e., the PTS system co-produces one pyruvate during glucose uptake whereas the symport system does not produce pyruvate. Since pyruvate can either be channeled to the TCA cycle for energy production (under aerobic conditions) or further be metabolized to acetate, succinate, lactate, ethanol etc., it is expected that glucose metabolism downstream of pyruvate

would be different in these two strains. Since intracellular energetic parameters such as ATP and ΔpH participate in many intracellular regulations, any perturbation in these parameters could have profound influence on the metabolic network. Similarly, intracellular PEP concentration is also an important regulator in glycolysis through its roles in regulating phosphofructokinase (PFK), pyruvate kinase (PK) and PEP carboxylase which connects glycolysis with TCA cycle.

This analysis prompts us to investigate the energetics of these strains and the metabolic changes brought about by switching the glucose transport system. ^{31}P NMR has been chosen as one of the tools in this study because of its capability to measure NTP, NDP, S-P while simultaneously determining the intracellular and extracellular pH values. Complementary to the whole cell experiments, concentrations of phosphorylated compounds were measured by taking ^{31}P NMR spectra on PCA extracted cell samples.

4.3 MATERIALS AND METHODS

Strains

E. coli strain MG 1655, an unmutagenized wild-type K-12 strain, was modified by a Tn 10 transposon insertion at galP (coding for galactose permease) in order to eliminate all residual glucose uptake activity by the galactose permease, GalP. The modified strain can transport glucose via the phosphotransferase (PTS) system and was named as PPA305 and also referred as wild-type PTS strain.

Strain PPA316, which is also derived from MG1655, carries a ptsHI-*crr* deletion (therefore has no PTS activity), and a mutation in galactose operon which

renders a constitutive expression of galactose permease. Glucose transport of this strain is via GalP, a H^+-galactose symporter, yielding glucose inside. Subsequent phosphorylation is through its native, constitutive glucokinase. This strain is also referred as the non-PTS strain.

Medium and culture conditions

The medium used in growth and metabolism studies contained (in grams per liter): Glucose, 20; tryptone, 10; yeast extract, 5; Na_2HPO_4, 3; KH_2PO_4, 1.5, NaCl, 5. Fermentations were conducted in a 3.5 L (working volume 2 L) LH fermentor (LH Fermentation, Hayward, CA). pH was controlled at 6.8 by adding 4 N NaOH. In aerobic experiments, the air flowrate was fixed at 2.0 (l/min.), and dissolved oxygen was controlled above 20% of air saturation by manually adjusting agitation speed. Anaerobic conditions were maintained by flushing nitrogen into the fermentor, with agitation speed set at 300 r.p.m. All fermentations were conducted at 37°C. The inocula were prepared with the same medium and grown overnight at the same temperature, either in a shaker for aerobic experiments, or in a water bath for anaerobic experiments, in the latter case, nitrogen was flushed and agitation was driven by an external magnetic stirrer. 1% (V-V) inoculation was used in all fermentation.

Analytical methods

Dry weight of cell suspension taken from the fermentor was measured. After two washes, cell pellet was transferred to a pre-weighed aluminum plate which was dried on a 105°C to constant weight. Metabolites in the supernatants were analyzed by

high performance liquid chromatography (HPLC). A BioRad Aminex HXP-87H (300 x 7.8 mm) column was used and 0.01N H_2PO_4 mobil phase at flow rate 0.4 ml/min. was found to be satisfactory in resolving metabolites of interest. Glucose concentration in the medium was determined with a Sigma test kit (510-A). Ethanol and D-lactate were assayed using Boehringer-Mannheim kits. All absorbance measurements were made using a Shimadzu UV-260 Spectrophotometer.

NMR whole cell experiments

Sample preparations

E. coli cells were grown in 2-L shake-flasks in 1 L of M63 growth medium supplemented with 5 g/l yeast extract. The cultivation of *E. coli* was carried out at 37°C and 275 rpm in a rotary shaker (New Brunswick Scientific). Glucose at an initial concentration of 5 g/l was used as the carbon source. Late-log phase cells were harvested by centrifugation at 7000 rpm using a JA-14 rotor for 5 minutes. This was followed by two washings using ice cold buffer containing: 100 mM Pipes (1,4-piperazinediethanesulfonic acid), 50 mM MES (2-[N-Morpholino]ethanesulfonic acid), 6mM Na_2HPO_4, 6mM KH_2PO_4, 60mM NaCl, pH adjusted to 7.3. Afterwards, cells were suspended in the same buffer with the cell density of the sample cell suspension approximately 100gDW/l [(grams dry weight)/l] for anaerobic NMR recording or 40gDW/l for aerobic samples to allow sufficient oxygenation of the suspension. More accurate dry weight values, required to quantify intracellular concentrations, were measured by transferring the cell suspension after each experiment to a pre-weighed aluminum plate which was dried in a 105°C oven to constant weight. A 12.5 ml aliquot of the sample suspension was placed in a 20 mm (diameter) NMR sample tube, 1 ml

D_2O was added as lock signal, and a sealed capillary with 0.1M methylene diphosphonic acid (MDP) was placed in the sample tube to provide a chemical shift reference. MDP resonates at 18.6 ppm downfield of 85% phosphoric acid which is assigned as 0 ppm.

^{31}P NMR operations

^{31}P NMR experiments were performed on a Brucker AM300 NMR spectrometer in the Fourier transform mode at a frequency of 121.5 MHz. A 20 mm NMR broad-band probe was used. After adding 0.5 ml of glucose (500g/l), spectra were accumulated in consecutive 1.5 minute blocks (120 transients), except where otherwise indicated, with a spectral width of 8000 Hz, and the free induction decays (FID) were sequentially stored on disk (8K). A pulse angle of 40^o and relaxation delay of 0.2 seconds (recycle time) were used. Routine tuning, lock, and shimming were applied. All experiments were conducted at 25^oC. A line broadening of 20 Hz was used in all the spectra from whole cell samples. At the end of each experiments, 80 µl Pi (1M) was added to the sample, and spectra were taken for calibration purposes (Shanks,1988).

PCA extract NMR experiments

Cell growth and harvest-washing-resuspension procedures are the same as whole cell experiments. After a desired elapsed time following glucose addition (until a quasi-steady-state metabolism is attained), 3.5 ml ice-cold perchloric acid (70%) was

added to the sample, 50 µl of MDP (1M) was also added to correct for any inaccuracy due to loss in the extraction procedure and to provide a chemical shift reference. Samples were vigorously vortexed for 2 minutes at maximum speed. After resting on ice for 15 minutes, precipitates were removed by centrifugation in a desk-top centrifuge at 2800 rpm for 15 minutes. Supernatants were neutralized with solid K_2CO_3, and precipitation was again removed by centrifugation. Extract was collected and diluted by a factor of 20 and pH was adjusted to 7.4. The resulting solution was passed through a Chelex 100 Biorad PolyPrep column (200-400 mesh) to remove paramagnetic cations. Post-ion exchange samples were frozen and then lyophilized using a LABCONCO freeze dry system.

For NMR spectroscopy of extracts, the lyophilized sample was redissolved in D_2O containing 20 mM EDTA of volume equal to the original sample volume. The samples were kept at -70°C until used in the NMR experiments. Samples were placed in 10-mm-diameter NMR tubes and ^{31}P NMR spectra were obtained on a Brucker AM 500 MHz spectrometer in the Fourier transform mode at a frequency of 202.49 MHz. using a pulse angle of 90° and relaxation delay of 1 second. Free Induction decays were accumulated for 1000 scans on 8K files. Composite pulse decoupling of protons was applied.

4.4 RESULTS

I. Metabolism and growth under aerobic conditions

The growth profiles and time courses of glucose and by-product acetate for both strains are presented in figure 4.3. The non-PTS strain PPA316 grew more slowly than the wild-type PTS strain PPA305. The specific growth rates in the exponential phase were 0.33 h^{-1} and 0.57 h^{-1} for PPA316 and PPA305, respectively. The maximal cell density obtained for PPA316 was 5.5 g/l (in dry weight), and the wild-type PPA305 reached a slightly lower cell density, 5.1 g/l.

Of all the metabolites analyzed (acetate, ethanol, succinate, pyruvate, formate and lactate), only acetate was accumulated in the growth medium at concentrations above detectable level (0.05 g/l) for the wild-type PTS strain, consistent with earlier studies (Clark,1989). Acetate concentration increased with the increase of the cell concentration and began to level off at 8 hr, when glucose concentration in the medium was low, reaching a maximal acetate concentration of 4.5 g/l. After the depletion of glucose, cells consumed acetate for additional growth, and a slow increment of cell concentration was observed during this period. Neither acetate nor other metabolites was found in the growth medium of the non-PTS strain. This is consistent with the difference in the maximal biomass concentrations obtained during growth, indicating that glucose was more efficiently used in the non-PTS strain because acetate excretion represents a waste of carbon and is equivalent to a lower flux to biosynthesis and less carbon oxidized for energy generation (Holms, 1986).

It was found that acetate production and excretion was triggered primarily by a large flux to pyruvate (Holms, 1986). It therefore follows that the non-PTS strain had a

smaller flux to pyruvate which prevented such overflow. The only route of pyruvate production is through pyruvate kinase (PK) which converts phosphoenolpyruvate (PEP) to pyruvate. Our NMR data showed that intracellular PEP concentration was significantly lower in cells of the non-PTS strain PPA316 than that in the wild-type PTS strain (Table 4.2). FDP was another factor favoring a smaller flux to pyruvate in this strain (FDP is a potent activator of PK). On the other hand, wild-type cells have an additional way to generate pyruvate. As illustrated in figure 4.2, one mole of pyruvate is coproduced for each mole of glucose transported through the PTS system. Pyruvate thus produced would not be converted back to PEP because gluconeogenesis and glycolysis are reciprocally regulated so that gluconeogenesis is inactive during glycolysis (Stryer, 1988). Therefore the flux to pyruvate was greater in the PTS strain than that of the non-PTS strain.

II. Anaerobic metabolism and growth

Compared to the aerobic experiments difference in growth rates between the two strains studied was more significant. As can be seen from figure 4.4, the wild-type PTS strain grew 5 times as fast as the mutant, with a specific growth rate of 0.43 h^{-1}. This is expected, because the relative effect of the additional energy cost for glucose uptake in the non PTS strain is maximized under anaerobic conditions when only two ATP is synthesized per each glucose metabolized. Consistent with this interpretation, the maximal biomass obtained for PPA316 was 3.0 g/l, which was 0.5 g/l lower than the wild-type PTS strain(13.4%).

Figures 4.5 a-e display fermentation products accumulated in the growth medium for both strains. Both strains produced acetate, ethanol, lactate, formate and succinate, to varying extent. Lactate was the only compound that was produced to similar amounts in both strains (fig. 4.5c), although rates of lactate production varied considerably. The profiles of ethanol were similar to those of acetate (fig. 4.5 a, b). The wild-type PTS strain produced approximately twice as much ethanol and acetate as the non-PTS strain. With respect to formic acid, the net rate of accumulation was similar to those lactate, acetate and ethanol for the wild-type PTS strain, but the non-PTS strain did not accumulate formate until the end of growth, with a final concentration of 0.2 g/l, only 1/16 as high as was reached by the wild-type PTS strain. The non-PTS strain accumulated succinate in the later stage of the fermentation. The highest succinate concentration was 5.9 g/l, approximately 3.7 times higher than the wild type.

Acetate, ethanol, lactate and formate were derived from pyruvate. In steady-state, flux to pyruvate should be equal to the combined fluxes from pyruvate to these four acids. The flux to pyruvate can then be evaluated by summarizing the specific production rates of these metabolites and taking proper stoichiometry coefficients. Therefore, the flux to pyruvate (F_{pyr}),

$$F_{pyr}=2/3\ Q_{acetate}+ 2/3Q_{ethanol}+ Q_{lactate} + 1/3Q_{formate} \qquad 4.3$$

where Q is for the specific production rates of acids, in unit of mmol per gram of cell dry weight per unit time (hr.) Results are given in figure 4.6. Therefore, the wild-type PTS strain had a much higher carbon flux to pyruvate except the final time point when glucose was exhausted (figure 4.4).

Succinate is believed to be derived from PEP and consumes 8 reducing equivalents for each succinate synthesized (Clark, 1989). Thus is one of the two most efficient ways in *E. coli* to recycle NADH to NAD^+(as efficient as ethanol pathway). Our NMR data (Table 4.1) show that the total concentrations of NADH and NAD^+ in this strain are substantially lower than the wild-type PTS strain. Since $NAD^+/(NADH+NAD^+)$ is in the range of 0.93-0.97 (Neihdardt et al. 1990), most of the nicotinamide adenine dinucleotide is in its oxidized form and therefore the NAD^+ concentration is much lower in the non-PTS strain than that of the PTS strain (Range of NAD^+ and NAD(H) is listed in Table 4.3). This might explain why succinate route was chosen in this strain.

III. NMR characterization

Figure 4.7 shows two typical ^{31}P NMR spectra for both strains in quasi-steady states. This steady-state is defined as a state in which NMR-visible intracellular parameters such as total sugar phosphate (S-P) , nucleotide triphosphate(NTP) and nicotinamide adenine dinucleotide [NA(D)H] concentrations remain constant. Under anaerobic conditions, PPA305 reached quasi-steady-state metabolism 5 minutes after the addition of glucose, during which NTP, S-P increased quickly from zero and its initial value, respectively, to the steady-state levels shown in fig 4.7 (top spectrum). During the quasi-steady-state, build-up of pH difference across the cytoplasmic membrane was manifested by the appearance of the intracellular inorganic phosphate (Pi^{cyt}) peak as a down-field shoulder of the extracellular inorganic phosphate (Pi^{ex}) peak. The steady-state lasted 10 minutes. PPA316 followed a similar trend, although it took 20 minutes to reach the quasi-steady state which lasted about 40 minutes.

The qualitative features of the spectra of both strains are very similar (figure 4.7) and are not different from those in the literature (Ugurbil et al. 1978; Axe and Bailey, 1987; Diaz-Ricci et al. 1990). Therefore, assignments of the peaks are based on these references. The resonances from 5 ppm to 3 ppm are in the sugar phosphate region (S-P), which contains glucose-6-phosphate (G-6-P), fructose-6-phosphate (F-6-P), fructose-1,6-bisphosphate (FDP), 3-phospho-glycerate (3-PGA) and 2-phospho-glycerate (2-PGA) and other phosphorylated intermediates of glucose metabolism. Cytoplasmic inorganic phosphate Pi^{cyt} and extracellular inorganic phosphate Pi^{ex} are the next observable resonances. From their chemical shifts and a Pi-pH titration curve, pH values of both cytoplasmic and extracellular medium can be evaluated. The nucleotide resonances at -5, -10 and -18.6 ppm were assigned to NTP_{γ}+NDP_{β}, NTP_{α}+NDP_{α} and NTP_{β}, respectively. NAD(H) includes both NAD^+ and NADH appears at -11 ppm. UDPG and similar compounds resonate near -12 ppm.

For the wild-type PTS strain PPA305, 120 scans (acquisition time of 1.5 minutes) is sufficient to obtain a spectrum with reasonable signal to noise ratio. However, for the non-PTS strain PPA316, due to the much lower NTP level, more scans are needed to detect NTP levels above the noise. In order to compare NTP and NAD(H) levels, 4 individual (120 scans each) are summed, Figure 4.7 is one of the summed spectra (total 480 scans, total acquisition time of 6 minutes) and is scaled so that the levels of a given resonance can be directly compared. Therefore, the non-PTS strain experienced a very different intracellular environment compared to the wild-type PTS strain. This was reflected from the lower levels of total sugar phosphate and total concentration of NAD(H), high-energy compound NTP and much smaller ΔpH, the latter two are two important energetic parameters.

Since inorganic phosphate is more abundant than NTP, their peaks were resolved in each individual spectrum, and thus pH in cytoplasmic and extracellular pH can be monitored with a time resolution of 1.5 minutes. Figure 4.8 shows pH evolutions for both wild-type and the mutant during steady-state glucose metabolisms. For PPA305, the extracellular pH decreased rapidly whereas the extracellular pH for PPA316 declined at a much slower rate, indicating much faster glucose metabolism for the wild-type PTS strain. The changes of cytoplasmic pH of PPA316 apparently followed closely with the changes of the extracellular pH, resulting in a roughly constant ΔpH over the time course, but the cytoplasmic pH of the wild-type did not show the same trend, instead, ΔpH increased with time (figure 4.9). A much lower cytoplasmic pH of PPA316 was observed. For example, at extracellular pH of 6.5, the mutant had a intracellular pH about 6.8, while the wild-type cell maintained an intracellular pH about 7.5 (figure 4.8).

Under aerobic conditions, similar pH profiles were observed. The only difference was that ΔpH maintained by the non-PTS strain was slightly higher (0.37 pH units).

Intracellular concentrations as measured by ^{31}P NMR are given in Table 4.1. In all intracellular concentration calculations, an intracellular volume of 2.7 μl per mg of cell dry weight was assumed (Henderson et al. 1977) and concentrations were corrected for saturation effects due to fast pulses. Under both anaerobic and aerobic conditions, the non-PTS strain had a very low NTP level, about 0.8 mM, in contrast to 4.0 mM and 5.2 mM for the wild-type under anaerobic and aerobic conditions, respectively. The availability of oxygen should, in principle, allow cells to use respiratory chain to generate more ATP, but this does not seem to be the case. NDP concentrations can be evaluated by subtracting $NTP\beta$ from $NTP\alpha$+$NDP\alpha$. While for

the wild-type the difference between these two peaks was negligible, indicating a very low concentration of NDP, the NDP for the mutant was estimated to be 0.2 mM under both anaerobic and aerobic conditions.

The total nicotinamide adenine dinucleotide NAD(H) concentration was also substantially lower in the mutant strain, more significant in anaerobic conditions.

Differences in the total sugar-phosphate concentrations were also observed. For the wild-type, ratios of S-P were 2.6 and 1.4 for aerobic and anaerobic glycolysis, respectively, with the non-PTS strain having lower concentrations in both cases.

It appears that there is no simple correlation between the level of the total S-P and rate of glucose metabolism. Therefore ^{31}P NMR experiments on cell extracts were also conducted in order to examine the S-P compositions and measure PEP concentrations.

Typical extract NMR spectra are shown in figures 4.10, 4.11 and 4.12. Many resonances resolved in the spectra were assigned by a combination of several methods. First tentative assignments were made based upon chemical shift values in the literature (Gadian et al. 1979; Robitaille et al. 1991), and were then checked by adding pure metabolites and taking additional spectra or by pH -titration.

Quantitative results of sugar phosphate analyses are presented in Table 4.2. The total concentrations of sugar phosphate agreed well with the whole cell experiments, indicating artifacts of extract procedures as detailed in the Materials and Methods are negligible.

In all cases, fructose phosphate (total concentration including both diphosphate and monophosphate) was the most abundant sugar phosphate, accounting for 68% and 76% of the total sugar phosphate in wild-type PPA305, under aerobic and anaerobic conditions, respectively. The percentages of fructose phosphate of PPA316 were

similar, being 76% under aerobic conditions and 62% under anaerobic conditions. Consequently, the differences in concentrations of FDP+F-6-P between these two strains largely accounted for the differences seen in the total S-P concentrations. PEP was much higher in the wild-type PTS strain, with more pronounced change in aerobic condition. For the other S-P components, with one exception of G-6-P in aerobic conditions, PPA305 had higher concentrations, by a factor ranging 1.2 to 3. Consistent with our NMR data, earlier NMR study showed that FDP was the dominating component found in the S-P region; in some cases, up to 90% of S-P were FDP (Ugurbil et al. 1978).

The ratios of steady-state glycolysis of PPA305 to PPA316 were 3.3 and 2.5, under anaerobic and aerobic conditions, respectively. Why do cells with a different glucose uptake system have lower glucose metabolism?

Glucose phosphorylation is a step which might be responsible for the lower rate of glucose metabolism in the non-PTS strain. Unfortunately, due to its minor role in glucose metabolism in wild-type strains, studies on glucokinase are scarce. Only one reference was found. The intracellular environments as determined by NMR measurement is unfavorable for normal glucokinase function. First of all, the intracellular pH of 7.1 at external pH 6.8 is well below its optimum, which is 9.5; it is estimated that the remaining activity at pH=7.1 is no more than 10% of its maximal activity. With an NTP level of 0.8 mM, assuming half of it is ATP (Lowry et al. 1971), it seems plausible that ATP is limiting the phosphorylation of glucose, which has a *Km* of 0.67 mM, higher than the estimated ATP concentration of 0.4 mM. Inhibition by G-6-P is a factor which further lowers the glucokinase activity. In vitro study showed (Fukuda et al. 1984) that, the G-6-P inhibition was most severe when G-6-P was

below 2 mM. The intracellular G-6-P concentrations as measured using PCA extract NMR fall into this region. ADP inhibition may also play a role because the estimated ADP concentration was 0.2 mM, which is close to the *K*i value of ADP for ATP.

At this point , it is logical to inspect whether or not any other part of the pathway also contributes to the low flux through the EMP pathway in this strain. With unusually low NAD^+ (Table 4.3) and ATP levels, it is possible that those reactions involving ATP and NAD^+ become rate limiting steps. Particularly, glyceraldehyde-3-phosphate dehydrogenase and fructokinase which uses NAD^+ and ATP, respectively, as their substrates. This is consistent with the succinate synthesis under anaerobic condition found in fermentation studies and the very low FDP concentrations in this strain (note: FDP is the immediate product of PFK). Another step that might hold responsibility is the reaction catalyzed by pyruvate kinase (PK), because PEP (substrate of PK) concentrations in the non-PTS strain are considerably lower than the wild-type PTS strain and the most potent activator of this enzyme FDP also exists in much lower concentrations.

4.5 DISCUSSION

Metabolic engineering, which utilizes recombinant DNA technology to restructure metabolic machinaries for strain improvement, often produces unpredictable and undesired results (Bailey, 1991). This is due to the inherently complicated and sophisticated regulation networks within the cell and is compounded by the fact that the regulatory interactions are largely unknown. Therefore, systematic study to fully

assess the consequences of each known genetic modification is necessary to advance the knowledge about cellular regulation and to approach the goal of rational design of living cells for industrial applications. In this study, we have demonstrated the usefulness of NMR as a tool in examining changes in intracellular metabolic environment and in analyzing energetic states of cells with a specific genetic modification in its substrate uptake system.

Our aerobic fermentation studies show that using galactose permease for glucose uptake lowers the carbon flux to pyruvate to an extent that prevents acetate excretion, while still sustaining a sufficient flux for biosynthesis and energy production as manifested by the comparable growth rate and higher cell density achieved. The situation is quite different in the PTS system, where glucose uptake is tightly associated with a concomitant flux to pyruvate, in addition to a flux from glycolysis. Consequently, restricting carbon flux to pyruvate in a PTS strain would necessarily be based on limiting the availability of the carbon source, just as commonly practiced in fed-batch cultivation (Zabriskie and Arcuri, 1986; Georgiou, 1988). For example, if F is the minimum flux to pyruvate that triggers acetate excretion, a non PTS system could operate its glucose metabolism at this flux, but a PTS system must lower its glycolytic rate to F/2 in order to prevent acetate production.

It is important to note that galactose permease is not under the control of the PTS system (Postma and Lengeler, 1985). However, deletion of the *crr* gene, coding for III^{glu} of the PTS system, may decrease cyclic adenosine-3', 5'-monophosphate (cAMP) levels in the non-PTS strain because adenylate cyclase is activated by phosphorylated III^{glu} (Postma, 1987). cAMP with its receptor protein (CPR)

influence a variety of functions in *E. coli*, such as induction of many catabolic enzymes (Adhya and Garges, 1982). In shake-flask cultivation, including cAMP (5 mM) in M63 glucose minimum medium did not increase cell growth rate of the non-PTS strain, in fact the growth rate was slightly decreased (15%). Therefore the metabolic changes observed here can not be attributed to the effect of lower cAMP levels induced by the deletion of PTS genes.

4.6 ACKNOWLEGMENTS

Ms. Wyanda Yap and Dr. P. W. Postma (The University of Amsterdam) constructed and provided strains used in this study. This work was supported by the Advanced Industrial Concepts Division of the U.S. Department of Energy and the National Science Foundation (Grant No. BCS 891284). The LH fermentor and instrumentation were generously provided by LH Fermentation (Hayward, CA). The assistance of Dr. Robert Lee with the Bruker AM500 NMR spectrometer is greatly appreciated.

4.7 REFERENCES

Adhya, S and Garges, S. How cyclic AMP and its receptor protein act in *Escherichia coli*. Cell. 1982, 29, 287-289.

Axe, D. D. and Bailey, J. E. Application of ^{31}P nuclear magnetic resonance spectroscopy to investigate plasmid effects on *Escherichia coli* metabolism. Biotechnology Letter, 1987, 9, 83-88.

Bailey, J. E. Toward a science of metabolic engineering. Science, 252, 1668-1674.

Cambell-Burk, S. L. and Shulman, R. G. High-resolution NMR studies of *Saccharomyces cerevisiae*. Ann. Rev. Microbiol. 1987, 41, 595-616.

Clark, D. P. The fermentation pathway of *Escherichia coli*. FEMS Microbiol. Rev. 1989, 63, 223-234.

Cooper, R. A. Intermediary metabolism of monosaccharides by bacteria. In: "International review of biochemistry, Biochemistry of carbohydrates II", Vol. 16, Manners, D.J.(ed.), University Park Press, Baltimore, 1978, 37-73.

Cooper, R. A. Convergent pathways of sugar catabolism in bacteria. In: "Carbonhydrate metabolism in cultured cells." Morgan, M. J. (ed.), Plenum Press, London, 1986, 461-491

Curtis, S. J. and Epstein, W. Phosphorylation of D-Glucose in *Escherichia coli* mutants defective in glucosephosphotransferase, mannosephosphotransferase, and glucokinase. J. Bacteriol. 1975, June, 1189-1199.

Dawes, E. A. Microbial energetics, Blackie, London. 1986.

Diaz-Ricci, J. C.; Hitzmann, B.; Rinas, U. and Bailey, J. E. Comparative studies of glucose catabolism by *Escherichia coli* grown in a complex medium under aerobic and anaerobic conditions. Biotechnol. Prog. 1990, 6(5), 326-332.

Driessen, M.; Postma, P. W. and van Dam, K. Energetics of glucose uptake in *Salmonella typhimurium*. Arch. Microbiol. 1987, 146, 358-361.

Fukuda, Y.; Yamaguchi, S.; Shimosaka, M.; Murata, K. and Kimura, A. Cloning of the glucokinase gene in *Escherichia coli* B. J. Bacteriol., 1983, Nov., 992-925.

Fukuda, Y.; Yamaguchi, S.; Shimosaka, M.; Murata, K. and Kimura, A. Purification and characterization of glucokinase in *Escherichia coli* B. Agric. Biol. Chem., 1984, 48(10), 2541-2548.

Gadian, D. G. et al Appendix 1: The ^{31}P chemical shifts of biological phosphorus compounds, measured as a function of pH. In: "Biological applications of magnetic resonance", Shulman, R. G. (ed.), Academic Press, 1979, 531-535.

Georgiou, G. Optimizing the production of recombinant proteins in microgranisms. AIChE J. 1988, 34(8), 1233-1248.

Henderson, P. J. F.; Giddens, R. A. and Jones-Mortimer, M. C. Transport of galactose, glucose and their molecular analogues by *Escherichia coli* K12. Biochem. J. 1977, 162, 309-320.

Henderson, P. J. F. and Maiden, M. C. J. Transport of carbohydrates by bacteria. In: " Carbon substrates in biotechnology", J. D. Stower et al. (ed.), IRL press, 1987, 67-92.

Holms, W. H. The central metabolic pathways of *Escherichia coli*: relationship between flux and control at a branch point, efficiency of conversion to biomass, and excretion of acetate. Current topics in cellular regulation, 1986, 28, 69-105.

Kundig, W. Molecular interations in the bacterial phosphoenolpyruvate-phosphotransferase system (PTS). J. Supramol. Struct. 1986, 2, 695-714.

Lowry, O. H.; Carter, J.; Ward, J. B. and Glaser, L. The effect of carbon and nitrogen sources on the level of metabolic intermediates in *Escherichia coli*. J. Biolog. Chem., 1971, 246(21), 6511-6521.

Lundberg, P.; Harmsen, E.; Ho, C. and Vogel, H. J. Nuclear magnetic resonance studies of cellular metabolism. Analyt. Biochem. 1990, 191, 193-222.

Navon, G.; Shulman, R. G.; Yamane, T.; Eccleshall, T. R.; Lam, K.; Baronofsky, J. J. and Marmur, J. Phosphorus-31 nuclear magnetic resonance studies of wild type and glycolytic pathway mutants of *Sacchromyces cerevisiae*. Biochem. 1979, 18(21), 4487-4499.

Neidhardt, F. C; Ingraham, J. L. and Schaechter, M. In: " Physiology of the bacerial cell, a molcular appoach", Sinauer Associates, Inc. Publishers, Sunderland, Massachusettes, 1990, 174-182.

Muir, M. Williams, L. and Ferenci, T. The influence of transport energization on the growth yield of *Escherichia coli*. J. Bacteriol. 1985, 163, 1237-1242.

Postma, P. W. and Lengeler, L. W. PEP: carbohydrate phosphotransferase system of bacteria. Microbiol. Rev. 1985, 49, 232-269.

Postma, P. W. Phosphotransferase system for glucose and other sugars. In: "*Escherichia coli* and *Salmonella typhimurium* cellular and molecular biology, volume I " Neidhardt F. C. (ed.), American Society for Microbiology, Washington, D. C. 1987, 127-141.

Roberts, J. K. M. and Jardetzky, O. Monitoring of cellular metabolism by NMR. Biochim. Biophys. Acta. 1981, 639, 53-76.

Robitaille, P. L.; Robitaille, P. A.; Brown, G. G. JR. and Brown, G. G. An analysis of the pH-dependent chemical-shift behavior of phosphorus-containing metabolites. J. Magn. Reson. 1991, 92, 73-84.

Saier, M. H. Mechanisms and regulation of carbohydrate transport in bacteria. Academic Press, New York. 1985.

Shanks, J. Metabolic engineering applications of *in vivo* ^{31}P and ^{13}C NMR studies of *Sacchromyces cerevisiae*. Ph.D. Thesis, Caltech, 1988.

Stryer, L. Chater 18: Pentose phosphate pathway and gluconeogenesis. In: "Biochemistry" (3rd. ed.) Freeman & Co. N. Y. 1988. 438-443.

Ugurbil, K.; Rottenberg, H.; Glynn, P. and Shulman, R. G. ^{31}P nuclear magnetic resonance studies of bioenergetics and glycolysis in anaerobic *Escherichia coli* cells. Proc. Natl. Acad. Sci. USA, 1978, 75(5), 2224-2248.

Ugurbil, K.; Shulman, R. G. and Brown, T. R. High resolution ^{31}P and ^{13}C nuclear magnetic resonance studies of *Escherichia coli* cells *in vivo*. In: "Biological applications of magnetic resonance" (Shulman, R. G. ed.), Academic Press, Inc. 1979, 537-589.

Zabriskie, D. W. and Arcuri, E. J. Factors influencing productivity of fermentations employing recombinant microorganisms. Enzyme Microb. Technol. 1986, 8, 706-717.

4.8 TABLES

Table 4.1. Intracellular concentrations measured by ^{31}P NMR

	SP	NTP	NAD(H)	UDPG
		Aerobic Condition		
PPA305	38.0±0.5	5.2±0.2	12.8±0.3	
PPA316	14.5±0.5	0.8±0.1	5.9±0.2	1.6±0.3
		Anaerobic Condition		
PPA305	39.3±0.5	4.0±0.2	14.7±0.3	
PPA316	28.0±0.5	0.8±0.1	5.4±0.2	2.8±0.3

Concentrations are in mM and averages of at least three separate experiments.

Table 4.2 S-P Concentrations measured by extract NMR

	Aerobic	Aerobic	Anaerobic	Anaerobic
	PPA305	PPA316	PPA305	PPA316
G-6-P	1.2	1.5	2.1	0.7
3-PGA	1.3	0.6	1.3	1.0
FDP+F-6-P	26.4	9.4	33.4	18.0
F-6-P	n.d.	2.9	n.d.	n.d.
2-PGA	6.0	2.2	3.8	3.2
S-P-Un	3.9	2.5	3.3	5.6
S-P total	38.8	16.2	43.9	29.1
PEP	7.9	0.8	30.0	18.4

Concentrations are in mM and are averages of at least three separate experiments. S-P-Un: unidentified sugar phosphate, other abbreviations are the same as figure 4.10, 4.11 and 4.12. The mean relative error: 20%.

n.d.--- not determined.

Table 4.3 Range of NADH and NAD^+

Concentration mM	NADH	NAD^+
Aerobic PPA305	0.4-0.9	11.9-12.4
Aerobic PPA316	0.2-0.4	5.5-5.9
Anaerobic PPA305	0.4-1.1	13.6-14.3
Anaerobic PPA316	0.2-0.7	4.7-5.2

Data from Table 4.1, assuming $NAD^+/(NAD^+ + NADH) = 0.93\text{-}0.97$.

4.9 FIGURES

Figure captions

Figure 4.1 Schematic presentation of the galactose-proton symport system. Glucose, as shown in the figure, as well as galactose can be transported by this system.

Figure 4.2 A simplified schematic presentation of the phosphoenolpyruvate: glucose phosphotransferase (PTS) system in *E. coli*. HPr, EI, EII and EIII are enzymes involved in PTS system. HPr, EI are the general PTS proteins. EII(glu) and EIII(glu) are specific for glucose. Phospho-EII(glu), Phospho-HPr are the phosphorylated forms of enzyme III and enzyme HPr.

Figure 4.3 Time-trajectories of biomass, glucose and acetate during growth under aerobic conditions. Open symbols are for the wild-type PPA305, solid symbols are for the mutant PPA316. (□) ----glucose; (O) ---- biomass; (Δ) ----acetate.

Figure 4.4 Time-trajectories of biomass and glucose under anaerobic conditions. Symbols are the same as figure 4.3.

Figure 4.5 Evolutions of fermentation products in the supernatant during growth under anaerobic conditions. Open circles are for the wild-type PPA305 and solid circles are for the mutant PPA316. a.) acetate; b.) ethanol; c.) lactate; d.) formate; e.) succinate

Figure 4.6 Flux to pyruvate, data taken from figure 4.4 and figure 4.5. Open circles are for PPA304 and solid circles are for PPA316.

Figure 4.7 ^{31}P NMR spectra acquired during anaerobic glycolysis of *E. coli* strains PPA305 (top spectrum) and PPA316 (bottom spectrum). Spectra were obtained using 40^{o} pulse and a relaxation delay of 0.2 s, other parameters as in the Materials and Methods. Abbreviations: SP: sugar phosphate; P_i^{cyt}: intracellular inorganic phosphate; P_i^{ex} : extracellular inorganic phosphate; NTP: nucleoside triphosphate; NDP: nucleoside diphosphate; NAD(H): nicotinamide adenine dinucleotide; UDPG: uridinediphosphoglucose.

Figure 4.8 pH evolutions of PPA305 (left part) and PPA316 (right part) during steady-state glycolysis under anaerobic conditions.

Figure 4.9 Plots of ΔpH versus time for PPA305 and PPA316 during steady-state glycolysis under anaerobic conditions. Data were taken from figure 4.9.

Figure 4.10 ^{31}P NMR proton decoupled spectra of PCA extract of PPA305. Spectra were obtained using 90^{o} pulse and a relaxation delay of 1.0 s,

other parameters as in the Materials and Methods. Abbreviations: Pi: inorganic phosphate; PEP: phosphoenolpyruvate. A line broadening (LB) of 2 Hz was used.

Figure 4.11 ^{31}P NMR proton decoupled spectra of PCA extract of PPA316. Parameters and abbreviations are the same as figure 4.10.

Figure 4.12 Expanded S-P region of the spectra shown in figure 4.10 and figure 4.11. Abbreviations: G-6-P: glucose-6-phosphate; F-6-P: fructose-6-phosphate; FDP: fructose-1,6-bisphosphate; 3-PGA: 3-phosphoglycerate; 2-PGA: 2-phosphoglycerate

Figure 4.1

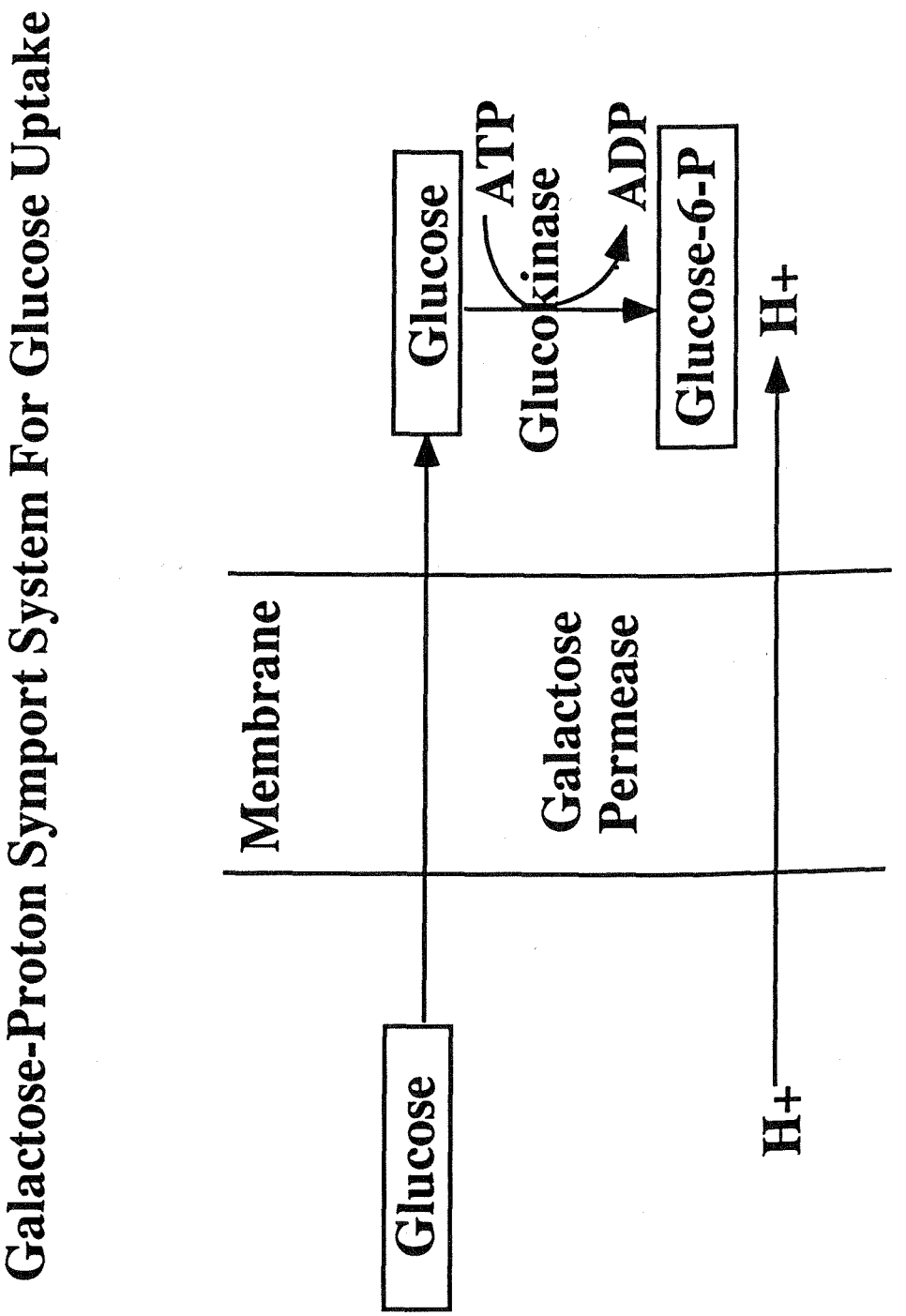
Galactose-Proton Symport System For Glucose Uptake
Glucose
Membrane
Galactose
Permease
Glucose
ATP
Glucokinase
ADP
Glucose-6-P
H+
H+

Figure 4.2

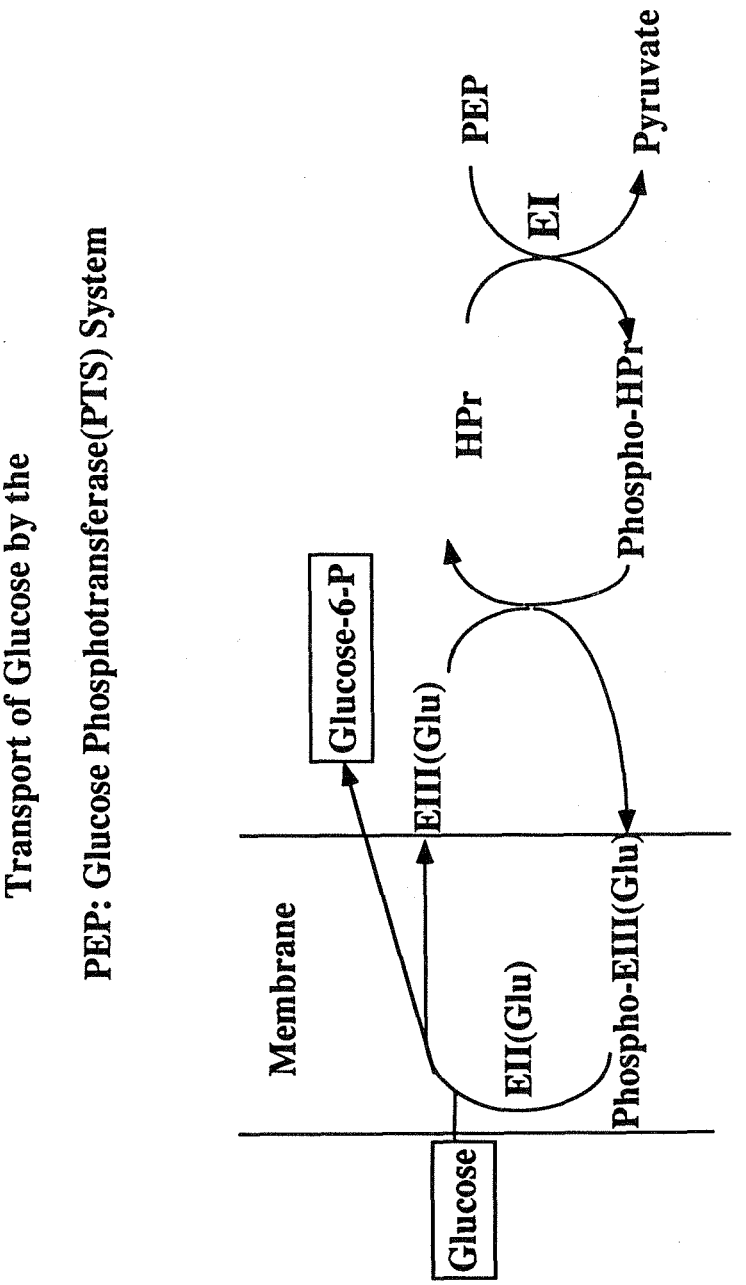
Transport of Glucose by the
PEP: Glucose Phosphotransferase(PTS) System
Membrane
Glucose
EII(Glu)
Phospho-EIII(Glu)
EIII(Glu)
Glucose-6-P
HPr
Phospho-HPr
EI
PEP
Pyruvate

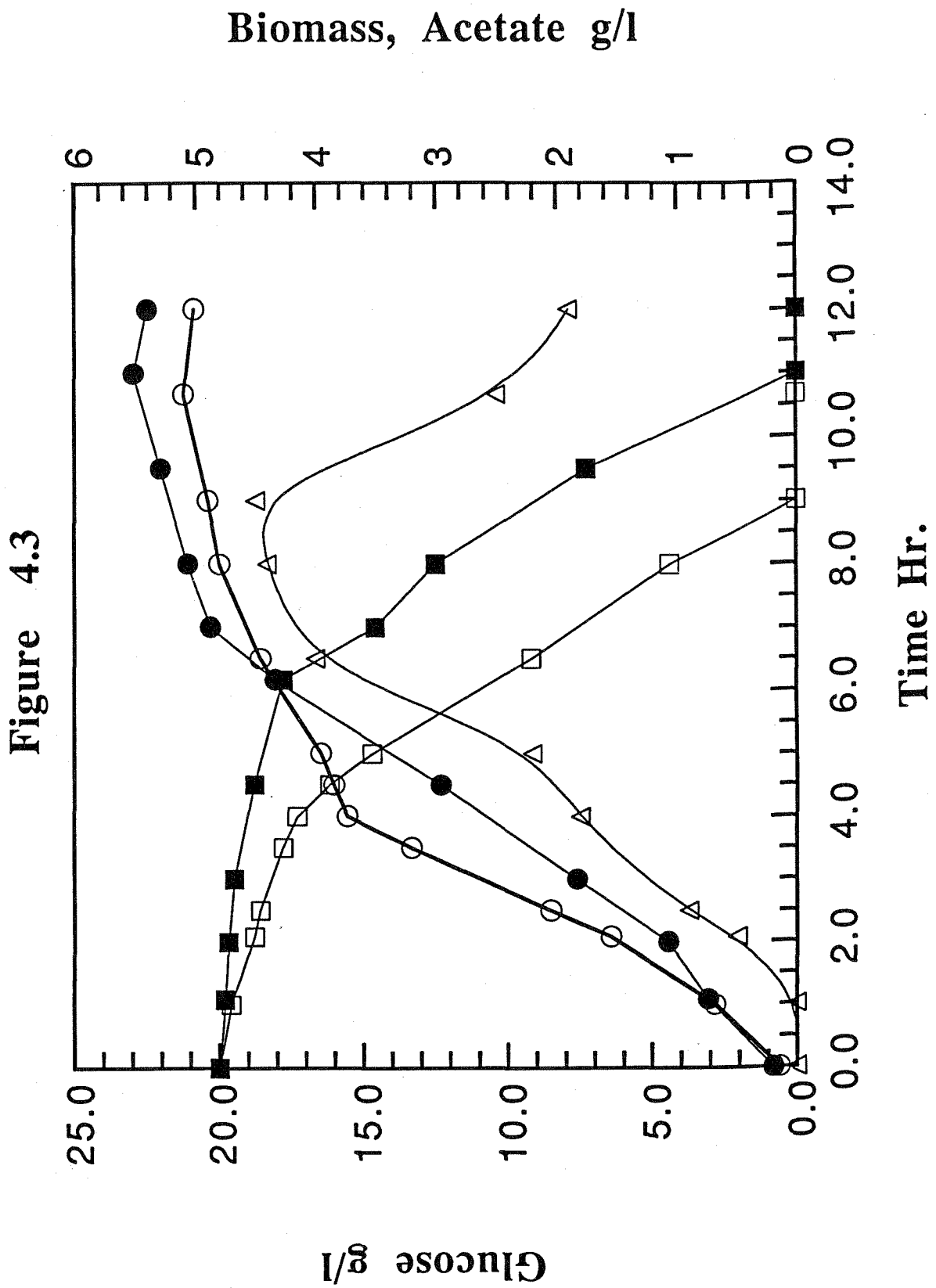
Biomass, Acetate g/l
Glucose g/l
Time Hr.
25.0
20.0
15.0
10.0
5.0
0.0
0.0
2.0
4.0
6.0
8.0
10.0
12.0
14.0
0
1
2
3
4
5
6

Figure 4.3

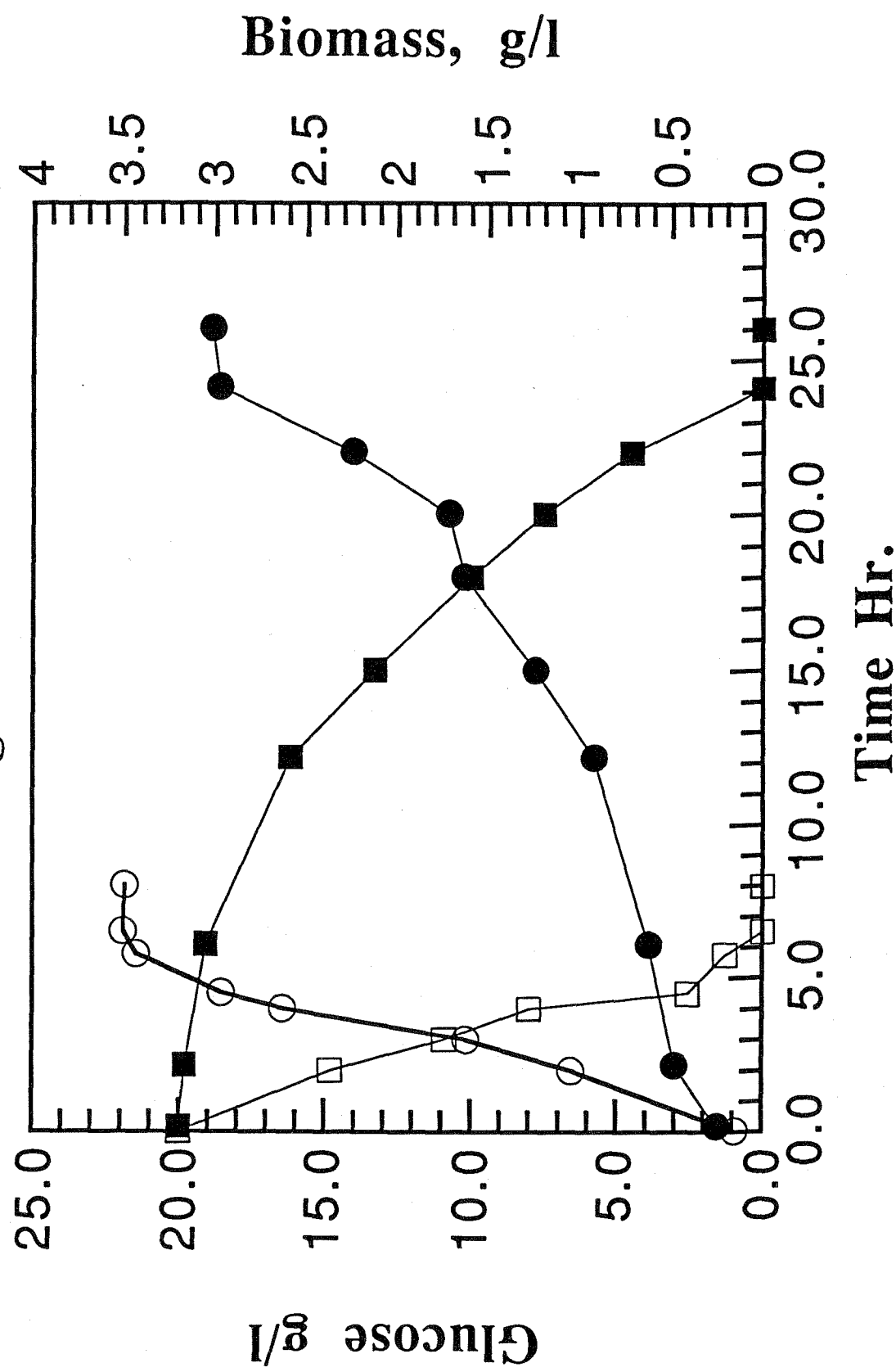
Biomass, g/l
4
3.5
3
2.5
2
1.5
1
0.5
0
30.0
25.0
20.0
15.0
10.0
5.0
0.0
Time Hr.
Glucose g/l
25.0
20.0
15.0
10.0
5.0
0.0

Figure 4.4

Figure 4.5 a-c

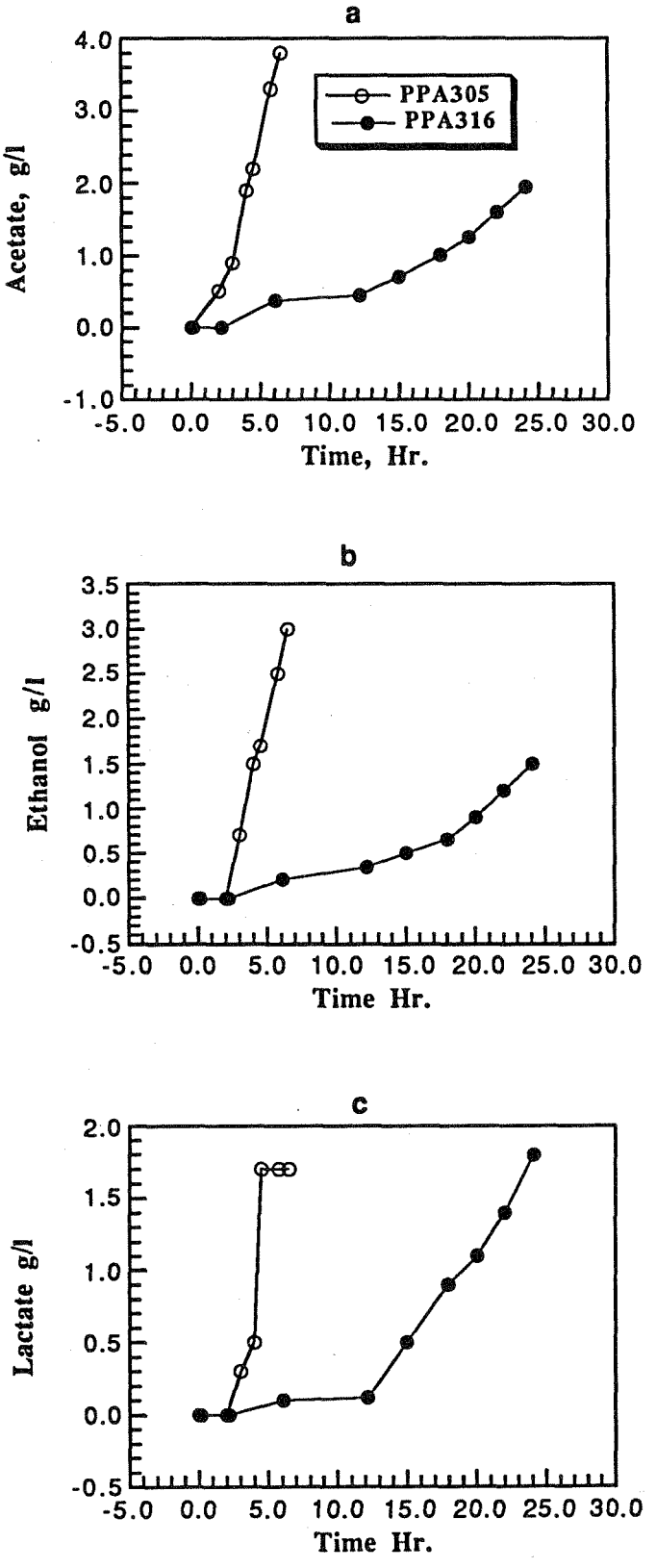
a
PPA305
PPA316
Acetate, g/l
4.0
3.0
2.0
1.0
0.0
-1.0
-5.0 0.0 5.0 10.0 15.0 20.0 25.0 30.0
Time, Hr.
b
Ethanol g/l
3.5
3.0
2.5
2.0
1.5
1.0
0.5
0.0
-0.5
-5.0 0.0 5.0 10.0 15.0 20.0 25.0 30.0
Time Hr.
c
Lactate g/l
2.0
1.5
1.0
0.5
0.0
-0.5
-5.0 0.0 5.0 10.0 15.0 20.0 25.0 30.0
Time Hr.

Figure 4.5 d-e

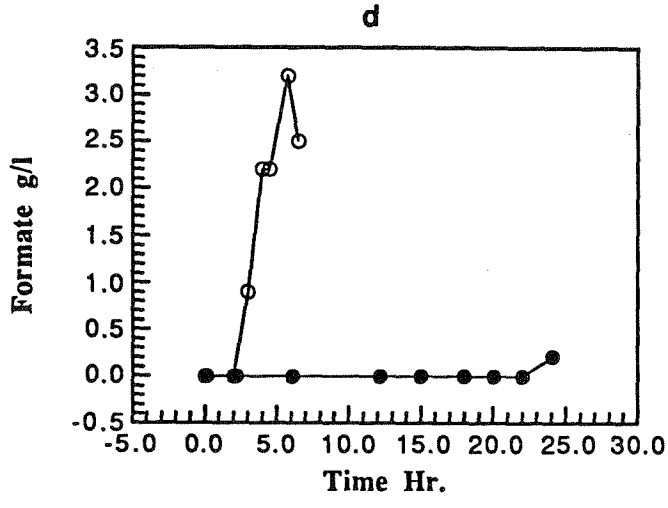
d
Formate g/l
3.5
3.0
2.5
2.0
1.5
1.0
0.5
0.0
-0.5
-5.0 0.0 5.0 10.0 15.0 20.0 25.0 30.0
Time Hr.

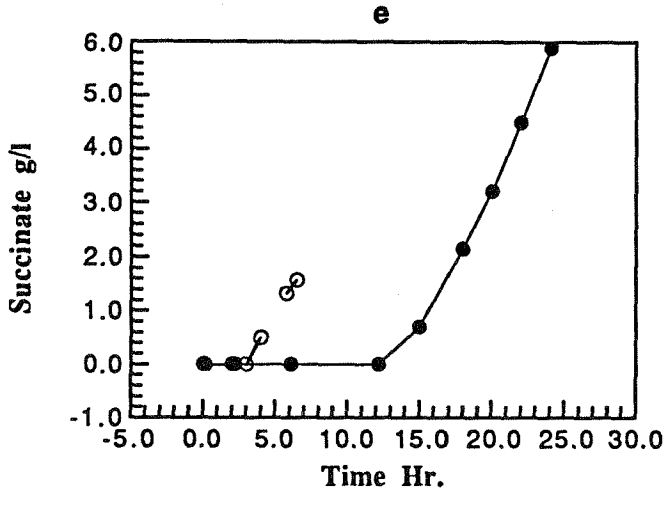
e
Succinate g/l
6.0
5.0
4.0
3.0
2.0
1.0
0.0
-1.0
-5.0 0.0 5.0 10.0 15.0 20.0 25.0 30.0
Time Hr.

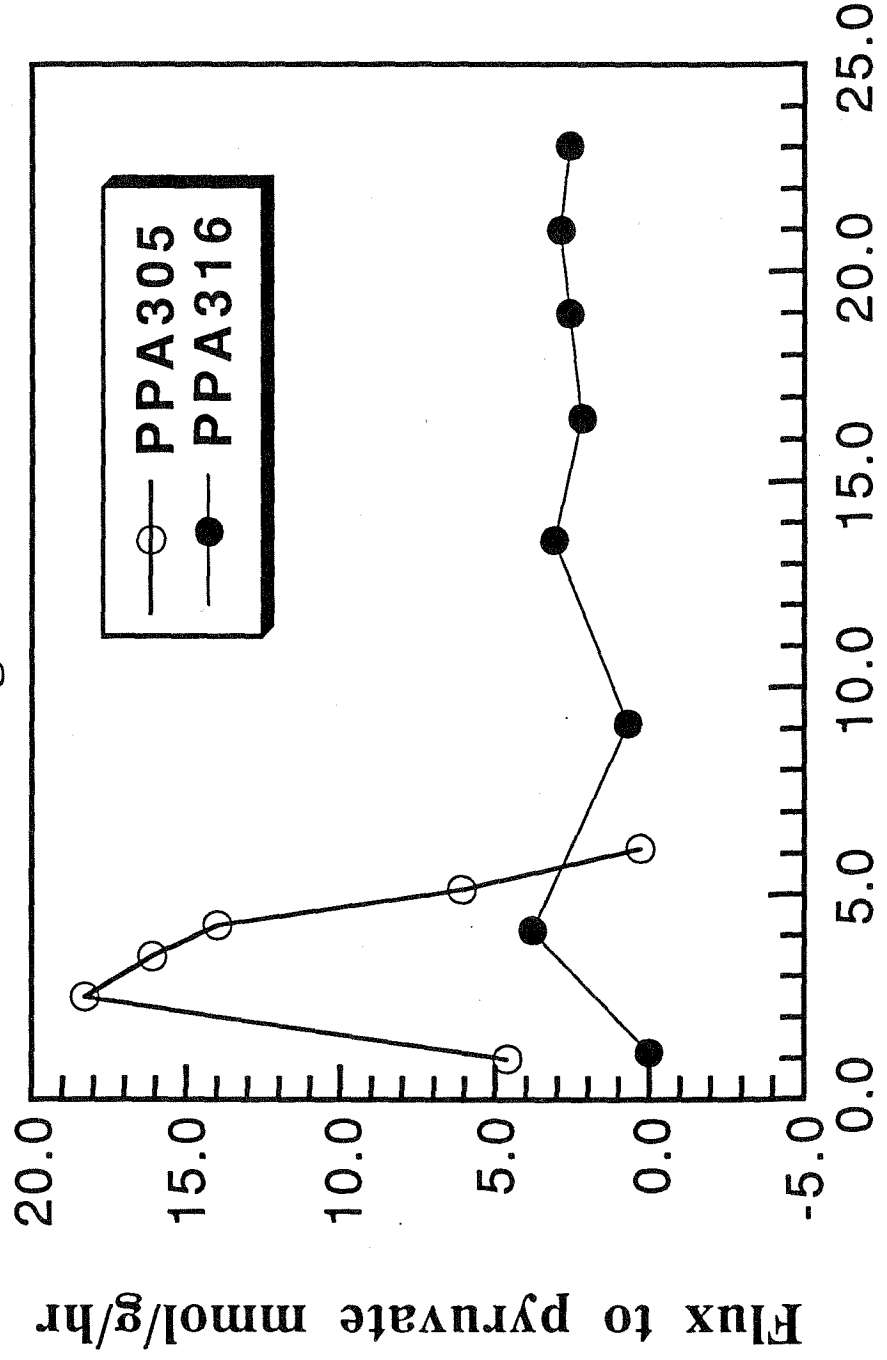
PPA305
PPA316
20.0
15.0
10.0
5.0
0.0
-5.0
0.0
5.0
10.0
15.0
20.0
25.0
Time Hr
Flux to pyruvate mmol/g/hr

Figure 4.6

Figure 4.7

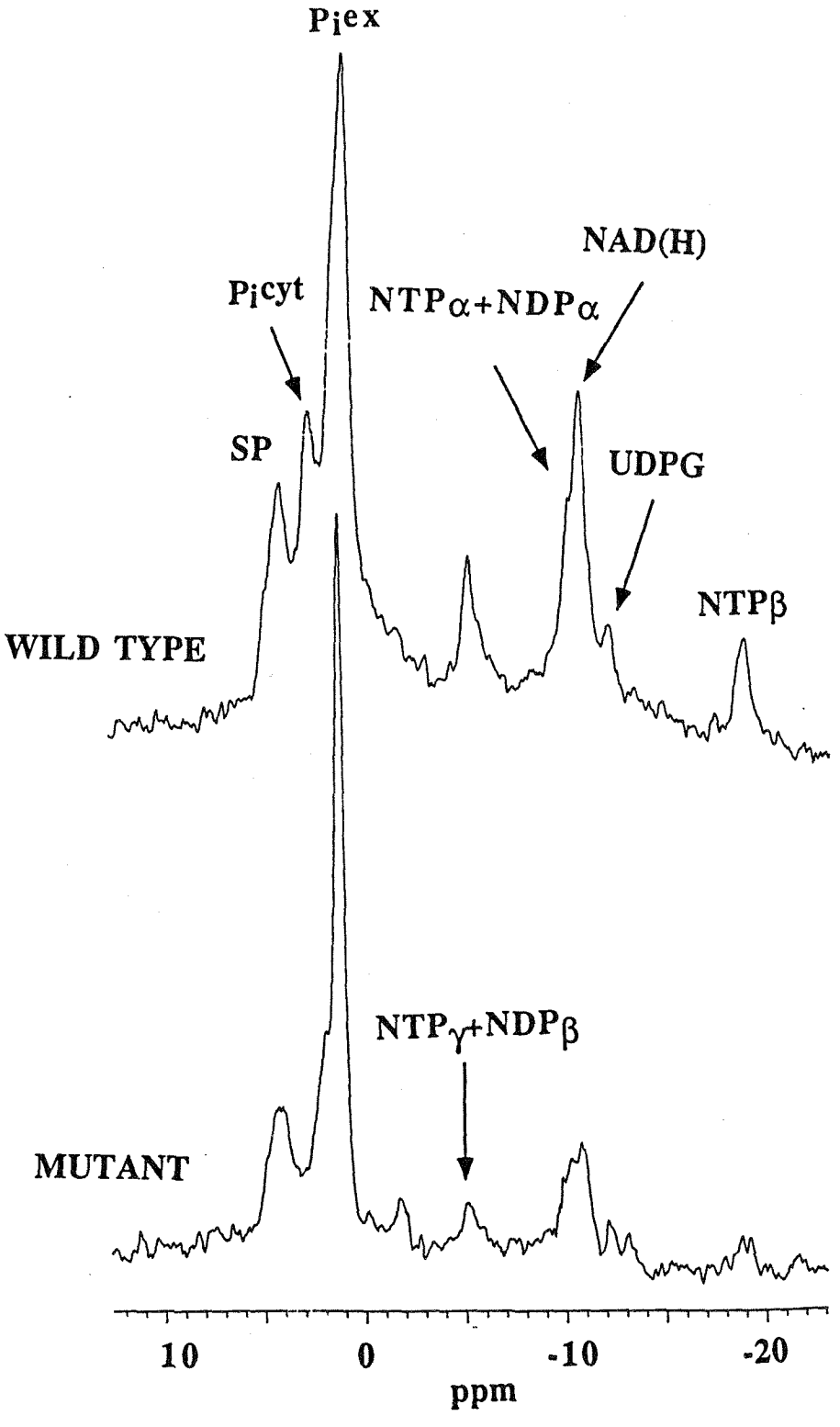
Piex
NAD(H)
Picyt
NTPα+NDPα
SP
UDPG
NTPβ
WILD TYPE
NTPγ+NDPβ
MUTANT
10
0
-10
-20
ppm

Figure 4.8

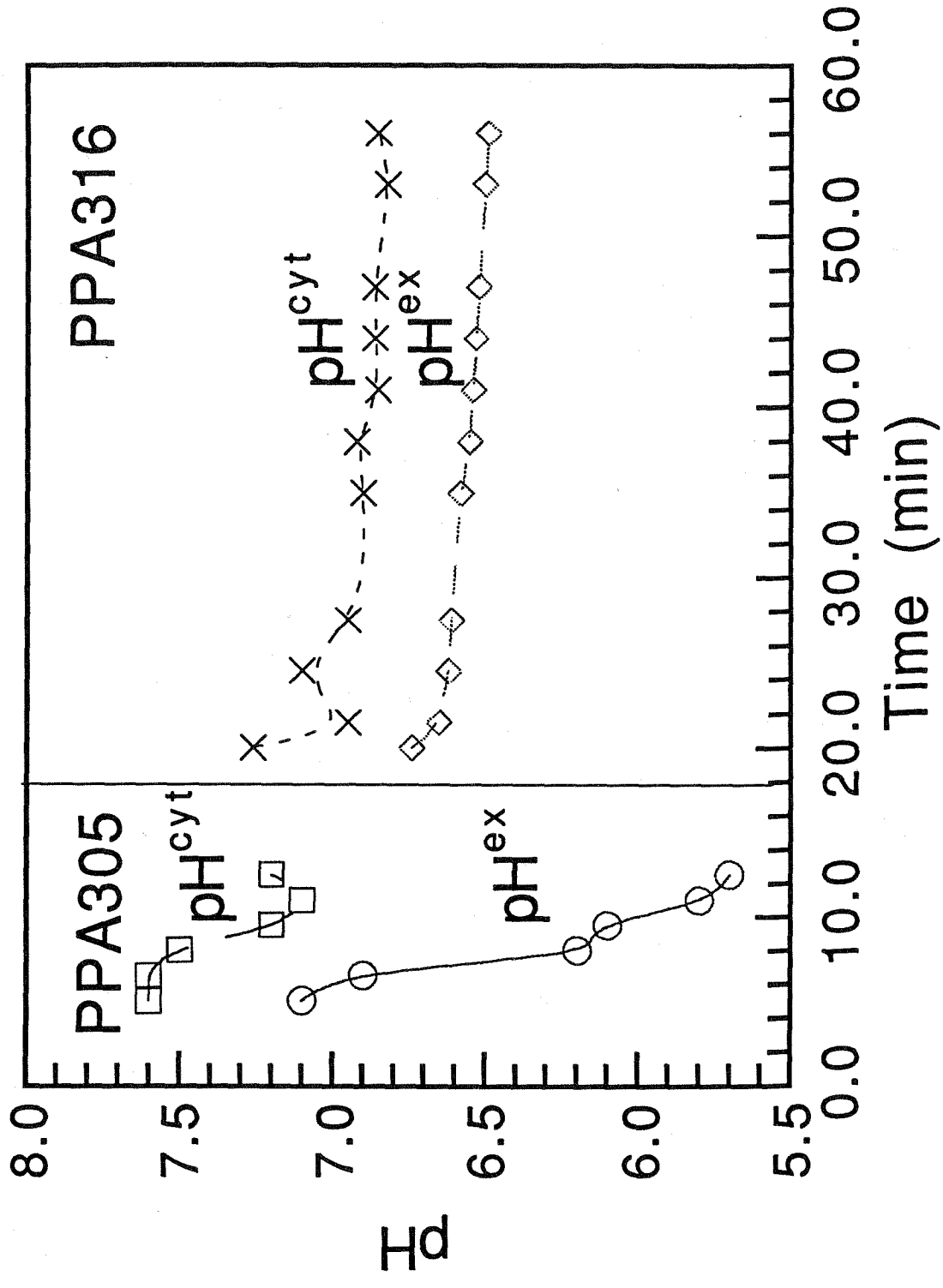
PPA316
PPA305
pH^cyt
pH^ex
pH^cyt
pH^ex
pH
8.0
7.5
7.0
6.5
6.0
5.5
0.0
10.0
20.0
30.0
40.0
50.0
60.0
Time (min)

Figure 4.9

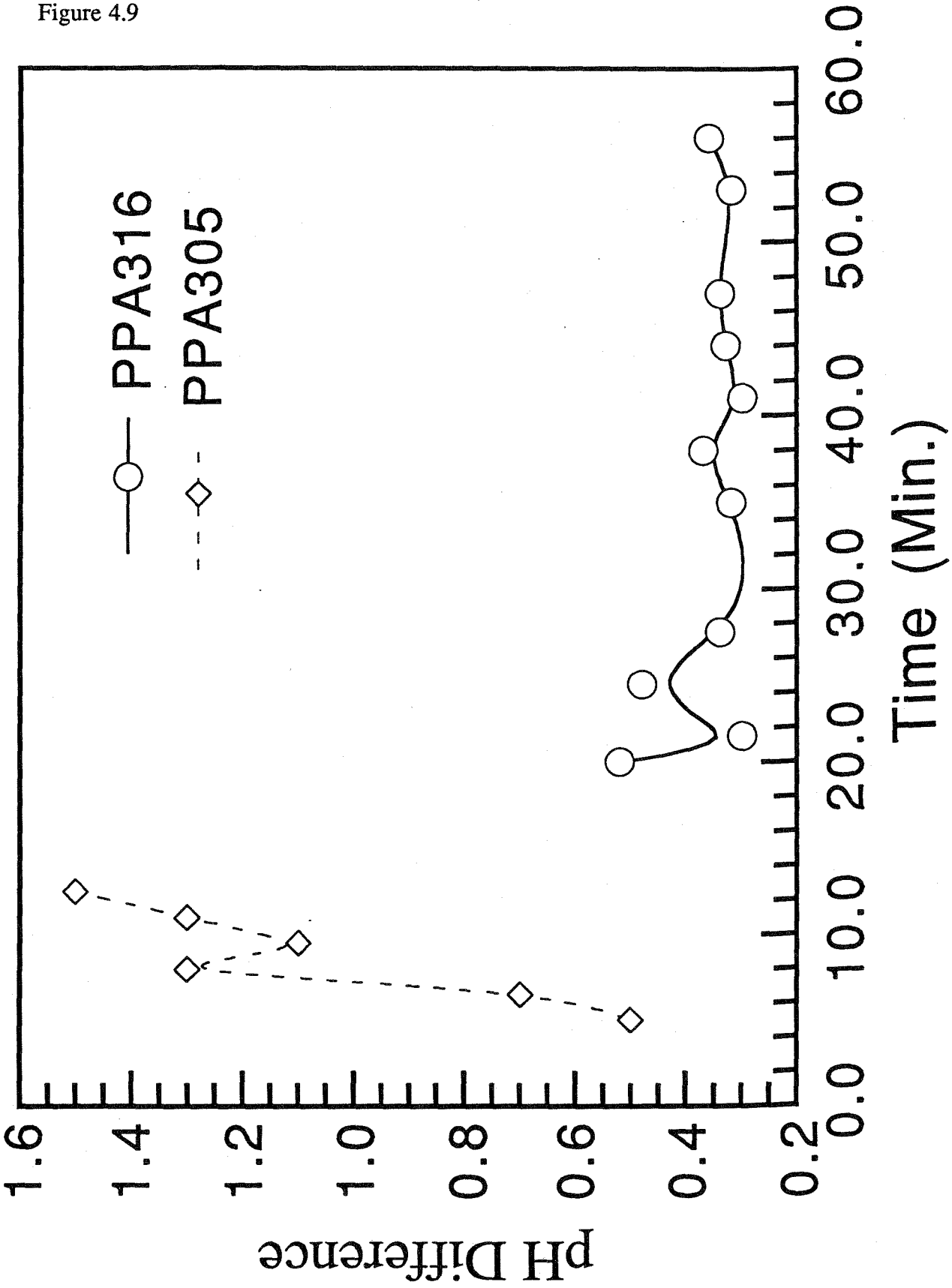
PPA316
PPA305
pH Difference
Time (Min.)
1.6
1.4
1.2
1.0
0.8
0.6
0.4
0.2
0.0
10.0
20.0
30.0
40.0
50.0
60.0

Figure 4.10

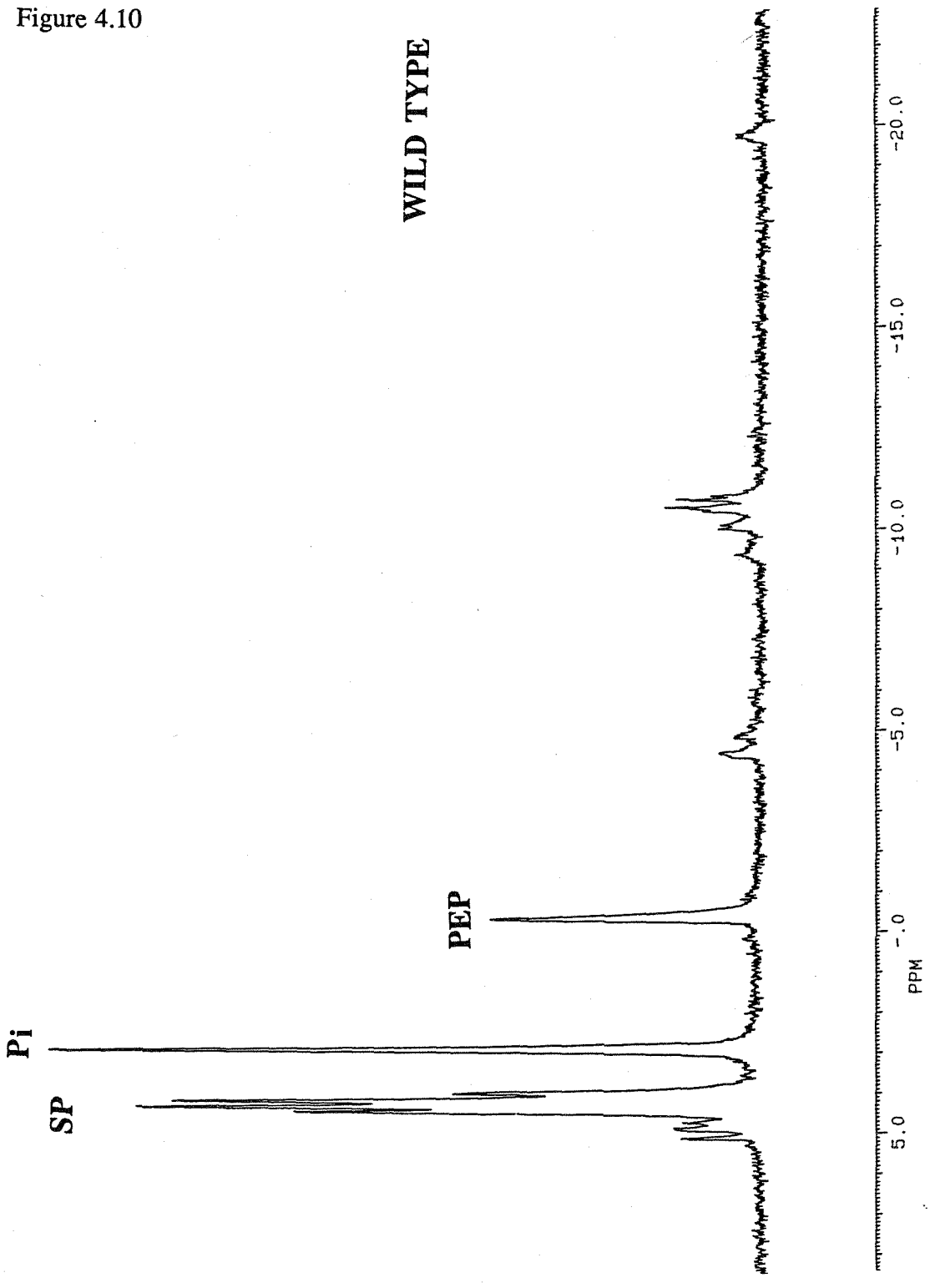

Figure 4.11

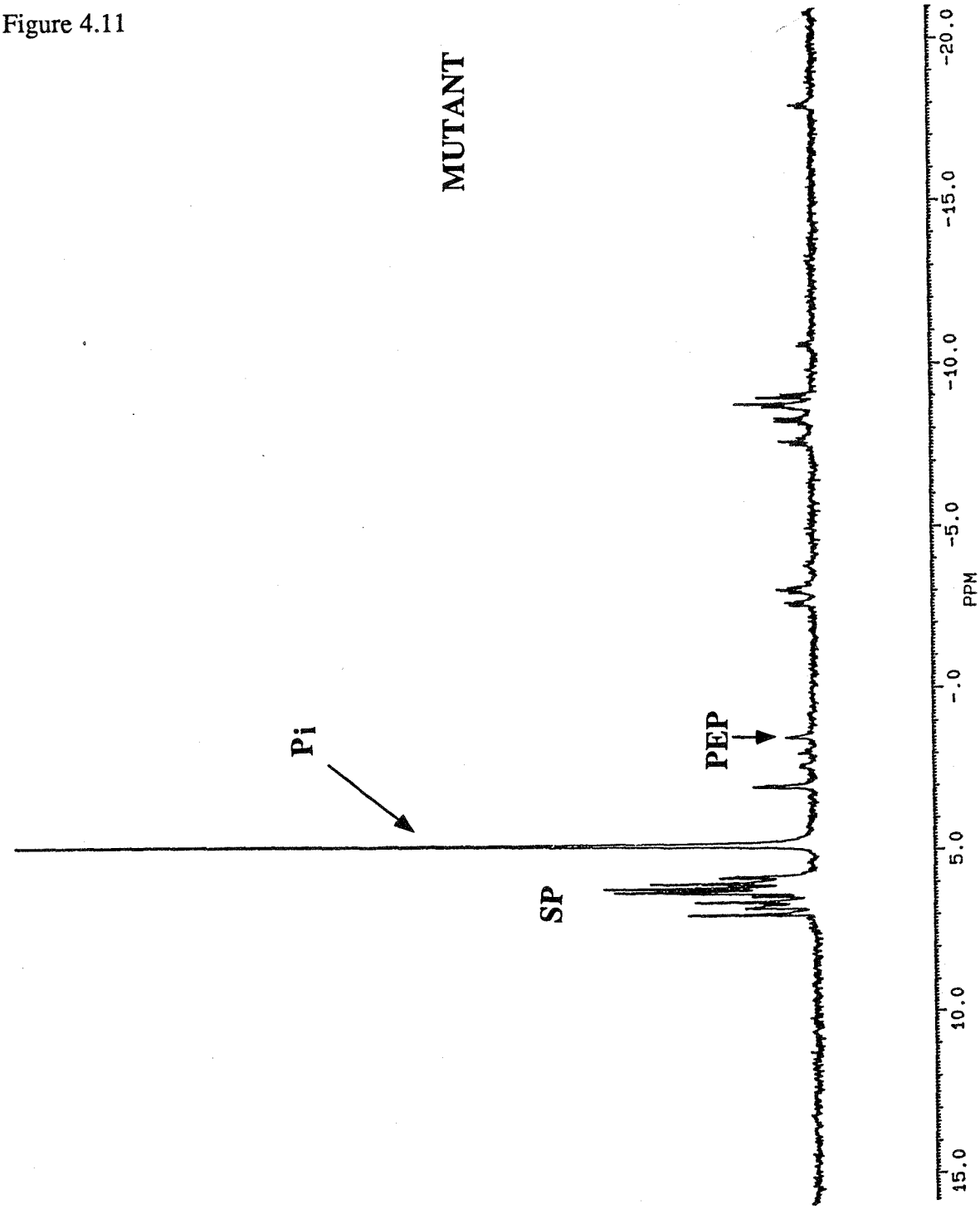

Figure 4.12

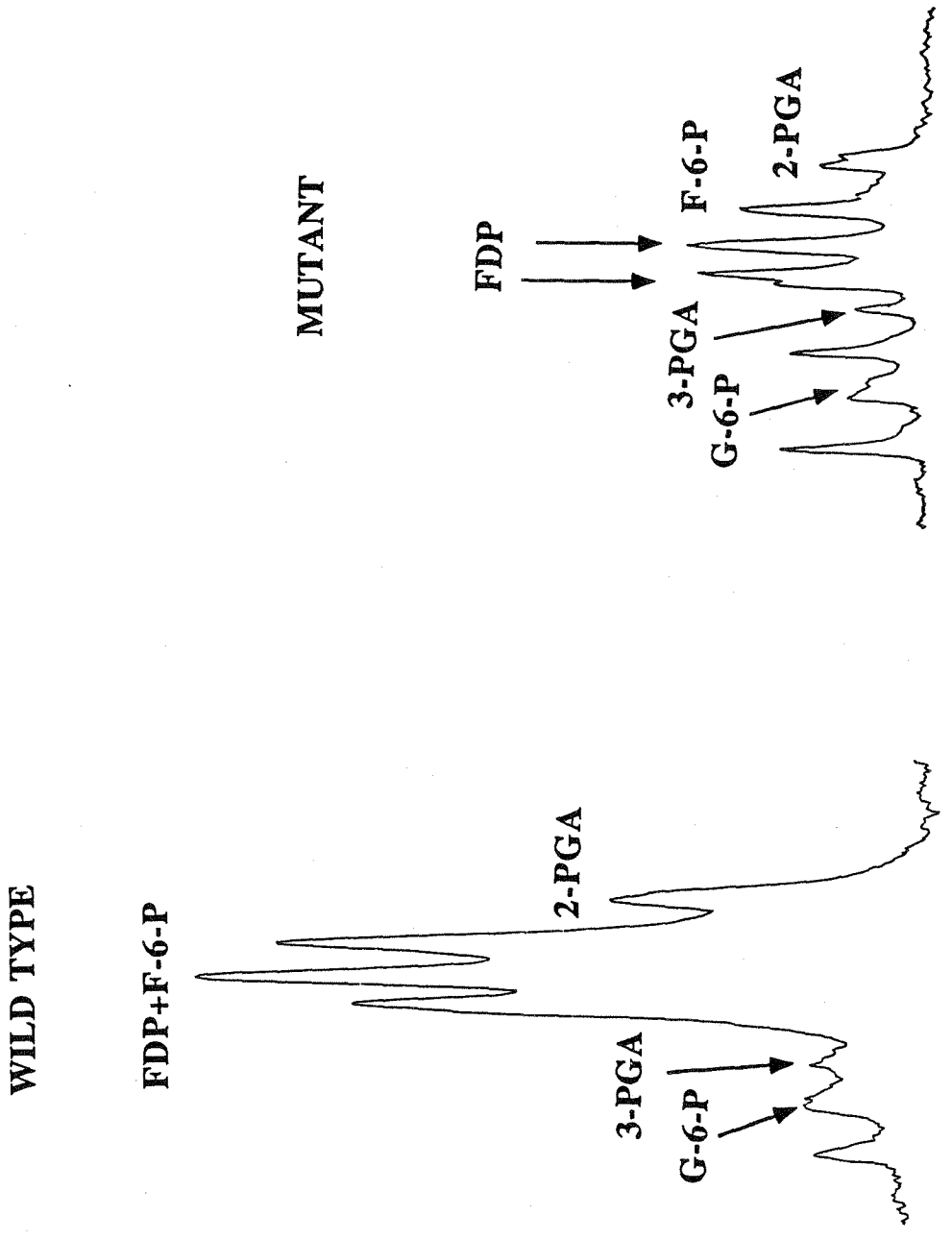

Chapter 5

Using a PTS Mutant for Phenylalanine Production

5.1 ABSTRACT

E. coli strains PPA305, which has a wild-type PTS system, and PPA316, which utilizes a proton-galactose symport system for glucose uptake, were used as host strains to harbor a phenylalanine overproduction plasmid pSY130-14 and to study the effects of using different glucose uptake systems on phenylalanine production. The non-PTS strain (PPA316/pSY130-14) produced much less phenylalanine, ranging from 0 to 67% of that produced by the PTS strain (PPA305/pSY130-14) depending on cultivation conditions used. The non-PTS strain PPA316/pSY130-14 had intracellular PEP concentration only one-sixth of the PTS strain, PPA305/pSY130-14. Additionally, PPA316/pSY130-14 had a substantially lower energy state in terms of the size of the pool of high-energy phosphate compounds and the magnitude of pH difference across the cytoplasmic membrane. The non-PTS strain consumed oxygen at a higher rate, attained lower biomass concentration and produced no acetate and phenylalanine during fermentation, suggesting more carbon was oxidized to CO_2, likely through the TCA cycle.

5.2 INTRODUCTION

Plants and microbes are known to possess abilities to convert simple carbohydrates such as glucose to aromatic amino acids and related metabolites (Weiss and Edwards, 1980). The aromatic amino acids phenylalanine, tyrosine and tryptophan are mainly used as human and animal dietary supplements. Industrial production of other compounds for example, indigo and eumelanin, derived from these three aromatic amino acids are being pursued for specific applications. Eumelanin has a unique UV-absorbing characteristics (Draths et al. 1992; Bell and Wheeler, 1986). The production of phenylalanine is of particular interest, because it is one of the essential raw materials in the manufacture of the low calorie sweetener " Aspartame," which is estimated to be at least 150 times sweeter than sucrose (Huang et al. 1985) and presently enjoys a large market worldwide.

Phenylalanine is synthesized from its precursors phosphoenolpyruvate (PEP) and erythrose-4-phosphate (E4P) through a highly controlled biosynthesis pathway. Figure 5.1 presents a simplified phenylalanine biosynthesis pathway of *E. coli,* showing the involvement of all major precursors, reducing equivalents and ATP. Also shown in the figure 5.1 are two regulatory enzymes whose controls are affected by a combination of feedback inhibition, feedback repression and attenuation (Pittard, 1987). DAHP synthase, which catalyzes the first committed step in the pathway, the condensation of PEP and E4P to synthesize 3-deoxy-arabino-heptulosonate-7-phosphate (DAHP), serves as the first control. *E. coli* has three isoenzymes of DAHP synthase, each subject to feedback control of a different amino acid at both genetic and enzymatic levels (aroG by phenylalanine, aroF by tyrosine and aroH by

tryptophan). The other regulatory enzyme is a bifunctional enzyme, chorismate mutase P-prephenate dehydratase, catalyzing two reactions from chorismate to phenylpyruvate (figure 5.1). The synthesis of chorismate mutase P-prephenate dehydratase is repressed by phenylalanine and is also regulated by transcriptional termination, i.e., attenuation (Brown, 1968; Zurawski et al. 1978). Phenylalanine also inhibits the activity of the enzyme. Because of the rigorous regulation of the pathway by the end product, only genetically modified strains would produce phenylalanine beyond the level needed for cell growth.

Metabolic engineering has been successfully used to deregulate the rigid control in phenylalanine biosynthetic pathway. Genetic strain improvement is facilitated by the fact that the detailed biosynthetic pathway and its regulation are known. Regulation at genetic level can be circumvented by replacing native promotors with a strong, synthetic promotor so that the expression of the enzymes involved in the phenylalanine production is controlled by a chemical added (e.g., IPTG), by temperature or other means (Sugimoto, 1987). Selecting resistance to a toxic phenylalanine analogue is a commonly used method to further desensitize feedback regulation (Backman et al. 1990; Sugimoto et al. 1985). Using these methods, a hyperproducing strain can be constructed. Notably, fermentation processes have been developed (Backman et al. 1990; Konstantinov, 1991), in which a final phenylalanine concentration of 50 g/l can be obtained with a yield approaching the theoretical yield (Forberg, 1988), 0.27 g/g (for PTS strains, in grams of phenylalanine produced per gram of glucose consumed).

It then follows that further improvements of the process would come from the modification of the primary carbon metabolism pathway, which supplies precursors

(PEP, E4P), reducing power (NADPH) and energy (ATP) required for the synthesis. Earlier studies showed that increasing the pool of PEP was important, although no measurements of PEP concentration were made. A transient accumulation of trehalose was observed in an aromatic amino acid overproducing strain, this phenomenon was speculated to be caused by a depletion PEP pool in this strain. Since phosphoenolpyruvate carboxylase (*ppc*) is responsible to divert PEP to the TCA cycle, it appears that mutations in *ppc* is effective in increasing PEP concentrations and thus also the phenylalanine production of aromatic amino acids. In fact, an industrial tryptophan producing strain (*Corynebacterium glutamicum)* carries a mutation in *ppc* gene (Hodgson, 1994). A mutation in *ppc* of an *E. coli* strain was also found to increase phenylalanine production by a factor of six (on cell mass basis), however, this mutation directed substantial glucose into waste products, especially acetate and pyruvate (Miller et al, 1987).

A stoichiometry analysis of phenylalanine synthesis using PTS and non-PTS glucose uptake systems leads to following two equations (Ahn, 1992):

For PTS strains:

$$4\ \text{Glucose} + NH_3 + 6NAD^+ + 2NADP^+ + 2ADP + 2Pi \Longrightarrow$$
$$\text{Phenylalanine} + 4\ \text{Pyruvate} + 3\ CO_2 + 6\ \text{NADH} + 2\ \text{NADPH} + 8\ H^+ + 2\text{ATP} \qquad 5.1$$

For strains using proton-galactose symport system:

$$2\ \text{Glucose} + NH_3 + 2\text{ATP} + 2NAD^+ + 2NADP^+ \Longrightarrow$$
$$\text{Phenylalanine} + 3\ CO_2 + 2\ \text{NADH} + 2\ \text{NADPH} + 5\ H^+ + 2\text{ADP} + 2\text{Pi} \qquad 5.2$$

This analysis predicts a 100% increase of theoretic yield of phenylalanine from glucose in a strain using a proton symport system for glucose uptake from 0.23 g/g (slightly different from 0.27 g/g, Forberg, 1988, due to different methods used) to 0.46 g/l. While CO_2 production remains the same, switching glucose uptake system from a PTS system to a non-PTS (galactose-proton symport system in this case) eliminates by-product pyruvate production. Assuming aerobic condition, by coupling to the respiratory chain, one mole NADH can generate 2 moles of ATP and expel 4 moles of H^+. From eqn. 5.1 and eqn. 5.2, 14 moles ATP would be produced and 16 moles proton be extruded per each mole of phenylalanine synthesized in a PTS system, compared to 2 moles ATP produced and 3 moles protons extruded in a proton symport system.

Consequently, it is perceivable that using different glucose uptake system for phenylalanine production can dramatically influence cell energetics (ATP levels and membrane energization) and metabolism as well as phenylalanine production.

^{31}P NMR was used in this study to monitor cell energetic states (ΔpH across the cytoplasmic membrane and NTP level), NAD(H) and also S-P total concentrations. Compositions of S-P were also analyzed using PCA extract NMR. Fermentation studies were performed to compare growth rates, phenylalanine and by-product productions between the two strains.

5.3 MATERIALS AND METHODS

Strain and plasmid

E. coli strains PPA305 and PPA316, each harboring a phenylalanine-overproduction plasmid pSY130-14 were used in this study. As described in the previous chapter, PPA305 is a wild-type strain, using the PTS system for glucose uptake, and PPA316 uses a proton-galactose symport system for glucose transport and subsequent ATP-dependent phosphorylation is catalyzed by glucokinase.

Plasmid pSY130-14 was kindly provided by Dr. Toshiomi Yoshida (Osaka University, Japan). pSY130-14 carries genes *aro*F^{FR} and *phe*A^{FR} for the enzymes involved in the critical and regulated steps in the phenylalanine synthesis pathway. The mutated gene *aro*F^{FR}, which encodes for 3-deoxy-D-arabino-heptulosonate-7-phosphate synthase, catalyzing the condensation of erythrose-4-P and PEP, is resistant to feedback inhibition by tyrosine. Similarly, the mutated gene *phe*A^{FR}, which encodes for chorismate mutase P-prephenate dehydratase, catalyzing the formation of Prephenate from chorismate, is resistant to feedback inhibition by phenylalanine. The expression of *aro*F^{FR} and *phe*A^{FR} is under a P_R-P_L promotor and temperature-sensitive repressor cI_{857} of bacteriophage lambda. The optimal temperature for best production of phenylalanine was found to be 38.5 ^{o}C. The detailed construction and characterization of the plasmid can be found in the reference (Sugimoto et al. 1987).

Medium and culture conditions

The medium used in this study contained (per liter): glucose, 20 g ; Na_2HPO_4 ·7 H_2O, 12.8 g; KH_2PO_4, 3 g; $NaCl$, 1 g; NH_4Cl, 2 g; $MgSO_4$· 7 H_2O, 3 g; sodium glutamate 0.4 g; $CaCl_2$, 11mg; $FeSO_4$· $7H_2O$, 10.7 mg; $ZnCl_2$·$7H_2O$, 0.8 mg; $MnSO_4$, 8 μg; $CuSO_4$· $5H_2O$ 10.7 μg; $(NH_4)_6Mo_7O_{24}$· $4H_2O$, 6.7 μg; $Co(NO_3)_2$, 6.7 μg. 1.0 ml/l antifoam Poly(propylene) glycol (M.W. 1,000) was added. 12.5 mg/l Kanamycin was used to provide selective pressure on the plasmid-containing strains.

Fermentations were performed aerobically in a 3.5 L (working volume 1.5 L) LH fermentor (LH Fermentation, Hayward, CA). pH was controlled at 7.0 by adding 30% NH_4OH. Air flowrate was fixed at 2.0 (l/min.), dissolved oxygen was controlled above 20% of air saturation by manually adjusting agitation speed for the PTS strain or by oxygen enrichment to the air for the non-PTS strain (the reason for using different oxygen supply conditions is explained in the Discussion section). All fermentations were conducted at 38.5°C. The inocula were prepared with LB supplemented with kanamycin and grown overnight at 30°C in a shaker. 2% (V-V) inoculation was used in all fermentations.

In shake-flask cultivation, cells were grown using 500 ml flasks containing 50 ml medium (the same as used in fermentation studies). The cultivation was carried out at 275 rpm in an INNOVA 4000 rotary shaker (New Brunswick Scientific) and at either a uniform temperature 38.5°C or at 30°C followed by an upshift to 38.5°C.

Analytical methods

Dry weight of cell suspension taken from the fermentor was measured. After two washes, cell pellet was transferred to a pre-weighed aluminum plate which was dried at 105°C to constant weight. Metabolites in the supernatants were analyzed by high performance liquid chromatography (HPLC). A BioRad Aminex HXP-87H (300 x 7.8 mm) column was used and 0.01N H_2PO_4 mobil phase at flow rate 0.4 ml/min. was found to be satisfactory in resolving metabolites of interest. Glucose concentration in the medium was determined with a Sigma test kit (510-A). Ethanol and D-lactate were assayed using Boehringer-Mannheim kits. All absorbance measurements were made using a Shimadzu UV-260 Spectrophotometer. Phenylalanine was measured using a Sigma kit F-60 on a Shimadzu spectrofluorophotometer at emission wavelength of 480 nm and excitation wavelength of 390 nm.

NMR experiments

E. coli cells were grown in 2-L shaker flasks in 1 L of the same medium as detailed above. Cultivation of *E. coli* was carried out at 38.5°C and 275 rpm in a rotary shaker (New Brunswick Scientific). All subsequent sample preparation procedures and NMR operations were the same as detailed in the previous chapter (Chapter 4).

5.4 RESULTS

I. Phenylalanine production

Initial experiments in comparing phenylalanine production between these two strains were performed using shake-flask cultivation. Results are presented in figure 5.2 a,b. Arrows show the time when temperature was shifted from 30°C to 38.5°C. Although PPA316/pSY130-14 grew to a much higher cell density than PPA305/pSY130-14 (70% higher in this case), the maximal phenylalanine concentration reached was considerably lower (330 mg/l versus 490 mg/l). Experiments using a uniform temperature 38.5°C gave qualitatively similar results, i.e., the mutant grew to much higher cell density (90% higher), but produced much less phenylalanine (only one-fourth, 240 mg/l versus 960 mg/l).

Further investigation was done in a fermentor. Figures 5.3 a-c show these fermentation results (substrate utilization in figure a; growth in figure b and phenylalanine in figure c). For PPA305/pSY130-14, phenylalanine production was highly growth-associated, reaching a highest concentration of phenylalanine of 220 mg/l at its highest biomass concentration of 4.8 g/l. Afterwards, with a depletion of carbon source, phenylalanine was consumed quickly, and it fell to one-tenth of its peak value within 3 hours. PPA316/pSY130-14, in contrast to the PTS strain, did not produce any phenylalanine during its growth phase and produced a little in stationary phase, and it reached a maximal biomass concentration of 4.4 g/l, slightly lower than the wild-type.

No by-product (acetate, pyruvate, formate, lactate, succinate) was detected in the supernatant for PPA316/pSY130-14. Only a trace amount of acetate was accumulated in the growth medium of PPA305/pSY130-14. The maximal acetate concentration reached was only 0.1 g/l.

Samples taken from fermentor or shake-flasks were properly diluted and spread on LB plates without kanamycin. After overnight cultivation, colonies on plates were counted. Colonies on replica plates (with kanamycin) were also countered. The plasmid stability as measured by this method was over 95% for both strains. There was no difference between two cultivation methods.

II. NMR characterizations

The same methodology as described in the previous chapter (Chapter 4), was applied here to further characterize these two strains carrying a phenylalanine overproduction plasmid.

Assignments of the peaks and experimental procedures are detailed in Chapter 4. Figure 5.4 shows typical spectra of whole cell experiments, taken in quasi-steady-state glycolysis under aerobic conditions. The left part of the figure is S-P and Pi region and the right portion of the figure shows vertically expanded nucleotide region (-4.5 ppm to -20 ppm). Quantitative results are given in Table 5.1.

The absence of the Pi^{cyt} peak in the Pi region of the spectrum (fig. 5.4 bottom, left) for PPA316/pSY130-14 indicates a much lower ΔpH across the cytoplasmic membrane, relative to PPA305/pSY130-14. Although the sensitivity of the measurement do not allow to estimation of an accurate value, the ΔpH was likely

below 0.3 units, as this magnitude of ΔpH would differentiate Pi^{cyt} from the total Pi peak as is the case in figure 4.6. pH difference of 0.3 units is likely the minimal pH difference that allows differentiation Pi peaks from two compartment (Campbell-Burk and Shulman, 1987). A substantially lower energetic state of the strain PPA316/pSY130-14, compared to PPA305/pSY130-14, was also reflected by the much smaller pool of high energy compound, NTP, which was three times lower. NAD(H) concentration in the non PTS strain was 1.8 times lower than its PTS counterpart (Table 5.1).

The ratio of the total S-P concentration in strain PPA316/pSY130-14, relative to that for strain PPA305/pSY130-14, was 2.4 measured in the whole cell experiments. The compositions of the S-P for both strains were determined by PCA extract NMR. Results are given in Table 5.2. As with PPA305 and PPA316 (Table 4.2), the most significant difference was found in fructose phosphate and PEP. PPA316/pSY130-14 had only one-sixth the PEP concentration and only one-seventh the fructose phosphate concentration of those of its wild-type.

5.5 DISCUSSION

In the course of fermentation of PPA316/pSY130-14, when cell density was over 3 g/l, using fixed air flow rate (the same flowrate as used for the other strain) and maximal agitation speed (higher than that used for the other strain at higher biomass concentration) could not maintain the dissolved oxygen above 20% of the air saturation. Oxygen enrichment was necessary in the later stage of the fermentation of this strain. Oxygen supply and utilization follows the following equation:

$$K_La\ \{[O_2]^*-[O_2]\} = q_{O2}X \qquad 5.3$$

where K_La is the mass transfer coefficient; $[O_2]^*$ is the dissolved oxygen concentration in equilibrium with the gas phase; $[O_2]$ is the dissolved oxygen concentration; q_{O2} is the specific oxygen uptake; and X is the biomass concentration. The observed difference in D. O. profiles indicated a higher specific O_2 uptake rate in PPA316/pSY130-14. This strain produced lower final biomass concentration and no phenylalanine and no acetate, indicating that more carbon was oxidized to CO_2. Studies in control of the TCA cycle suggest that citrate synthesis plays a key role in regulating carbon flux to the TCA cycle, for which ATP, among others, is an inhibitor. Since ATP level in this strain was unusually low as measured by NMR methods (Table 5.1, note: half of NTP is ATP, see Chapter 4). Therefore more carbon flux through the TCA cycle in this strain is likely responsible for the higher specific oxygen uptake rate and higher yield of CO_2.

Contrary to the expectations, mutation in PTS system and switching to a non-PTS system did not increase the PEP pool, and did not enhance the production of phenylalanine.

Both strains behaved quite differently in different cultivation conditions, shake-flask cultivation and fermentation. Particularly, phenylalanine production was substantially decreased in fermentations, this is unexpected as earlier studies (Sugimoto et al. 1987) showed that control of pH and D.O. led to higher production of phenylalanine. We observed that during fermentation the specific growth rates were approximately twice as much as the specific growth rates in shake-flask cultivations for both strains. Faster growth rate in fermentation could be responsible for the poor

performance in phenylalanine. For both strains, final biomass concentrations were higher in fermentations, indicating a larger portion of carbon was channeled to biomass formation.

In our fermentation studies, we used the optimal temperature 38.5°C determined in a different host strain AT2471 by Sugimoto et al. (1987). Different genetic background may have different temperature optimum. Whether this is the case remains an interesting subject for future work.

5.6 ACKNOWLEDGMENTS

Ms. Wyanda Yap and Dr. P. W. Postma (The University of Amsterdam) constructed and provided the host strains used in this study. The plasmid pSY130-14 was kindly provided by Dr. Toshiomi Yoshida (Osaka University, Japan). This work was supported by the Advanced Industrial Concepts Division of the U.S. Department of Energy and the National Science Foundation (Grant No. BCS 891284). The LH fermentor and instrumentation were generously provided by LH Fermentation (Hayward, CA). The assistance of Dr. Robert Lee with the Bruker AM500 NMR spectrometer is greatly appreciated.

5.7 REFERENCES

Ahn, I. Effect of glucose uptake systems on the yield of amino acids in *Escheriahia coli*. Master thesis. Caltech, 1992

Backman, K.; O'Connor, M. J.; Maruya, A.; Rudd, E. et al. Genetic engineering of metabolic pathways applied to the production of phenylalanine, Ann. N. Y. Acad. Sci. USA. 17-24.

Bell, A. A. and Wheeler, M. H. Annu. Rev. Phytopathol. 1986, 24, 411.

Brown, K. D. Regulation of aromatic amino acid biosynthesis in *Escherichia coli* K-12. Genetics. 1968, 60, 31-48.

Draths, K. M.; Pompliano, D. L.; Conley, D. L. and Frost, J. W. et al. Biocatalytic synthesis of aromatics from D-glucose: the role of transketolase. J. Am. Chem. Soc. 1992, 114, 3956-3962.

Forberg, C.; Eliaeson, T. and Haggstrom, L. Correlation of theoretical and experimental yields of phenylalanine from non-growing cells of a rec *Escherichia coli* strain. J. Biotech. 1988, 7, 319-332.

Forberg, C. and Haggstrom, L- Phenylalanine production from a rec *Escherichia coli*-strain in fed-batch culture. J. Biotech. 1988, 8, 291-300.

Hodgson, J. Bulk amino-acid fermentation: technology and commodity trading. Bio/technology. 1994, 12, 151-155.

Huang, S. O.; Gil, G. H.; Cho, Y. J. Kang, K. R.; Lee, J. H. and Bae, J. C. The fermentation process for L-phenylalanine production using an auxotrophic regulatory mutant of *Escherichia coli*. Appl. Microbiol. Biotechnol. 1985, 22, 108-113.

Konstantinov, K. B.; Nishio, N.; Seki, T. and Yoshida, T. Physiologically motivated strategies for control of the fed-batch cultivation of recombinant *Escherichia coli* for phenylalanine production. J. Fermen. and Bioeng. 1991, 71(5), 350-355.

Miller, J. E.; Backman, K. C.; O'Connor, M. J. and Hatch, R. T. Production of phenylalanine and organic acids by phosphoenolpyruvate carboxylase-deficient mutants of *Escherichia coli*. J. Industrial Microbiol. 1987, 2, 143-149.

Ogino T.; Garner, C.; Marley, J. L. and Hermann, K. M. Biosynthesis of aromatic compounds: ^{13}C NMR spectroscopy of whole *Escherichia coli* cells. Proc. Natl. Acad. Sci. USA. 1982, 79, 5528-5832.

Pittard, A. J. Biosynthesis of the aromatic amino acids. In: "*Escherichia coli* and *Salmonella typhimurium* cellular and molecular biology, volume II " Neidhardt F. C. (ed.), American society for microbiology, Washington, D. C. 1987, 127-141.

Sugimoto, S.; Yabuta, M.; Seki, T.; Yoshida, T. and Taguchi, H. Expression of pheA gene using P_R-P_L tandem promoter of bacteriophage lambda. Appl. Microbiol. Biotechnol. 1985, 22, 336-342.

Sugimoto, S.; Yabuta, M.; Kato, N.; Seki, T.; Yoshida, T. and Taguchi, H. Hyperproduction of phenylalanine by *Escherichia coli*: application of a temperature-controllable expression vector carrying the repressor-promotor system of bacteriophage lambda. J. Biotech. 1987, 5, 237-253.

Weiss, U. and Edwards, J. M. The biosynthesis of aromatic compounds. Wiley, New York, 1980.

Zuraski, G.; Brown, K. D.; Killingly, D. and Yanofsky, C. Nucleotide sequencing of the leader region of the phenylalanine operon of *Escherichia coli*. Proc. Natl. Acad. Sci. USA. 1978, 75, 4271-4275.

5.8 TABLES

Table 5.1 Intracellualr concentrations measured by ^{31}P NMR on whole cell samples

Concentration in mM	SP	NTP	NAD(H)	UDPG
PPA305/pSY130-14	36.1±0.4	4.8±0.2	9.0±0.3	
PPA316/pSY130-14	15.2±0.5	1.4±0.2	5.1±0.2	1.2±0.3

Concentrations are averages of at least three separate experiments.

Table 5.2 S-P concentrations measuredy by extract ^{31}P NMR

S-P Conc. in mM	PPA305/pSY130-14	PPA316/p130-14
G-6-P	1.0	2.2
3-PGA	0.6	1.3
FDP+F6P	28.6	4.2
2-PGA	5.5	2.1
S-P-Un	1.4	3.3
S-P TOTAL	37.1	13.1
PEP	18.6	3.1

Concentrations are in mM and are averages of at least three separate experiments. S-P-Un: unidentified sugar phosphate, other abbreviations are the same as figure 4.10, 4.11 and 4.12. The relative error: 20%.

n.d.--- not determined.

5.9 FIGURES

Figure captions

Figure 5.1 Phenylalanine synthesis pathway of *E. coli*.

Figure 5.2 Time trajectories of biomass (a) and phenylalanine (b) during shaker-flask cultivation. (O) ----PPA316/pSY130-14; (Δ) ----PPA305/pSY130-14.

Figure 5.3 Time trajectories of glucose (a), biomass (b) and phenylalanine (c) during fermentations under aerobic conditions. (O) ----PPA316/pSY130-14; (Δ) ----PPA305/pSY130-14.

Figure 5.4 ^{31}P NMR spectra acquired during aerobic glycolysis of *E. coli* strains PPA305/pSY130-14 (top spectrum) and PPA316/pSY130-14 (bottom spectrum). The left part is for S-P and Pi region and the right portion of the figure is vertically expanded nucleotide region. Spectra were obtained using 40° pulse and a relaxation delay of 0.2 s, NS (number of scans) 480, other parameters as in the Materials and Methods. Abbreviations: SP: sugar phosphate; P_i^{cyt}: intracellular inorganic phosphate; P_i^{ex} : extracellular inorganic phosphate; NTP: nucleoside triphosphate; NDP: nucleoside diphosphate; NAD(H): nicotinamide adenine dinucleotide; UDPG: uridinediphosphoglucose.

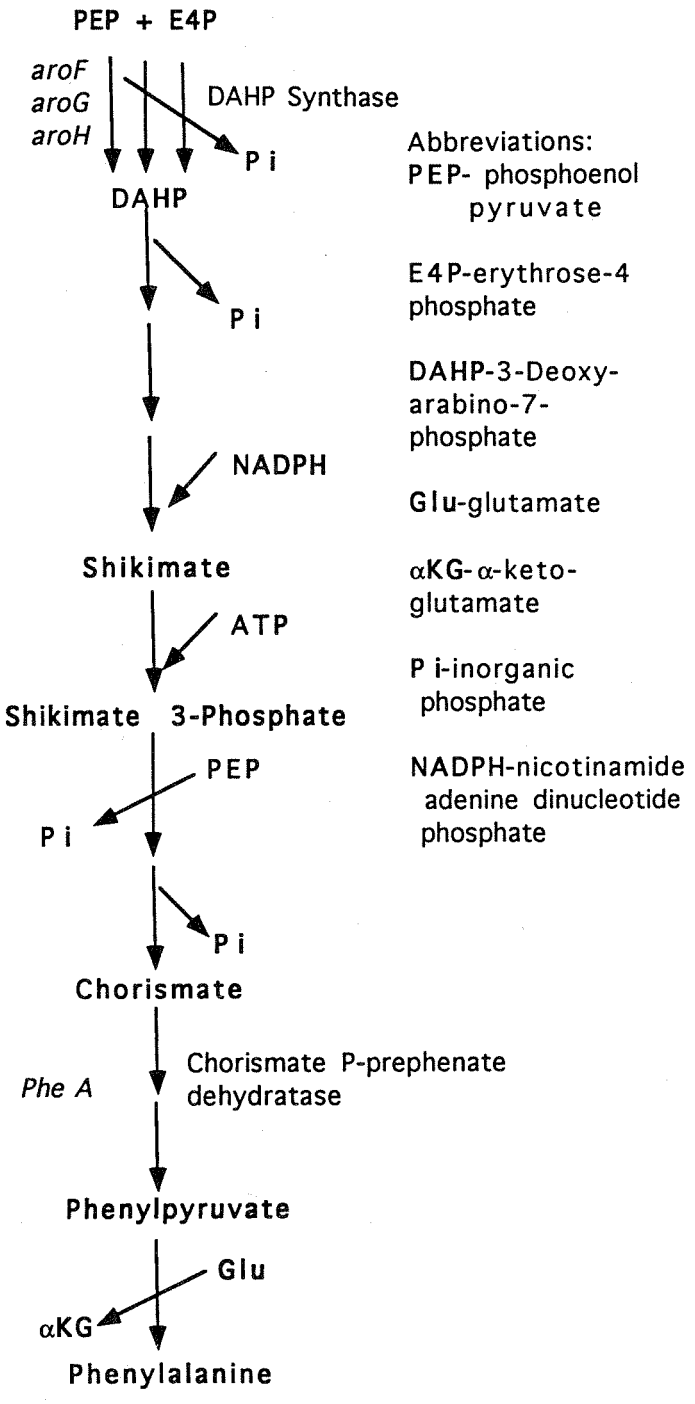

Figure 5.1 Phenylalanine biosynthesis pathway

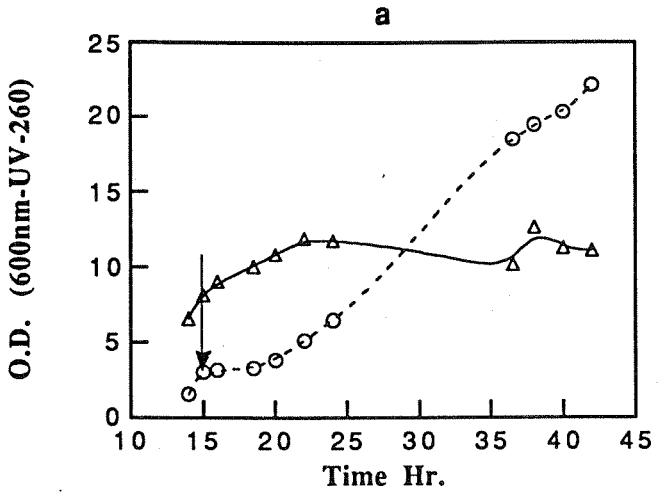
a
O.D. (600nm-UV-260)
25
20
15
10
5
0
10 15 20 25 30 35 40 45
Time Hr.

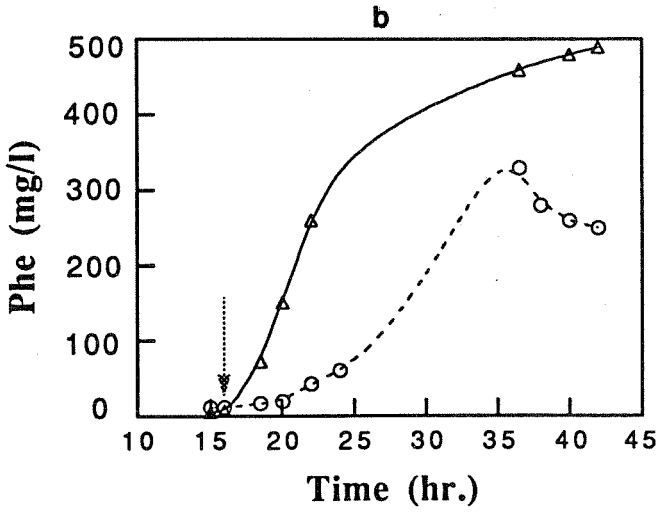
b
Phe (mg/l)
500
400
300
200
100
0
10 15 20 25 30 35 40 45
Time (hr.)

Figure 5.2

Figure 5.3

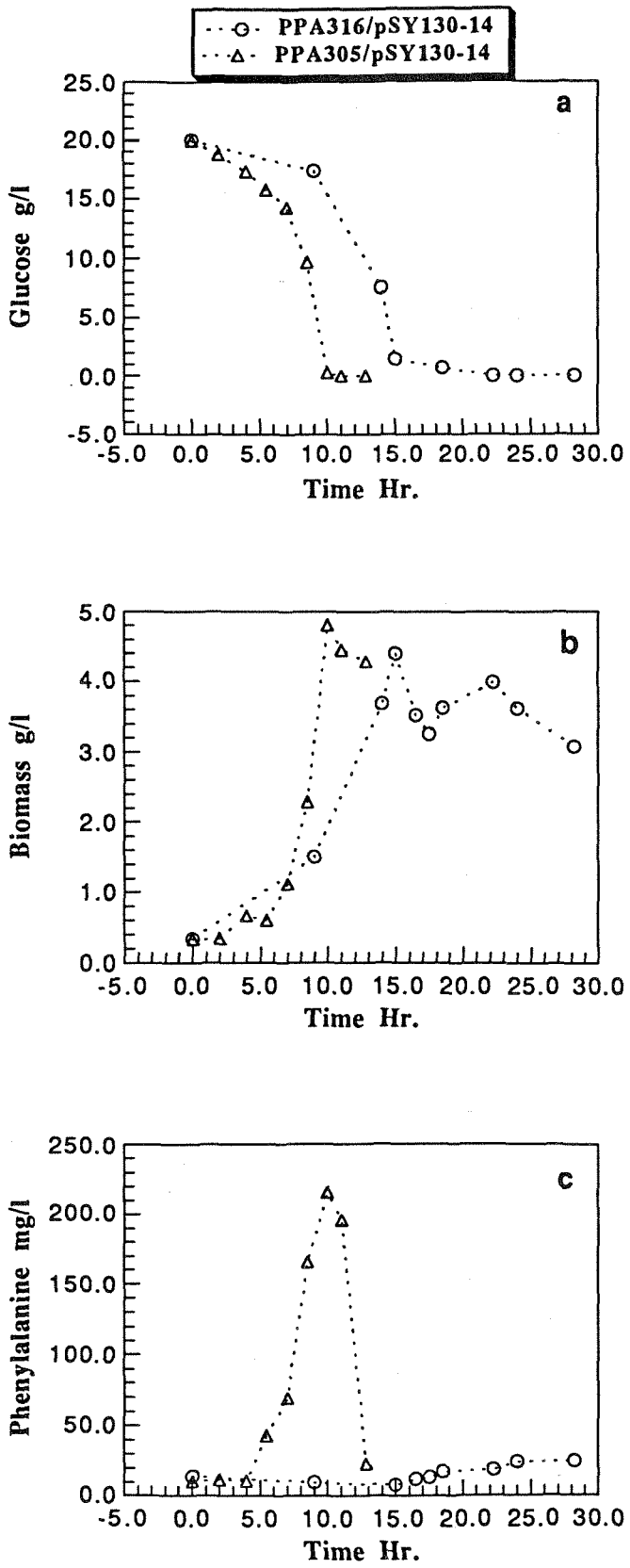
PPA316/pSY130-14
PPA305/pSY130-14
a
Glucose g/l
25.0
20.0
15.0
10.0
5.0
0.0
-5.0
-5.0 0.0 5.0 10.0 15.0 20.0 25.0 30.0
Time Hr.
b
Biomass g/l
5.0
4.0
3.0
2.0
1.0
0.0
-5.0 0.0 5.0 10.0 15.0 20.0 25.0 30.0
Time Hr.
c
Phenylalanine mg/l
250.0
200.0
150.0
100.0
50.0
0.0
-5.0 0.0 5.0 10.0 15.0 20.0 25.0 30.0
Time Hr.

Figure 5.4

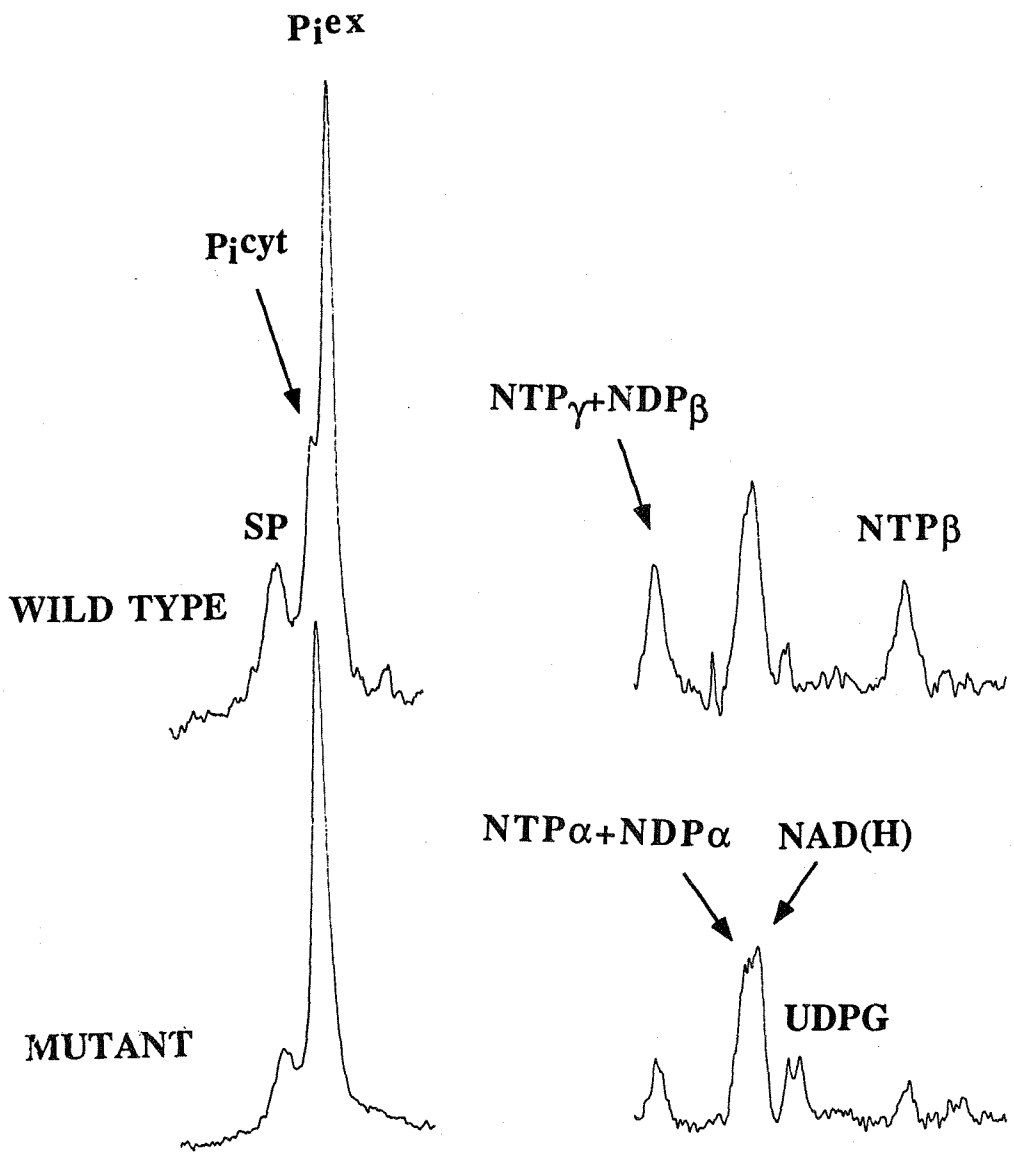
Piex
Picyt
NTPγ+NDPβ
SP
NTPβ
WILD TYPE
NTPα+NDPα
NAD(H)
UDPG
MUTANT

Chapter 6

Conclusions

6.1 CONCLUSIONS

It has been demonstrated that ^{31}P NMR is a useful tool in metabolic engineering studies. It provides information on concentrations of various metabolites, NTP and cofactors NAD(H), intracellular pH and the pH difference across the cytoplasmic membrane. NMR thus can be used for analyzing changes in cell energetics, metabolism and intracellular environments which correspond to specific genetic manipulations. NMR data, when combined with growth and fermentation studies, enrich our understanding regarding cellular responses to particular genetic modifications and point out new directions of further improvement of the cell genome.

On-line NMR system

A novel on-line NMR system has been developed in this work which further strengthens the power of NMR by extending its applications to growing cell cultures. This system allows fermentor-grown cells to directly circulate to an NMR spectrometer for on-line monitoring. Cell growth conditions such as pH, D.O., air supply and temperature can be easily controlled in the fermentor. Additional oxygen supply in the circulation loop and in the NMR sample tube, and monitoring D.O. in the loop, ensure that oxygen limitation is avoided. Fluctuations in other parameters such as pH, temperature during circulation are marginal under typical operation conditions.

Experiments can then be conducted under well-defined conditions, eliminating time-limitations in the conventional method. A simple exponential glucose feeding protocol enables cell to grow to concentrations high enough for NMR measurements and thus eliminates the need of concentrating cells and possible artifacts associated with such procedures. Both anaerobic and aerobic metabolism can be monitored. The on-line NMR system also offers the hope to do new types of physiological studies. Examples illustrating this are provided by the studies of acetate inhibition on growth of *E. coli* and on VHb effects described in this thesis.

Acetate effects

Acetate effects on cell growth rates and the energization of the cytoplasmic membrane (ΔpH) were monitored simultaneously. ΔpH collapsed when acetate concentration was high (ca. 20g/l). This coincided with a significant decrease of the specific growth rate and a sudden increase of D.O. concentration in the fermentor. Results from this study confirmed that acetate acts as an uncoupler of membrane energetics, as suggested for another microorganism.

VHb work

Using the on-line NMR system, the steady-state levels of ATP, ΔpH and other NMR-visible parameters were measured in *E. coli* strains with and without VHb expression (GRO21 and MG1655) during their growth under oxygen-limiting conditions. It has been concluded that both strains had similar ATP levels and ΔpH. The specific growth rates measured in late exponential phase showed a 65% increase in

VHb-expressing strain. This means that the net ATP accumulation rate (the rate at which ATP increases per unit volume of culture per unit time) is increased in the VHb-expressing strain.

Employing the saturation transfer NMR technique, ATP synthase kinetics have been measured for the two strains respiring on succinate. ATP synthesis rate catalyzed by the ATPase is accelerated by 30% by the presence of VHb.

Studies on strains with different glucose transporters

The PTS system is considered the most energy efficient glucose-uptake system in *E. coli*. Using an alternative uptake system brings about many consequences. Although the specific growth rate under aerobic conditions of the non-PTS strain (PPA316) is not much affected, reaching 60% of the specific growth rate of the PTS strain (PPA305), the anaerobic specific growth rate is reduced by a factor of five. Significantly different fermentation patterns have been observed. Lowered flux of the non-PTS strain to pyruvate is a plausible explanation for this under aerobic conditions, which prevents carbon overflow to acetate. A lower flux of this strain to pyruvate in anaerobic conditions is evidenced from analyzing end-products. Substantial flux to succinate for the non-PTS strain is considered to be the consequence of low NAD^+ level of this strain.

NMR data show that the non-PTS strain experience a considerably different intracellular environment. NTP and ΔpH concentrations are lower, while NDP is higher. NAD(H) is also much lower. With respect to S-P, not only the total concentration is lower, but the S-P composition is substantially different. Notably the FDP and PEP concentrations are also at much reduced level.

The much decreased glycolysis rate in this strain may be attributed to the lower NAD^+, ATP, FDP and PEP concentratios which in turn may limit reactions catalyzed by glucokinase, glyceraldehyde-3-phosphate dehydrogenase, PFK and PK.

Phenylalanine production

The non-PTS strain carrying a phenylalanine overproduction plasmid exhibits much lower energy levels (NTP and ΔpH) and lower S-P total concentration than its PTS counterpart. NAD(H) and PEP concentrations are also significantly lower. The composition of S-P is considerably different, Particularly FDP is much lower in the non-PTS strain.

Using the non-PTS proton symport system for glucose uptake does not increase phenylalanine production under the conditions studied here.

The non-PTS strain also has a higher specific oxygen uptake rate, reaches lower biomass concentration, and produces no phenylalanine, acetate and other products, suggesting a larger portion of carbon is oxidized to CO_2.

6.2 FUTURE WORK

In addition to using the galactose-proton symport system for glucose uptake, there is another alternative to uncouple glucose uptake from its phosphorylation. Mutated II^{glu} of the PEP-dependent phosphotransferase system has been shown capable of transporting glucose in the absence of the general phosphoryl-carrying proteins of the PTS, enzyme I and HPr (Ruijter et al. 1992). Glucose transport is via

facilitated diffusion and requires no energy, and subsequent phosphorylation is catalyzed by glucokinase. Thus the net cost of glucose uptake and phosphorylation is one ATP equivalent per each molecule of glucose transported and phosphorylated. This scheme of glucose uptake is energetically equivalent to the PTS system. It is particularly interesting to study the energetics and metabolism of such a system as well as phenylalanine production and to compare the data and conclusions reached in this study.

Carbon-flux partition between pentose phosphate pathway (PP) and EMP pathway is likely different in cells overproducing one or more aromatic amino acid(s) from the 30%-70% partition found in normal cells. One of the precursors of aromatic amino acids, erythrose 4-phosphate (E-4-P), is from the PP pathway. Also, reducing equivalent NADPH required for biosynthesis of aromatic amino acids is mainly generated from the PP pathway. It is not always true the PEP is limiting phenylalanine, E-4-P may well be limiting under certain conditions (Draths et al. 1992). Evaluation of the flux apportionment between the two pathways can provide such valuable information. This can be done with the isotopic tracer (^{14}C) method and, in principle, also by ^{13}C NMR.

6.3 REFERENCES

Draths, K. M.; Pompliano, D. L.; Conley, D. L. and Frost, J. W. et al. Biocatalytic synthesis of aromatics from D-glucose: the role of transketolase. J. Am. Chem. Soc. 1992, 114, 3956-3962.

Ruijter, G. J. G.; van Meurs, G.; Verwey, M. A. Postma, P. W. and van Dam, K. Analysis of mutations that uncouple transport from phosphorylation in enzyme II^{glu} of the *Escherichia coli* phosphoenolpyruvate-dependent phosphotransferase system. J Bacteiol. 1992. 2843-2850